Scuola Internazionale Superiore di Studi Avanzati - Trieste

SISSA 40!

In silico and *in vitro* screening of acridine and phenothiazine derivatives as anti-prion agents

Candidate:

Ludovica Zaccagnini

Supervisor:

Prof. Giuseppe Legname

A thesis submitted for the degree of
Doctor of Philosophy
in Functional and Structural Genomics
October 2018

SISSA - Via Bonomea 265 - 34136 TRIESTE - ITALY

Scuola Internazionale Superiore Studi Avanzati
(SISSA)

In silico and *in vitro* screening of acridine and phenothiazine derivatives as anti-prion agents

Candidate: Supervisor:

Ludovica Zaccagnini **Prof. Giuseppe Legname**

A thesis submitted for the degree of
Doctor of Philosophy
in Functional and Structural Genomics
October 2018

ABSTRACT

Although in the last decades there has been a growing interest in neurodegenerative diseases, there are still no effective therapies. Some of these diseases are considered protein misfolding disorders (PCDs), since they are mainly caused by a conformational change of a native protein into a disease-associated one, that can aggregate and form an infective seed; Alzheimer's disease with Aβ and Tau proteins, Parkinson's disease with α-synuclein, and prion diseases with prion protein.

Recently, transmissible spongiform encephalopathies (TSEs), also known as prion diseases, have been considered as a prototype of neurodegenerative diseases for their ability to be sporadic, inherited and also infectious. Indeed, the infectivity was long thought to belong exclusively to prion diseases, but in the last years accumulating evidence suggest that other proteins follow a similar mechanism of seed self-propagation and cell-to-cell spreading *in vitro* and *in vivo*.

TSEs are mainly characterized by vacuolation, neuronal loss, cognitive and motor impairments. They include kuru, Creutzfeldt-Jacob disease, Gerstmann Sträussler-Scheinker syndrome and fatal familial insomnia in human, bovine spongiform encephalopathy in cattle, scrapie in sheep and chronic wasting disease in elk and deer. The etiology agent is the scrapie prion protein (PrP^{Sc}), the abnormal, misfolded form of the cellular prion protein (PrP^{C}). The normal protein is anchored to the cell surface through a C-terminal moiety of glycophosphatidyl-inositol (GPI). Even though the two isoforms share the same primary sequence, they have several different aspects: PrP^{C} is rich in α-helices, is soluble and protease K (PK) sensitive; while the PrP^{Sc} has a high level of β-sheets, is insoluble and partially PK resistant.

The molecular mechanism underlying the conversion of PrP^{C} to PrP^{Sc} is still not completely understood. Several studies in literature focus on the ability of small molecules to inhibit the conversion by either binding the PrP^{C} or blocking the PrP^{Sc} aggregation. The majority of compounds screened for this action were already used as antivirals, antimalarials, antifungals and antidepressants. Drug repositioning is a strategy that uses known compounds to treat new diseases. By using this approach quinacrine (antimalarial), Pentosan Polysulfate (heparin mimetic), Doxycycline (antibiotic) and Flupirtine (analgesic) were tested in human clinical trials, unfortunately without the expected results. Other approaches applied to develop anti-prion therapies are medicinal chemistry, multi-target approaches and *in silico* methods.

In drug screening, the *in silico* method is useful to increase the discovery speed of new drugs, thus reducing costs and lab work. In particular, we developed a quantitative structure-activity relationship model (QSAR) and by using it performed a virtual screening of some purchasable compounds. With the help of the QSAR model, we obtained a library of 10 molecules with a predicted IC_{50} in the nanomolar range. Immortalized neuroblastoma (N2a) and hypothalamic (GT1) mouse cell lines chronically infected with prions were used to assess the cell viabilty of the library and to measure the anti-prion infectivity.

After performing western blot analysis and Real-Time Quaking-Induced Conversion (RT-QuIC) assay, compound **1** emerged as the most promising molecule, since it was able to completely cure N2a-RML cells from PrP^{Sc}, either after acute or chronic treatments. Additionally, we designed a competitional assay, which shows that compound **1** blocks prion conversion by binding to the cellular prion protein. These results make this molecule an interesting and promising therapeutic tool for prion diseases.

LIST OF PUBLICATIONS:

All the work reported here arises from my own experiments and data analysis performed in SISSA or as a result of joint collaborations with other groups.

-**Zaccagnini L.**, Brogi S., Brindisi M., Gemma S., Chemi G., Legname G., Campiani G. and Butini S. Identification of novel fluorescent probes preventing PrPSc replication in prion diseases. Eur J Med Chem. 2017 Feb 15;127:859-873.

-**Zaccagnini L.**, Rossetti G., Tran TH., Gandini A., Salzano G., Bolognesi ML., Carloni P., Legname G. In silico and in vitro screening of acridine and phenothiazine derivatives as anti-prion agents. Eur J Med Chem. 2018 *submitted*

LIST OF ABBREVIATIONS

3D: three-dimensional
α-syn: α-synuclein protein
Aβ: amyloid-β protein
AD: Alzheimer's disease
ALS: amyotrophic lateral sclerosis
ASA: amyloid seeding assay
BBB: blood brain barrier
CC_1: charged aminoacid cluster 1(residue 23-27) in the HuPrP sequence
CC_2: charged aminoacid cluster 2 (residue 95-110) in the HuPrP sequence
CNS: central nervous system
CJD: Creutzfeldt-Jakob disease
CSF: cerebral spinal fluid
CWD: chronic wasting disease
Dpl: Doppel
DWI: Diffusion-weighted magnetic resonance imaging
Edbg: Edimburg, a PrP^C-null mice strain
EEG: Electroencephalography
ER: endoplasmic reticulum
f: familial
FL: full length
FLAIR: fluid attenuated inversion recovery
FFI: Fatal familial insomnia
FSE: Feline spongiform encephalopathy
FT: Fourier Transform
FTIR: Fourier transform infrared spectroscopy
GAGs: glycosaminoglycans
GPI: glycosylphosphatidylinositol
GSS: Gerstmann-Sträussler–Scheinker
GT1: mouse hypothalamic cells line
HD: hydrophobic domain
HD: Hungtington's diseases
Hu: human
i: iatrogenic
IC_{50}: half maximal inhibitory concentration
Ig: immunoglobulin
LRP1: low density lipoprotein receptor-related protein
LTP: long term potentiation
MD: molecular dynamic
MM: minimal medium
Mo: mouse
MRI: Magnetic resonance imaging
N2a: mouse neuroblastoma cells line
NFTs: neurofibrillary tangles
Ngsk: Nagasaki, a PrP^C-null mice strain
NMDA: N-methyl-D-aspartate glutamate receptors
NMR: nuclear magnetic resonance
OR: octapeptide-repeat region
ORF: open reading frame

PCD: protein conformational disorder
PD: Parkinson's disease
pIC_{50}: predicted IC_{50}
PMCA: Protein Misfolding Cyclic Amplification
PNS: peripheral nervous system
PrP: prion protein
PrP^{C}: physiological cellular form of PrP
PrP^{Sc}: misfolded, pathogenic form of PrP^{C}, also denoted as prion.
^{Ctm}PrP: C-terminal transmembrane PrP form
^{Ntm}PrP: N-terminal transmembrane PrP form
PrP^{res}: PK-resistant PrP
PK: protease K
PRNP: human prion protein gene
Prnp: prion protein gene in non human species
Prnd: Doppel gene in non human species
PSS:
RTQuIC: Real-time quaking-induced conversion
Sh: Syrian Hamster
SOD-1: Superoxide dismutase
rec: recombinant
RT: room temperature
s: sporadic
ScGT1: chronically PrP^{Sc} infected mouse hypothalamic cells line
ScN2a: chronically PrP^{Sc} infected mouse neuroblastoma cells line
SPR: surface plasma resonance
STED: stimulated emission depletion nanoscopy
STI1: stress-inducible protein I
TDP-43: TAR DNA-binding protein 43
Tg: transgenic
ThT: thioflavin T
TME: Transmissible Mink Encephalopathy
TSEs: transmissible spongiform encephalopathies, also denoted as prion diseases
v: variant
VGCC: voltage-gated calcium channel
WHO: world health organization
WT: wild-type
ZrchI: Zurich I or $Prnp^{0/0}$, a PrP^{C}-null mice strain

TABLE OF CONTENTS

Chapter II

Chapter III

Chapter IV

CHAPTER I

Introduction

1.1 Neurodegenerative diseases

Over the last decades different disorders caused by protein misfolding have been studied and grouped together under the name of protein conformational disorders (PCDs). Many of these diseases are neurodegenerative disorders, such as Alzheimer's disease (AD), transmissible spongiform encephalopathies (TSEs), Huntington's disease (HD), Parkinson's disease (PD), and amyotrophic lateral sclerosis (ALS) [1].

The neurodegenerative diseases can be caused by mutations or sporadic events, in any case the onset of the disorder increases with aging. These age-related pathologies have high societal costs and lead to a dramatic loss of life quality for patients and caregivers. Nowadays, there is still no cure for any of these disorders. Furthermore, 45 million people worldwide are affected by some form of neurodegeneration, and data from 2015 report of World Health Organization (WHO) claims that in 2030 the affected are expected to reach 76 million.

Neurodegenerative diseases are debilitating conditions that affect the nervous system resulting in progressive degeneration and death of nerve cells. This causes many different symptoms, such as problems with movement (tremor, ataxia, balance impairment) and mental functions - (apathy, insomnia, dementia) [2].

Each neurodegenerative disease is caused by specific misfolded protein. For example, amyloid-β (Aβ) and tau as neurofibrillary tangles (NFTs) in AD [3, 4], α-synuclein (α-syn) in PD [5], Cu/Zn superoxide dismutase (SOD1) and TAR DNA-binding protein 43 (TDP-43) in ALS [6, 7], prions (PrP^{Sc}) in prion diseases, also known as TSEs [8], and others (Table 1).

The protein folding determines the three-dimensional (3D) structure, given by amino acid sequence, and the biological function of a protein. The protein misfolding is due to a lack of a correct three-dimensional structure. This conformational change in the secondary or tertiary structure, but not in the primary, can lead the protein to toxicity and/or loss of its biological activity. Misfolded proteins are rich in β-sheets, that is a specific conformation which consist of alternating peptide-pleated strands linked by hydrogen bonding between the amino and the

carboxyl groups of the peptide bond. This type of structure allows the stabilization of oligomers and aggregated proteins. On the contrary, natively folded proteins are mainly enriched in α-helix structures, where the hydrogen bonds are between groups in the same strand. So, there is a correlation between the protein misfolding and the aggregation.

Disease	Clinical Features	Protein
AD	Progressive dementia	Aβ and tau
PD	Movement disorders	α-syn
ALS	Movement disorders	SOD1
TSEs	Dementia, ataxia, psychiatric problems, insomnia	Prion protein

Table 1. List of some neurodegenerative disorders with their clinical features and proteins involved

The conformational change and the onset of aggregation can be caused by many factors, such as mutations, environmental changes and chemical modifications. These factors reduce the conformational stability of the protein's native form and lead to a shift of the equilibrium between the folded protein and the misfolded protein. In physiological conditions, the population of partially folded protein is refolded by molecular machineries such as molecular chaperones (i.e. heat-shock proteins, calnexin) and ubiquitin-protease pathway [9].

Under destabilizing conditions, general physiochemical features such as net charge, hydrophobicity and propensity to alpha and beta structure formation, affect the tendency of the unfolded or partially folded protein chain to aggregate and form amyloid fibrils [10]. All amyloid fibrils share the same main features, they are straight, unbranched, 6.12 nm wide and formed by a different number of elementary filaments (protofilaments) that are around 1.5-2.0 nm in diameter, twisted around each other in a rope-like structure. These structural features are studied by transmission and cryo-electron microscopy, atomic force microscopy, NMR and X-ray diffraction[11].

1.1.1 Prion Diseases

Prion diseases, also known as transmissible spongiform encephalopathies (TSEs), are infective neurodegenerative disorders. The main hallmarks are spongiform lesions, glial activation and cell apoptosis, which lead to many different motor and cognitive symptoms. TSEs were defined as transmissible in early 1930s, by an experiment performed by Cuille and Chellè showing transmissibility of scrapie to goats [12]. Originally, this transmissibility hypothesis was considered as an unorthodox hypothesis. Afterward, Griffith speculated that a protein alone, without the presence of nucleic acids, could be the infectious moiety responsible for the disease [13]. Finally, in 1982 Stanely B. Prusiner proposed the prion hypothesis, stating that TSEs result from the conformational change of the native isoform of the prion protein (PrP^{C}) into the scrapie isoform (PrP^{Sc}) [14].

Prion diseases affect humans and a wide range of animal species. These disorders can arise sporadically, be inherited, or acquired through infection (Table 2). Animal TSEs include bovine spongiform encephalopathy (BSE) of cattle [15], scrapie of sheep [16], chronic wasting disease (CWD) of moose, elk and deer [17] and transmissible mink encephalopathy (TME) [18].

Human prion diseases include fatal familial insomnia (FFI) [19], Gerstmann-Sträussler-Scheinker syndrome (GSS) [20], Kuru syndrome [21] and Creutzfeldt-Jakob disease (CJD). CJD can be classified as:

- sporadic (sCJD), the most common form, although very rare with an incidence of 0.6-1.2 x 10^{-6} per year. The etiology is unknown, because no cause has been identified due to the failure of finding either an infectious or genetic etiology [22].
- familial (fCJD), which is the autosomal dominant form, caused by PRNP mutation.
- iatrogenic (iCJD), which is attributed to tissue transplantation or to the use of neurosurgical instruments contaminated by individuals suffering of unrecognized TSEs. iCJD is considered one of the biggest catastrophes in the history of medicine.
- variant (vCDJ), caused by the transmission of BSE prions to humans, as it occurred in the '90s [23].

Kuru is another infectious prion diseases, like iatrogenic and variant CJD [21]. In this case, the transmission of prions was due to a ritualistic cannibalism of brain from relatives of New Guinea highlanders dying of Kuru [24].

Specie	Disease	Sporadic	Genetic	Infectious
Humans	CJD			•
	GSS		•	
	FFI	•	•	
	vCJD		•	•
	Kuru			•
Cattle	BSE	•	•	•
Sheep	Scrapie	•	•	•
Cervids	CWD	•	unknown	•
Mink	TME	•	unknown	unknown
Feline	FSE	•	unknown	unknown

Table 2. Human and animal prion diseases

1.2 Prion Protein

The term "prion", acronym of PRotinaceous Infective ONly particle, was coined by Stanley B. Prusiner [14]. The cellular prion protein (PrP^C) is a ubiquitous protein expressed in the heart, immune system, skeletal muscle, pancreas, kidney, and both the central nervous system (CNS) and peripheral nervous system (PNS). In CNS and PNS it is localized in the membranes of neurons, astrocytes, oligodendrocytes, and Schwann cells.

PrP^C is a detergent-soluble, protease-sensitive, glycoprotein localized mainly in the extracellular membrane, attached throughout a glycosylphosphatidyl inositol (GPI) anchor [25].

1.2.1 Biogenesis of PrP^C

The prion protein gene (*PRNP* in human or *Prnp* in other species) is highly conserved among different species. The open reading frame (ORF) encoded within a single exon [8, 26]. In humans, Syrian hamsters and opossums, the PrP gene comprises of two exons with the ORF localized in the exon 2, while in mice, sheep, cattle and rats the gene has 3 exons, with ORF present in the third exon. The other exons contain untranslated sequences including the promoter and termination sites. The PrP promoter contains multiple copies of GC rich repeats and is devoid of TATA box [27, 28]. In humans, *PRNP* is a single copy gene mapped in the short arm of chromosome 20, which corresponds to the homologous region of mouse

chromosome 2 where *Prnp* is located. PrP mRNA has been detected in a wide range of tissues and cell types, but the highest concentration is found in the brain, where *in situ* hybridization has demonstrated that the greatest abundance of mRNA is located in neurons [29, 30].

PrP^C is highly expressed in the central (CNS) and peripheral nervous system (PNS), however, its content varies among different cell types, neurons and glial cells. The expression of mRNA and the protein is developmentally regulated, increasing postnatally with distinct time course for distinct regions. Indeed, the earliest expression is in the hippocampus, thalamus and hypothalamus.

The pre-pro protein, as a typical cell-surface glycoprotein, is translocated to the endoplasmic reticulum (ER) and the presence of the 23 amino acids, that act as N-terminal peptide are then cleaved in the ER lumen. Here, the immature prion protein is susceptible to many post-translational modifications, such as N-glycosylation at human residues N181 and N197, the formation of a disulfide bond at position C179 and C214 and cleavage of the C-terminal signal peptide and subsequent attachment of the glycosylphosphatidyl inositol (GPI) moiety at position 231 [31, 32]. In the co-translational translocation in the ER, PrP can be synthesized with three topologies in the ER. The secreted form of PrP that follows the traditional exocytic pathway to the cell surface, and two C- or N- terminal transmembrane forms, known as PrP^{Ctm} and PrP^{Ntm}, respectively, due to transmembrane insertion of the PrP hydrophobic domain (residues from 110 to 134) in the ER compartment [33, 34] (Figure 1).

The GPI-anchored form is derived from the secreted form, which is fully translocated in the ER and is trafficked in the Golgi apparatus. In the Golgi, further processing of the N-linked oligosaccharides results in modified glycosylation to include complex-type sugar chains. N-glycosylation of PrP^C is variable, resulting in un-, mono- and diglycosylated forms, depending on the number of glycosylation sites occupied with the oligosaccharide chains [35]. The lipid rafts are membrane domains with a high level of mature PrP^C. These membrane regions are detergent-resistant with many important cellular receptors and other GPI-anchored proteins [36]. Interestingly, the association of PrP^C with lipid rafts seems to be required for its correct folding, as cholesterol depletion leads to its misfolding [37-39].

PrP^C endocytosis occurs between the cell surface and endocytic compartments, in two possible ways: by clathrin-dependent pathway or mediated by caveolae -like domains.
From the cell surface, PrP^C can be endocytosed to internal endosomal compartments, delivered from early to late endosomes, and routed to lysosomes for degradation or recycled to the cell surface for ensuing cycles [40].

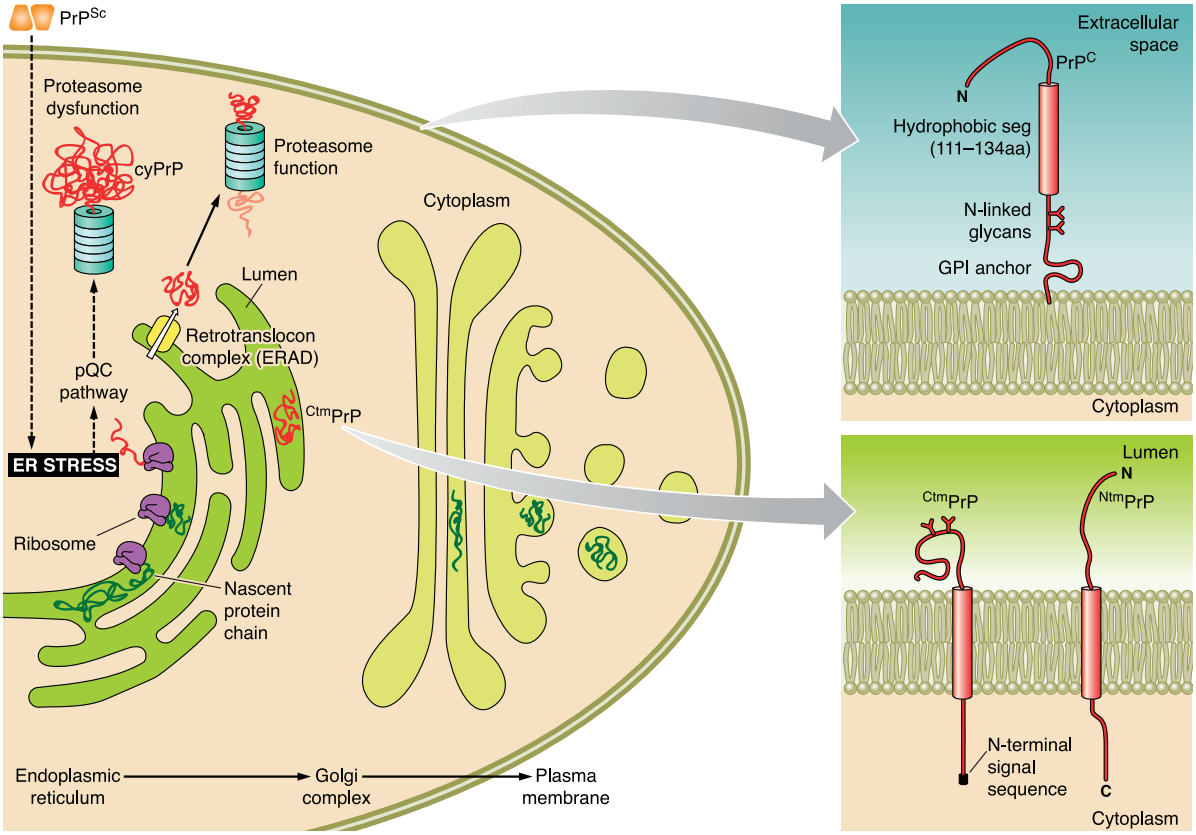

Figure 1. Biogenesis of PrP^C. PrP^C (green coils) is synthesized, folded, and glycosylated in the endoplasmic reticulum (ER), where the glycosylphosphatidylinositol (GPI) anchor is added, before further modification in the Golgi complex. Mature PrP^C translocates to the outer leaflet of the plasma membrane. Instead, PrP^{Ctm} and PrP^{Ntm} are unusual transmembrane forms, generated in the ER, which have their COOH or NH_2 terminus in the ER lumen, respectively (modified from [41]).

1.2.2 PrP structure

The human PrP (HuPrP) gene encodes a 253 amino acids long pre-pro-protein that is subsequently processed as mentioned before. In the mature form, the first 22 residues are cleaved after translation, whereas the last 23 amino acid residues are cleaved prior to the addition of the GPI anchor to Ser231 [42, 43]. The mature human PrP^C (HuPrP) is composed of 209 residues with a molecular weight of 35-36 kDa.

The majority of the structural data of PrP^C were obtained by using the bacterially expressed recombinant PrP (recPrP) as a model. Although recPrP is not subjected to post-translational modifications, it is structurally equivalent to the physiological PrP^C.

Atomic structure obtained by NMR [44-46] and X-ray crystallography studies [47, 48] showed that the full length PrP has a very specific structure: a well-defined C-terminal part and a flexible N-terminal domain. The globular C-terminal domain consists of three α-helices (aa

144-154 α_1, 173-194 α_2 and 200-228 α_3) and two antiparallel β-sheets (aa 128-131 β_1 and 161-164 β_2) siding the first α-helix (Figure 2). A third β-sheet strand has been recently identified and named β_0 [49, 50]. The α-helices have been shown to undergo a vast structural rearrangement into β-sheets in the pathogenic form. Indeed, in literature it is shown that, using a Fourier transform infrared spectroscopy (FTIR), the α-helix content of PrP^C passes from 48% to ~24% in the pathogenic form, while the β-sheet content increases from 8%, in the physiological condition, to ~50% in PrP^{Sc} form. The α_1 and α_2 are the bulk of the structure and are linked by the disulfide bond between two cysteine residues, Cys179 and Cys 214 [51, 52].

The N-terminal (aa 23-124) is the unstructured domain and because of the flexibility of the chain this domain may be divided into four different consecutive domains: a first charge cluster or CC1, the octapeptide repeat (OR), a second charge cluster or CC2, and a hydrophobic domain (HD). The OR is a series of four or five octapeptide repeat of eight amino acids (PHGGGWGQ). The OR repetitions have a high affinity for copper ions (Cu^{2+}) and a low affinity for other bivalent cations, for example Zn^{2+}, Fe^{2+}, Mn^{2+}, Ni^{2+}. Histidine and tryptophan residues were found to be essential for the coordination of copper and other bivalent metals, suggesting a role for PrP^C in regulating the homeostasis of these cations [53]. CC1 and CC2 (residues 23-27 and 95-110, respectively) seem to be involved in glycosaminoglycans (GAGs) [54, 55] and nucleic acids binding [56]. The CC1 region seems to be involved in recycling and internalizing PrP^C from the cell surface [57]. However, mice lacking CC1 or CC2 domains did not show pathologies and are susceptible to prion infection [58]. The HD is believed to play a role in the PrP^C function in concert with CC2. Indeed, ablation of CC2 in combination with a partial or complete deletion of HD causes severe pathologies in transgenic (Tg) mice, suffering from ataxia to cerebellar granule cell loss. While a partial deletion of HD is not toxic [59]. The HD contains the palindromic alanine-rich sequence AGAAAAGA, that lies within the so called "toxic peptide". It has been shown that peptides corresponding to the palindrome are important in the conversion of PrP^C to PrP^{Sc}; in fact, deletion of this region prevents conversion of PrP into the pathogenic form, and interferes with in vitro formation of protease-resistant PrP [52, 60, 61].

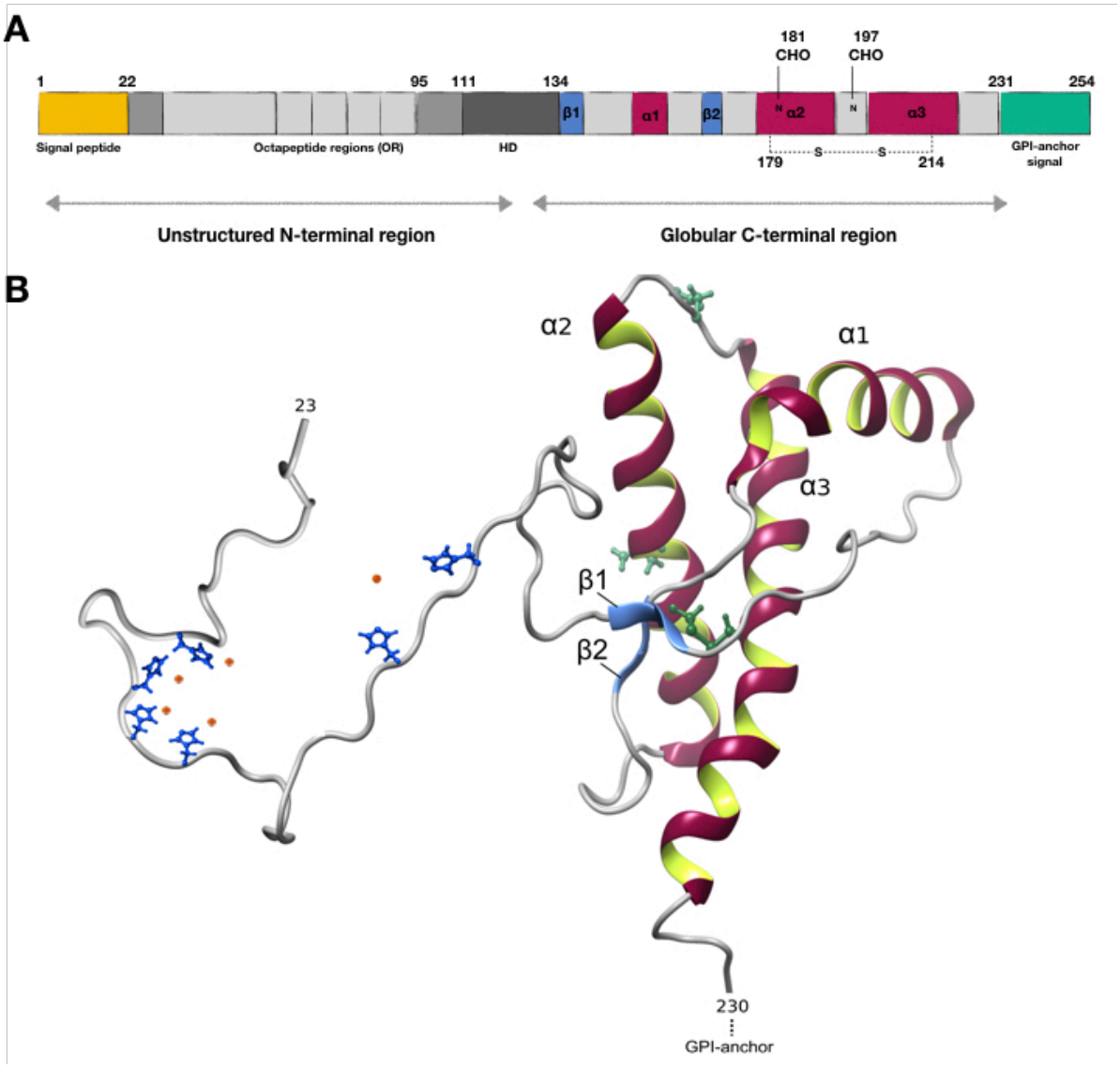

Figure 2. The structure of cellular prion protein. (**A**) Schematic illustration of primary PrP^C structure, including post- translational modifications. (**B**) Secondary structure of PrP^C. Histidine residues are highlighted in blue, copper ions in orange. The two cysteins of the disulfide bond are in light green, the two asparagines residues for N-glycosylation in dark green.

1.2.3 PrP^C physiological functions and distribution

Historically, the study of the PrP^C started simultaneously with the discover of TSEs, since from the beginning it was clear that the cellular prion protein was the counterpart of the PrP^{Sc}. A fully understanding of its physiological role has been lacking for a long time. To look at the localization of PrP^C is an important starting point to comprehend its biological functions.

1.2.3.1 Expression and localization

PrP^C is a cell surface protein, expressed in different tissues and organs, but more present at the level of CNS and PNS. Even in the brain, the amount of PrP^C varies from one region to another and from one cell to a different one, but in any case, the neurons are the cells where the PrP^C is mainly expressed, indicating that this protein has a singular significance in these cells. The higher concentration of PrP^C in the neuron is at the synapse level [62], but it is still under debate where exactly it is expressed, if at pre- or postsynaptic level or both [63].

Based on these findings, many studies report that PrP^C could have a crucial role in the synaptic maintenance, structure and function [64]. Likewise, appreciable amount of the cellular prion protein has been found in peripheral tissues, such as immune system, bone marrow and blood, indicating a different role also in these tissues [65].

It is also important to understand when the protein is expressed. In literature, different works can be found that have been studying the PrP^C presence in embryonic development. *Prnp* mRNA expression starts around the embryonic day 6.5 (E6.5) in extraembryonic tissues [66], E7.5 in the cardiac mesoderm [67] and E8 in the developing CNS [68, 69]. The involvement of PrP^C in neuronal differentiation is confirmed by its high expression in all the regions where neurogenesis occurs, such as the ventricular zone, hippocampus, thalamus and hypothalamus, thus explaining the possible involvement in neuronal differentiation [70]. In human adult brain, PrP^C is not only expressed in neurons, but it is consistently present in glia and endothelial cells of the blood-brain-barrier [71].

1.2.3.2 Knockout models

In the beginning of 1990s, many groups created *Prnp* knockout mice to assess the primary PrP^C function and to investigate whether the loss of this physiological function could bring to neurodegeneration in prion diseases.

In 1992, Büeler and his colleagues produced the first *Prnp* null mouse strain ($Prnp^{-/-}$), named Zurich I (ZrchI), mixing C57BL/6J x 129/Sv(ev) background, by replacing codon 4–187 with a

neomycin phosphotransferase expression (neo) cassette [72]. The second line of *Prnp* null mouse, the Npu or Edimburgh (Edbg) was generated by interruption of the *Prnp* ORF at position 93 and introduction of a neo cassette [66, 73]. These two lines of mice, in a first round of characterization did not present any developmental alterations, suggesting that normal PrP^C is not necessary for normal physiological functions in the mice strains, but they were resistant to prion infection, demonstrating that PrP^C is fundamental for developing TSEs [73].

In contrast with these first findings, Nagasaki (Ngsk) PrP^C-deficient mice, in which the entire *Prnp* gene was removed, develop ataxia and Purkinje cells degeneration. This phenotype, which is completely abolished by the reintroduction of PrP^C, was imputed to the loss of the protein [74, 75]. The same phenotype was observed in other two *Prnp* null mice strains, Rcm0 [76] and Zurich II [77]. Later it was demonstrated by several groups that the presence of this phenotype was due to the upregulation of Doppel (Dpl), a protein expressed in testes and encoded by the gene *Prnd*, located 16 kb downstream *Prnp*, which generally is not expressed in the brain [76, 78]. Thus, showing that only the ectopic expression of Dpl, rather than the absence of PrP^C, was the cause of the neurodegeneration observed, precludes an association of these differences with the lack of PrP^C expression.

Although ZrchI and Edbg mice did not present any obvious physiological abnormalities, these mice lines provided a platform for experiments aimed at gaining further insight on the role of PrP^C in the context of behaviour, sleep-wakefulness cycle, memory, synaptic activity and neuronal excitability.

1.2.3.3 Role of PrP^C at the synaptic level

As mentioned above, the cellular prion protein in highly expressed in both neurons and glial cells. In neurons, PrP^C is mainly localized in pre- and post- synaptic compartments. Immunocytochemical studies showed that PrP^C is enriched along axons and in pre- and postsynaptic terminals [79] and that it undergoes anterograde and retrograde axonal transport. Recently, it has been shown that sialic acid within GPI-anchor is important for targeting PrP^C to synapses [80]. These observations suggest a role of PrP in preserving normal synaptic structure and function by regulating synaptic transmission plasticity; indeed, synaptic dysfunction and synaptic loss are early events in prion diseases.

The long-term potentiation (LTP), that is correlated with synaptic plasticity and so with learning and memory formation, is affected by the presence of PrP^C. Indeed, some studies report deficiencies in spatial learning and memory in PrP^C-deficient mice. Interestingly, these results are in contrast with a work carried out in *Prnp* ZH1/ZH1 mice that did not show any

memory impairment. Thus, the role of the cellular prion protein in memory and learning has not been established yet [81].

Another important activity that has been related to the synaptic PrP^C is the sleep homeostasis and the sleep continuity. A study from 1996 conducted by Manson's group revealed that *Prnp*$^{ZH1/ZH1}$ and co-isogenic *Prnp*$^{Edbg/Edbg}$ mice display altered circadian rhythms, increased sleep fragmentation, and increased slow wave activity (SWA) following sleep deprivation [82]. These findings explain the typical symptoms that occur during different prion diseases such as the sporadic [83] and fatal familial insomnia [84], where this phenotype is completely rescued by the reintroduction of PrP^C expression [85]. However, the molecular mechanism of sleep regulation activity of PrP^C is still not understood; even if a recent study claims that the calcium-dependent hyperpolarization is critical to sleep duration, and that sleep deterioration is associated with impairment of calcium-dependent potassium channels, voltage-gated calcium channel (VGCC) and N-methyl-D-aspartate (NMDA) glutamate receptors, which are activated by S-nitrosylation mediated by PrP^C and copper ions [50, 86].

1.2.3.4 Interaction of PrP^C with other proteins

The cellular prion protein interacts with several different proteins, that have been identified and analyzed to better understand the PrP^C functions.

STI1 is a heat shock protein characterized in a macromolecular complex with Hsp70 and Hsp90 chaperone family protein, that are localized in the cytoplasm and a small part at the cell membrane, where it seems to bind PrP^C [87]. The interaction between STI1 and PrPC induces neuroprotective signals that rescue cells from apoptosis *via* cAMP/protein kinase A and the Erk signaling pathways [88].

LRP is another cell surface PrP^C ligand. This protein mediates the internalization of the cellular prion protein and directs the complex through clathrin coated pits. LRP was suggested to act as a putative PrP^C receptor because it was shown to co-localize with PrP^C on the surface of both N2a and baby hamster kidney cells [89].

PrP^C has also been identified in a complex with NCAM, which is the neuronal cell adhesion molecule. This complex mediates a signaling cascade involving the p59fyn, inducing the neurite outgrowth and neuronal survival [90, 91].

The PrP^C is involved in many other physiological activities, such as the regulation of copper concentration at the synaptic level [92], protection against oxidative stress [59, 93], secretion of exosomes [94], and many others that are not cited here (Table 3). So, it seems that the cellular

prion protein is fundamental for myriads of functions, but at the same time appears to be dispensable for the development. Achieving a complete picture of PrP^C biological functions is crucial for the development of drugs able to restore PrP^C activity in prion diseases and other pathological settings.

Role of PrP^C	Phenotype of Prnp-/- model system
Synaptic transmission and plasticity	-Reduced long-term potentiation -Reduced excitatory and inhibitory synaptic transmission
Memory formation	-Reduced spatial learning and memory -Reduced avoidance learning and memory
Stabilization of sleep and circadian rhythm	-Altered circadian rhythm, increased sleep fragmentation, increased SWA after sleep deprivation
Neuronal excitability	-Reduced Kv4.2 currents -Reduced sAHP and calcium-activated potassium currents
Calcium homeostasis	-Reduced VGCC currents -Increased calcium buffering
Glutamate receptor function	-Upregulation of Kainate receptor subunits -Increased NMDA currents, nociception and depressive-like behavior
Neurite outgrowth	-Reduced neurite outgrowth in vitro -Delayed development of cerebellar circuitry
Toxicity elicited by oligomeric species	-Protected from LTP reduction induced by toxic Aβ species
Neuroprotection	-Larger lesions in model of acute cerebral ischemia
Copper, zinc, iron, and lactate metabolism	-Reduced zinc content in primary neurons -Increased lactate-uptake in cultured astrocytes
Peripheral myelin maintenance	-Age-dependent demyelinating neuropathy

Table 3. Physiological roles of cellular prion protein [81].

1.3 PrP^{Sc}: the infectious agent

PrP^{Sc} is the alternative and misfolded isoform of the PrP^C. This abnormal conformation of the prion protein accumulates and forms deposits around neurons. The common feature of all prion diseases is the presence of PrP^{Sc} aggregates. For a long period, it has been thought that the scrapie prion protein was the only misfolded protein that could be transmitted, but in the last decades many different studies showed the transmission of the other misfolded proteins, such as amyloid Aβ [95], tau [96] and α-synuclein [97].

The conversion process is associated with conformational changes of the secondary structure from α-helices to β-sheets. Indeed, when the conformational change occurs, PrP^{C} switches from a structure composed by 45% α-helices and a few β-sheets (~3%), to a form with 30% α-helices and 45% β-sheets [98]. With this composition, the PrP^{Sc} aggregates are partially resistant to protease K digestion, in fact, limited protease digestion of PrP^{Sc} produces a smaller, protease-resistant molecule of approximately 142 amino acids, referred to as PrP 27–30 (PrP^{res}) while PrP^{C} gets entirely degraded (Figure 3). Protease K is the common method to distinguish PrP^{Sc} from PrP^{C}, by means of Western blot technique and although resistance to limited proteolysis has proved to be a convenient tool for detecting PrP^{Sc}, not all PrP^{Sc} molecules are resistant to protease digestion [98, 99]. These protease-sensitive PrP^{Sc} forms are denoted $sPrP^{Sc}$ [100, 101]. Furthermore, PrP^{Sc} from different species or prion strains may show different degrees of protease resistance.

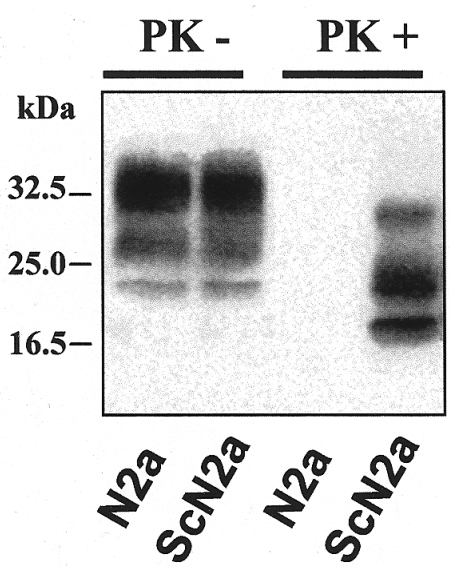

Figure 3. Detection of PrP^{Sc} in prion infected and uninfected cells. Western blot. Lysates of N2a or prion-infected N2a cells (ScN2a) were treated with proteinase K and analysed by SDS-PAGE and Western blotting with anti-PrP antibody [102].

1.3.1 Prion strains and species barrier

The prion strain phenomenon is another unique feature of TSEs respect to the other neurodegenerative disorders. It has been observed that animals affected by prion diseases can develop different pathologies and that the clinical and biochemical outcomes could be maintained through several passages in rodent's models of prion diseases. Similar to other infectious agents, these variants have been termed "strains". Due to the fact that prions are

composed only of proteins and replicate using the PrP^{C} substrate present in the host, differences in prion strains cannot be attributed to genetic variability, which accounts for the existence of viral strains. Rather, prion strains arise from conformational variability, because PrP can assume several different, self-propagating conformations, each of which enciphers a distinct prion strain. However, currently it is widely accepted that the main differences between prion strains arise from alternative conformations of PrP^{Sc} that can be stably and faithfully propagated [103, 104]. The differences in these conformations result in differences in resistance to PK digestion and electrophoretic mobility after PK digestion [105-107], varying glycosylation patterns [108], sedimentation velocities and resistance to urea and guanidinium hydrochloride denaturation [109]. Also, recent studies with synthetic prions support this theory [99, 110].

The transmissibility of PrP^{Sc} between mammalian species is another really important feature of this infectious agent. But, the transmission is limited by the so called “species barrier” [111]. The phenomenon refers to the difficulty to transmit the infectious prion agent from one specie to another, and can be characterized by extended incubation times, but if prions are then re-isolated from the recipient host and re-transmitted to another host of the recipient species, the incubation period decreases and the prions are “adapted” [112]. (One of the causes for the species barrier are the sequences of the potential prion proteins of the two species.) In 1939, the first experimental transmission of TSE between species was carried out with scrapie between sheep and goats, showing 100% susceptibility, demonstrating that goats are highly susceptible. Then, further experiments were performed with other species to test their susceptibility to TSEs. The results demonstrated that some animals have a very low susceptibility to prion infections (i.e. rabbits and guinea pigs) [113], in contrast to other species, which are unusually susceptible (i.e. hamsters and bank voles) [114].

In the last decades, this topic has been a subject of great interest because of the epidemic of BSE in cattle. BSE is the only example of TSE agent transmission to humans from another specie. It is thought that the source of BSE infection in the United Kingdom was sheep scrapie contamination resulting from the practice of feeding cattle with rendered sources of mammalian ruminant protein, such as meat and bone meal, derived from the offal of cattle, sheep, and pigs as a high-protein nutritional additive. Overall, more than a million cattle are thought to have been infected and after some years of this epidemic a new form of CJD, called variant CJD (vCJD) emerged [106]. Many studies demonstrated the hypothesis that vCJD emanated from BSE in cattle, but just a small portion considering the 60 million people and all visitors present in Britain during the peak of BSE epidemic. Indeed, just around 170 cases of vCJD have been

documented since 1996 and now the epidemic has stopped, thus demonstrating the poor transmissibility of BSE to humans by ingestion [115]. Nowadays, the scientific community is alerted by another TSE epidemic, the CWD in cervids, that is continuously spreading not only in the North America [116, 117] and Canada [118], where the cervids meat is commonly used as food [119], but even in Europe [120] and a single case in South Korea [121]. Several laboratories are now studying whether the species barrier exists in this case, and recently Race showed that the cynomolgous macaques are immune to intracerebral and oral CWD infection [122].

1.3.2 Conformational conversion of PrP^{C} to PrP^{Sc}

According to the protein-only hypothesis, the central molecular event in the replication of prions is the self-propagating conversion of PrP^{C} to PrP^{Sc}, but unfortunately the mechanism remains subject of debate. It is thought that PrP^{C} binds PrP^{Sc} forming an intermediate complex before forming new PrP^{Sc}.

Once prions enter an organism, an exponential replication process begins generating more and more PrP^{Sc} particles. When a critical threshold level of particles is reached, animals show clinical symptoms of neurologic dysfunction and then die [123]. The time between inoculation and the appearance of clinical signs is denominated incubation time.

There are two models to explain the conformational conversion of PrP^{C} to PrP^{Sc}, the "refolding" and the "seeding" models.

- In the "refolding" model or template assistance model, PrP^{Sc} has an instructive role towards PrP^{C}. There is an interaction between the exogenous PrP^{Sc} and the endogenous PrP^{C} and the products of this reaction are new molecules of endogenous PrP^{Sc}, which can transform other endogenous cellular prions in the scrapie isoform with a consequential propagation and aggregation. A high energy barrier can prevent the spontaneous conversion (Figure 4) [123]. This model is supported by spectroscopy at high pressure [124] and changes between hydrogen-deuterium studies [125].
- The “seeding” model, also known as seeded nucleation model, suggests that PrP^{Sc} can be physiologically present in the organism. The two forms are in a reversible equilibrium, but the PrP^{C} isoform is thermodynamically favored. Only when several molecules of PrP^{Sc} are aggregated (into oligomeric or fibril-like seeds), the replication can start. In this case, the seed recruits other monomeric PrP^{Sc} molecules and stabilizes

them, thus creating the amyloid. The fragmentation of aggregates increases the number of nuclei, which can recruit further PrP^{Sc} with an acceleration of the process, thus resulting in apparent replication of the agent [41].

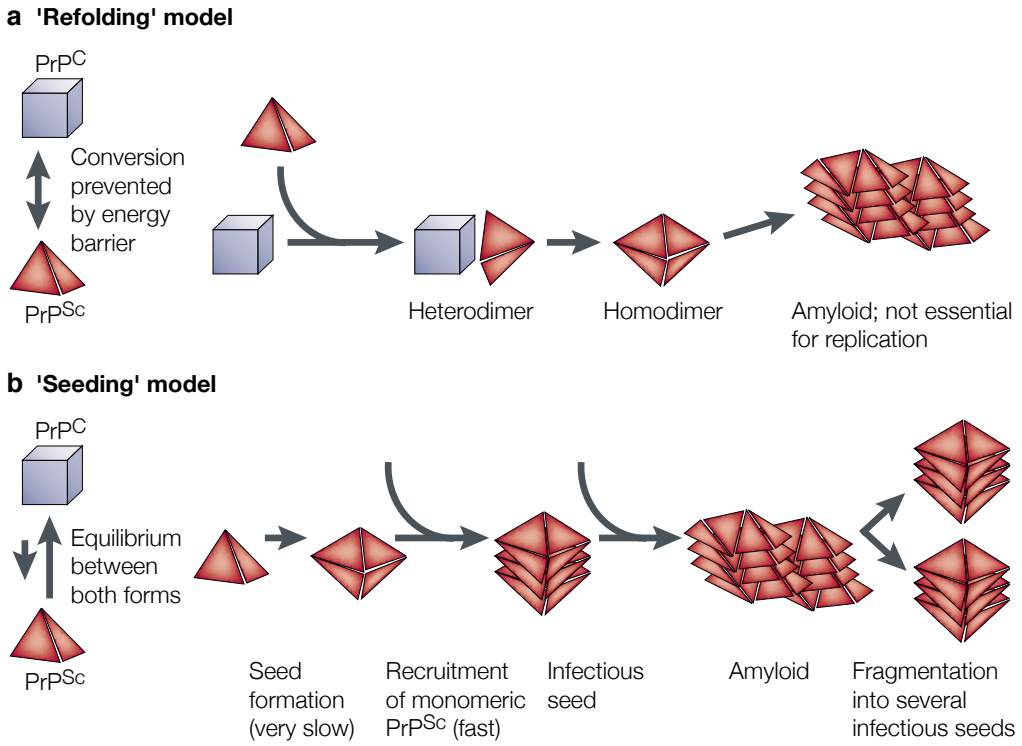

Figure 4. The protein-only hypothesis and the two models for the conformational conversion of PrP^{C} into PrP^{Sc}. (a) The refolding model. (b) The seeding model. [126].

These models do not exclude each other, rather they are relevant to any types of diseases:

- in the genetic type, the *PRNP* mutation leads PrP^{C} to change spontaneously its tertiary conformation or the mutation can decrease the energy barrier between PrP^{C} and PrP^{Sc}, thus facilitating and accelerating PrP^{Sc} aggregation;
- in the infective type, the ingestion of PrP^{Sc} can directly convert endogenous molecules of PrP^{C};
- in the sporadic form, the unknown biochemical modifications can change tertiary structure and promote the conversion in PrP^{Sc}.

PrP^{C} is generally localized in lipid rafts onto the plasmatic membrane. There are two proposed conversion sites of PrP^{C} into PrP^{Sc}: the cell surface or the endosomes. In ScN2a cells, particularly, PrP^{Sc} aggregates in endosomes and lysosomes, while a small amount is converted on the cell surface [127]. The PrP^{Sc} that is formed in the endosomes aggregates and causes the impairment of the proteasome, while the cellular surface PrP^{Sc} creates extracellular oligomers, fibrils and then amyloid plaques. Both, the extracellular and the intracellular PrP^{Sc} promote

neurotoxicity [128, 129].

The literature points to the presence of cellular co-factors in prion replication. These factors are present only in mammals, not in bacteria, yeast or flies. They are mainly referred to as "protein X", but there is no evidence for the nature of this factor. Many *in vitro* studies suggest that different molecules, such as RNA, may be involved in this mechanism [36]. Five scenarios are proposed to explain the cofactor rules in prion conversion:

1. The cofactors bind the infective agent and promote PrP^{Sc} aggregation.
2. The cofactors act as catalysts and favor PrP^{C} to initiate PrP^{Sc} conversion.
3. The cofactors only stabilize the PrP^{Sc} conformation.
4. The cofactors promote the fragmentation of PrP^{Sc} in small seeds, which allows for prion replication.
5. The cofactors bind PrP^{Sc}, decreasing its clearance in vitro.

Therapies that target these factors could be effective in blocking prion replication [1].

It is important to keep in mind that these co-factors can help the replication, but they are not crucial for the prion replication. Indeed, the final proofs for the “protein-only hypothesis” have been provided by:

- the first PrP knockout transgenic mice models [72]. These mice develop normally in the absence of PrP and are resistant to prion infection [130].

- techniques able to mimic the prion conversion and replication *in vitro*: the protein misfolding amplification technique (PMCA) [131], amyloid seeding assay (ASA) [132] and Real Time Quaking Induced Conversion (RTQuIC) [133], that will be dealt with here.

1.3.3 Prion infectivity and neuroinvasion in humans

As mentioned above, the media and the scientists have devoted particular attention to the infectious TSEs, because of the epidemic of BSE in the United Kingdom and its capability to cross the species barrier and infect humans, but unfortunately the route of infection is still poorly known.

In transmission experiments, there are different possible routes of infections, due to different routes of prion inoculation:

- Intracerebrally, in which prions replicate directly in the brain, where PrP^{C} expression level is higher [134]. However, this is not what happens in nature.

- Intraocularly, that can occur both in animal experiments [135], either in iCJD patients [136], these cases were caused by the transplant of prion-contaminated corneal grafts.
- Intravenously [137], with less efficiency than intracerebral injection [138]. Accidental prion transmission via this pathway was long underestimated due to the low presence of prions in human blood. However, reports exist of vCJD cases due to blood transfusion [139].
- Intraperitoneally [137]

In acquired prion diseases, Kuru, vCJD, BSE, TME, the most common route of infection is due to oral exposure of PrP^{Sc} contaminated food (Table 4).

After an oral infection, prions can be found in Peyer's patches in the gut, then the prion propagation continues into splenic lymphoid tissue and/or in gut-associated lymphoid tissue (GALT, which includes tonsils), resulting in prion transport by splenic innervation to the brainstem and spinal cord [140, 141].

The route of infection is defined by three phases:

1. In the first phase, after ingestion, there is the PrP^{Sc} invasion of the gut-associated lymphoid tissues (GALT). The incorporation of PrP^{Sc} into the intestine is mediated by a Fc receptor (nFcR), which contributes to the uptake of maternal antibodies into the intestine [142]. Another study demonstrated that the iron binding protein ferritin forms a complex with a fragment PrP^{Sc} to enhance the transport of PrP^{Sc} in an intestinal endothelial cell model, suggesting a role for ferritin in transport of infected prion protein across the intestine [143].

2. After incubation in lymphoid tissues such as GALT and spleen, the PrP^{Sc} spreads to the CNS via the enteric nervous system. This invasion occurs in the retrograde direction along efferent fibers of both sympathetic and parasympathetic nerves.

3. The final phase is the infection of the spinal cord and brain leading to a characteristic spongiform degeneration and astroglial activation.

The natural horizontal transmission is another way of prion infection, typical for some TSEs such as scrapie or CWDs. This transmission is maintained within their animal population through their persistence in the environment. It was believed that this transmission route was caused by prion excretion because of the important role played by lymphoid tissues in prion dissemination and pathogenesis [144]. Prions should spread from lymphoid tissue to other tissues and be secreted in placenta, saliva, urine, and feces into the environment [145, 146]. But it is also known that, the lymphoid tissue has a minor role in the pathogenesis of BSE in cattle and BSE prions are mostly confined to the central nervous system [147, 148]. While, BSE prions in sheep accumulate mainly in the lymphoid organs [149]. It is not known why some

prion strains are capable of such dissemination outside the central nervous system while others remain in the brain even if elicited by oral challenge but it seems to be a consequence of complex prion strain–host interactions [150].

Infection route	Source of prions	Prion diseases	Several animal models
Intracerebral	Experimental	Several TSEs	Several animal models
	Prion-contaminated neurosurgery material, electrode probes, and dura mater grafts	iCJD	Human
Oral	Prion-contaminated food products	Kuru, vCJD, BSE, TME	Human, cattle, mink
Ocular	Experimental	Several TSEs	Several animal models
	Prion-contaminated corneal grafts	iCJD	Human
Intravenous	Experimental	Several TSEs	Several animal models
	Prion-contaminated blood products	vCJD	Human
Horizontal transmission	Environmental contamination	Scrapie, CWD	Sheep, goat, cervid species

Table 4. Summary of Prion Infection Routes and Corresponding Prion Diseases [150]

1.4 Diagnosis

As mentioned above, prion diseases are illnesses that affect the CNS. For all the neurodegenerative pathologies, the diagnosis is based mainly on clinical examination and the diseases are considered possible depending whether the clinical symptoms fit the standard guidelines [151], because the most reliable technique is the immunohistochemical detection of brain tissue. This is due to the fact that each neurodegenerative disease has a very specific neuropathological feature. For example, an AD brain contains amyloid plaques, neurofibrillary tangles, dystrophic neurites containing hyperphosphorylated tau, that are accompanied by astrogliosis and microglial cell activation [152]; PD is characterized by neuronal inclusions composed of α-synuclein, called Lewy bodies, that lead to a loss of dopaminergic neurons of the substantia nigra that project to the putamen [153]; and CJDs are associated with presence of prion deposits, spongiform degeneration and a strong astrogliosis [154].

1.4.1 Diagnostic Tests

The definitive diagnosis can only be made post-mortem by brain histological analysis or by brain biopsy. Although brain biopsy has been used to establish a definitive diagnosis, it is strongly discouraged because it is invasive, costly and can lead to brain injury and other side effects. Recently, some less invasive biopsy options were evaluated, such as the use of olfactory mucosa and skeletal muscle, but in the end, they were not validated or adopted [155]. It is also known that PrP^{Sc} of vCJD, but not from sCJD patients, could be detected in tonsils [156]. The main technique used to detect the presence of prions in the tissue taken from the brain biopsy is PK treatment followed by a Western blot analysis.

The electroencephalography (EEG) has been used to diagnose CJDs since 1954. Periodic sharp wave complexes are the hallmark EEG finding in patients with CJD and are thus very helpful to substantiate the clinical diagnosis of suspected CJD. The EEG is useful to detect patients with sCJD, because very specific bilateral alpha activity with irregular theta, delta, and intermittent high amplitude rhythmic delta waves were found during the early stages of sCJD [157]. But the pattern just mentioned could change for different sCJD subtypes and is also present only in the sporadic form of CJD, for instance, in vCJD patients the EEG does not present the specific wave. In addition, this technique has a low sensitivity causing false positives [158] and can bring to a diagnosis of AD [159, 160].

Another non-invasive technique used to diagnose prion diseases in humans is the magnetic resonance imaging (MRI). Despite the increasing use of MRI, it is generally accepted that imaging technologies are used mainly to exclude other causes of pathology [161], because also in this case characteristic changes in MRI features are different for each prion diseases. Indeed, MRI is useful to discriminate between vCJD and sCJD, changes in the nucleus caudatus are usually seen in sCJD, while most changes are observed in the posterior thalamus [162] and the bilateral pulvinar in vCJD [163]. It is important also to specify that in sCJD changes are observed mainly using diffusion-weighted images (DWI), while in vCJD using fluid-attenuated inversion recovery (FLAIR) [164], where the sensitivity and specificity based on objective criteria are at approximately 80% [165]. The limitation of MRI on CJD diagnosis is associated with the interpretation, skill, and expertise of clinicians. The MRI features associated with CJD, especially in its early stages, may not be detected by a clinician or a radiologist as opposed to an experienced neuro-radiologist or a prion disease specialist. Thus, diagnoses may be missed, delaying further investigation. This suggests that even if an initial MRI is regarded as normal, a specialized review should still be carefully considered.

An increase of many neuronal and astroglial proteins during the TSEs have been identified [166]. For example, in the cerebral spinal fluid (CSF) of sCJD patients the level of the proteins S-100 [167] and neuron-specific isoenzyme [168] are markedly spread. The 14-3-3 protein is mostly used as a neuronal death marker to help with the diagnosis of sCJD and fCJD [169], but it is absent in the CSF of patients with GSS and FFI. As the 14-3-3 protein might be elevated in the cerebrospinal fluid of patients with other neurological illnesses, the usefulness of this test depends on the exclusion of other pathologies [151].

It is evident that there is still not an efficient and completely reliable diagnostic test for TSEs, so the clinicians make the diagnosis combing the use of these techniques, and the recognition of the specific clinical symptoms. The sCJD patients are mainly affected by a combination of rapidly progressive multifocal dementia with pyramidal and extrapyramidal signs, and visual or cerebellar signs [161]. vCJD appears initially as a progressive neuropsychiatric disorder characterized by symptoms of anxiety, depression, apathy, withdrawal and delusions [170]. While GSS is characterized by dementia, Parkinsonian symptoms and a relatively long duration (5–8 years) [171]. Symptomatically, the GSS is similar to AD, but in GSS ataxia and seizures are really common. In all the inherited prion diseases, the diagnosis is established by genetic screening for prion mutations.

1.4.2 The need of a pre-symptomatic diagnosis

Pre-symptomatic detection of CDJs in live patients is so far, not possible, but it is extremely important for different reasons:

- To develop an efficient anti-prion therapy. It is known that when people start to have symptoms in all the neurodegenerative diseases, the brain alterations and impairments are extensive and irreversible. This is also evident from the animal models data, several compounds can delay the onset of the disease and increase the survival time, but none of them has shown a significant effect when the treatment was started at the symptomatic stage [126].
- To assess the possibility of people incubating the disease. This necessary started with the BSE epidemic and then with the appearance of vCJD. In order to completely stop the epidemic, it could be important to have tests able to detect bovine that are incubating the disease at the symptomatic stage, because it is possible that infected animals that do not show the clinical signs of BSE and that give a negative result using

the available biochemical tests are still entering the food chain and presenting a serious risk to human health [172]. Also, the iCJD transmission is born by corneal transplants, implantation of electrodes in the brain, dura mater grafts, contaminated surgical instruments and treatment with human growth hormone derived from cadaveric pituitaries of people with sCJD [173].

1.4.3 New approaches: PrP^{Sc} amplification

Recently, two techniques able to mimic the prion conversion *in vitro* and to amplify the PrP^{Sc} have been developed: the protein misfolding cyclic amplification (PMCA) and the Real-Time Quacking-Induced Conversion (RT-QuIC). These techniques can detect and promote the amplification of a very low amount of PrP^{Sc} present in a several types of samples, such as brain homogenates, blood, urine and olfactory mucosa.

1.4.3.1 PMCA

In 2001 Soborio et al. developed a system able to mimic *in vitro* the PrP^{Sc} conversion process that takes place *in vivo*, and that amplifies in an exponential fashion minute quantities of PrP^{Sc} present in a sample, based on the nucleation/polymerization model [131]. Basically, it consists of the incubation of a large excess of PrP^{C} from a healthy brain homogenate (usually 10^{-10} dilution factor) with PrP^{Sc} derived from TSEs infected sample. In each cycle, there are two different phases present. In the first one, the sample that contains a low amount of PrP^{Sc} and an excess of PrP^{C} is incubated to promote growing of PrP^{Sc} aggregates. While during the second phase, the sample is sonicated in order to break the PrP^{Sc} polymers, increasing the number of nuclei (or seeds) (Figure 5). It follows that, as it happens for the DNA in PCR, if the cycles are more than one, the number of seeds increases in an exponential fashion. So, one round of 144 PMCA cycles leads to a 6000-fold increase of sensitivity of detection, whereas 2 and 7 rounds of successive PMCA result in 10 million and 3 billion folds amplification [174]. It has been shown that PMCA is able to detect and amplify a single molecule of PrP^{Sc}. The presence of newly generated PrP^{Sc} has been confirmed by different biochemical assay, such as the resistance to PK digestion or insolubility in non-ionic detergents.

This assay was developed using animal models of TSEs (infected mice [175], hamster [151], cattle[176] and cervids [177]).

But recently, PMCA has been studied as a possible diagnostic tool to detect prions in many different human tissues, such as blood in patients with vCJD [178], the olfactory mucosa (OM) of FFI individuals [179], urine in vCJD [180] and also plasma in symptomatic and pre-symptomatic vCJD patients [181]. In all these tissues and prion diseases, the efficiency of PMCA to detect PrP^{Sc} is extremely high. So, it is probable that soon this technique will be introduced as a usual diagnostic test for human and animal TSEs.

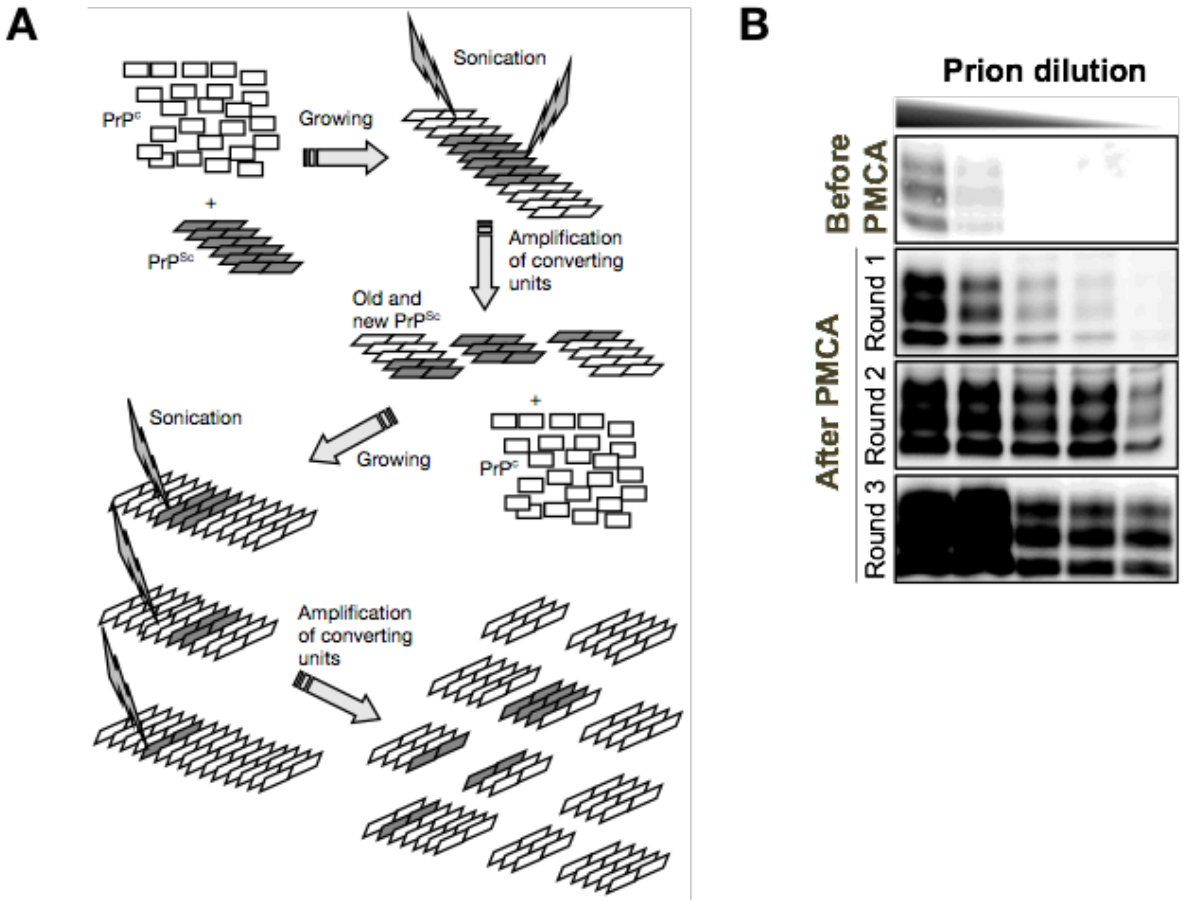

Figure 5. PMCA (A) Representation of PMCA procedure**.** [131] (**B**) Amplification of PrP^{Sc} detected by Western blot [182].

1.4.3.2 RT-QuIC

The RT-QuIC assay was illustrated by Atarshi and collegues in 2008 [183], then it was applied for human [184] and animal [185] diagnostic purpose. In this assay, the test samples, which can or cannot contain prions, are added and mixed to a large excess of recombinant PrP. The readout is based on 96-well plate format, where the seeds of PrP^{Sc} bind the PrP^{C} monomer inducing their conformational conversion into amyloid fibrils. The fibrils are bound to

florescent Thioflavin-T dye (ThT), a compound known to stick all the β-sheet enriched aggregated molecules. The eventual increase of fluorescence is read by a shaking fluorescence plate reader. This method is extraordinarily efficient, leading to billion- to trillion-fold seed amplifications. As a result, attograms (1^{-18} grams) of PrP^{Sc}, which are approximately 10–40 particles, can be detected [186, 187]. Analogous to end-point dilution titrations classically used in animal bioassays but with greatly reduced times and costs.

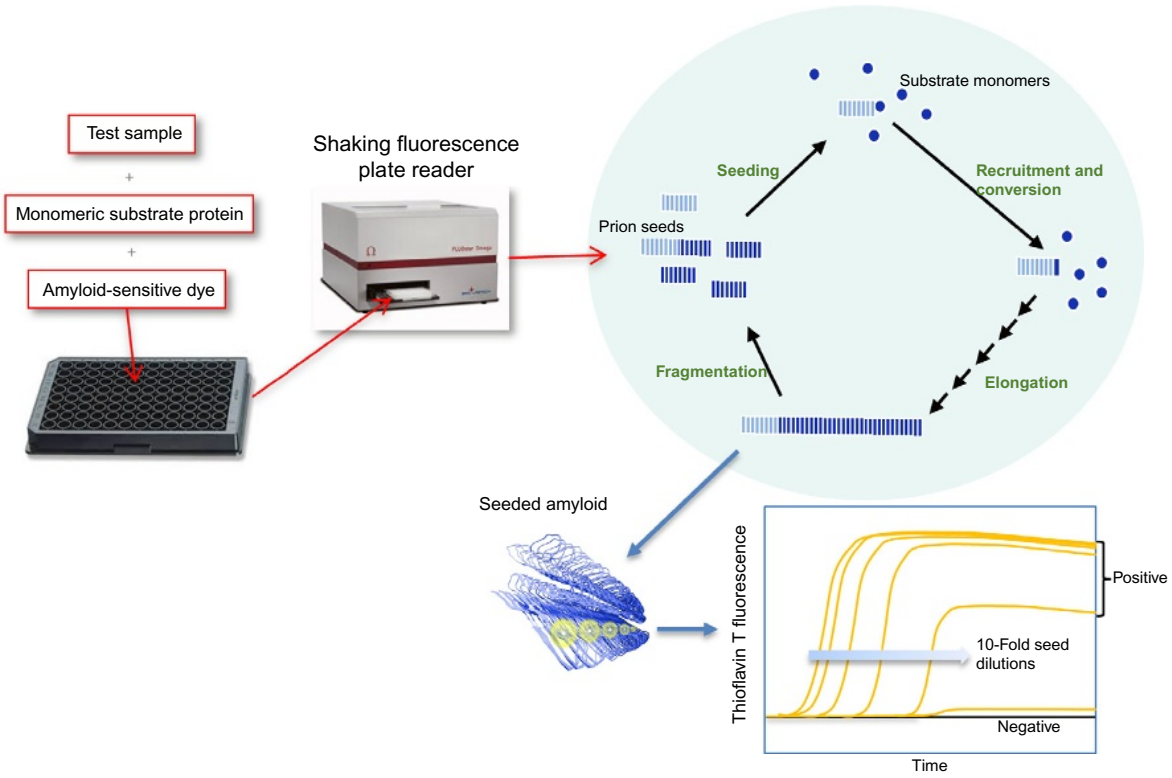

Figure 6. The basis of RT-QuIC amplification. (Modified from [188])

Many studies conducted by different groups showed the possible use of RT-QuIC as a tool for ante-mortem diagnosis for human TSEs. Indeed, the ability of RT-QuIC to detect prions in the cerebral spinal fluid of patients with sCJD has been demonstrated [184]. Another important work is the one published by Zanusso and colleagues, where they detected prions in the CJD OM. The tissue is collected by a gentle brushing in the upper nasal cavity using flexible flocked swabs, without any kind of discomfort for the patients and a complete recovery of blood cells [189, 190].

This technique can also be used to detect prion diseases in many animals, such as BSE in cattle [191], scrapie in sheep [185], CWD in cervids [192, 193].

Recently, the use of RT-QuIC has been expanded to the therapeutic application. It is possible to control the efficacy of a treatment in a noninvasive way (OM samples) during a clinical trial.

It is also possible to perform a prescreening of compounds to check if they are able to block the PrP^C conversion just by adding the tested compounds in the 96-well plates [194].

1.5 Therapeutic approaches

The importance to diagnose TSEs before the symptoms is fundamental to develop an appropriate treatment. It is known that the appearance of symptoms corresponds to an irreversible impairment of the brain, due to the presence of amyloid plaques, spongiosis and a strong astrogliosis. Indeed, there is still no therapy to cure human prion diseases. Since TSEs were discovered, efforts have been made to cure or at least modify the course of these disorders, but unfortunately the scientific community collected just failures and frustrations [195]. Before 2010 the interest in this field was limited, but there was a change with the publications of several studies proving a prion-like mechanism for all the neurodegenerative misfolding disorders. They proposed prion diseases as a prototype of neurodegenerative diseases, because there is evidence that not only the prion protein, but also other proteins such as Aβ, α-synuclein and tau are able to aggregate and spread in AD and PD [97, 196]. This commonality is not irrelevant as it allows drug discovery progresses in such rare diseases with low public health priority and visibility. But also involving other neurodegenerative diseases the situation does not change much. For instance, the Food Drug Administration (FDA) has not approved any new treatment for these disorders since 2003, and from 2002 to 2012, 244 compounds were evaluated in 413 trials for AD, but just 1 (Memantine) was approved for marketing [195]. So, it seems that in any case, the research for new possible drugs in the neurodegenerative field is a challenge.

There are different reasons for this difficulty:

- The lack of a specific diagnostic tool. As it is mentioned before, the late administration of a drug candidate leads directly to its failure [197].
- The lack of a validated target. These pathologies are not yet completely understood, so use as a target just the protein of interest is probable not enough [198].
- The blood-brain barrier (BBB) crossing. All the compounds directed to CNS need to cross the BBB to reach the brain, the cross efficacy has to be very high, so that the compounds have to arrive in a sufficient concentration to achieve their biological activity.
- The treatment must be no toxic also for a long period.

1.5.1 Clinical trials in human TSEs

The term “clinical trials” indicates biomedical and behavioral research studies to explore if a medical intervention is safe and effective on human patients. The medical interventions consist of new or repurposed drugs, psychological therapy, surgery or dietary choices [199].

In the neurodegenerative diseases, clinical trials include two types of goals: “cure” the disease in the most optimistic situation or improve the patient’s lifestyle, by improving a specific symptom or disability.

In prion diseases, no compound specifically designed for these disorders has been tested in clinical trials. There are different reasons that can explain this situation. The first one is that the prion diseases are a very rare illness and the costs for a clinical trial is very high, so finding a way to cover the expenses is not that easy. The rapidity of disease progression (for sCJD is around 4-6 months) is not helping too, the diagnosis and the referral to specialist centers are typically made late in the clinical course when patients have advanced disability, and the priority is palliative care. Since 1971, fourteen clinical trials have been tried, the majority of them are antivirals, antimalaria and antifungals [197].

The first compound used in TSEs clinical trials was the Amantadine. Amantadine is an antiviral molecule. It is not a case that it was tested prion diseases, because TSEs were initially considered as slow viral illnesses. Two studies were published regarding the treatment with Amantadine on CDJ patients during 1983 and 1984. In both cases the molecule did not show any kind of anti-prion activity, because there was no statistical increase of survival time between the treated patients and the controls [200, 201].

In the same period a nucleoside analog was used to treat CJD patients, the Acyclovir. Unfortunately, also in this case the treatment resulted to be unsuccessful [202, 203].

Similar negative results were obtained using other two antiviral molecule: interferon [204], that is a signaling protein known to induce a nonspecific resistance to viral infection, and the vidarabine [205], a nucleoside analog able to bind and interfere with the synthesis of viruses.

So, all the treatments with antivirals were negative and ineffective.

Amphotericin B was the first antibiotic tested. This compound was previously used in two animal models: hamsters infected with 263K strain and CJD monkeys [206]. In both cases a significant increase of survival time was documented. Thus, in 1992 Masullo et al. decided to use this molecule to treat two CJD patients, but after 8-10 months the clinical situation of the patients worsened and they died [207].

In 2001 the synergistic activity of an antidepressant (Clomipramine) and a

serotine/norepinephrine reuptake inhibitor (Venlafaxine) was tested in France on a vCJD patient. The treatment lasted for 7 weeks, but after 14 months of the symptoms onset, the woman died [208].

In the same period, Korth and others were looking for some known compounds able to cross the BBB. They focused the attention on some tricyclic acridine and phenothiazine molecules used to treat psychosis. One of them, the Quinacrine, obtained excellent results in the inhibition of PrP^{Sc} protein in cells chronically infected with prions (on ScN2a cells EC_{50}=0.25 μM) [209]. When the compound was tested in mice models, the strong efficacy previously described in cells was lacking [210]. But for the good safety profile and ability to cross the BBB, the compound was tested in humans. The first clinical trial with Quinacrine was made in France in 2004, 32 CJD patients were treated with 1 g dose for 1 day and followed by 300 mg daily. In this case, no effect was obtained [211]. [211]. In 2009, Collinge and his colleagues in UK opened a new trial, called PRION-1 involving 107 patients. The large majority of them were affected by vCJD. They noticed that 300 mg of Quinacrine were well tolerated but it was not sufficient to achieve the hoped results [212]. The last Quinacrine trials were performed between 2005 and 2009 at the University of San Francisco. 425 patients were randomly treated with 300 mg of Quinacrine or with placebo. The results of this study did not show significant differences between the placebo and Quinacrine treated patients [213]. In the same years, some studies conducted on cells demonstrated that even if Quinacrine reduces PrP^{Sc}, a continuous chronic treatment results in strain selection of PrP and so drug-prion resistance [214]. The combination of Quinacrine and another tricyclic compound, Chlorpromazine, was tested in an iCJD patient, but again without the expected results [215].

In 2003 some cases of sCJD were treated with an anticonvulsant, Phenyotin, in combination with Topiramate or Quinacrine and Chlorpromazine. After a short period of treatment, in both cases the patients started to have seizures and to increase muscle rigidity without any other type of improvement [216].

A very interesting trial came from the use of Flupirtine, a nonopioid analgesic, with an encouraging cytoprotective activity in prion diseases *in vitro* [217]. In 2004, it was used to treat 28 patients with a probable CJD, and although tests demonstrated a slowdown of cognitive decline in the treated patients, there were no significantly statistic differences in the survival time [218].

Pentosan polysulfate (PSS) promotes an increase of the survival time in humans [219]. PSS is a semisynthetic pentasaccharide heparinoid able to act in competition with endogenous heparin sulfate proteoglycans as coreceptor for PrP^{C} on the cell surface [199]. Unfortunately, it is

known that it does not cross the BBB, so in the all clinical trials performed, even if there was a strong increase in the survival time (~ 50%), there were many adverse effects due to the intraventricular administration [220].

Recently, the antibiotic Doxycycline was tested in human clinical trials with high expectation, after several *in vitro* and *in vivo* studies that showed its ability to reduce PrP^{Sc}, inhibit prion formation and destabilize aggregates, increase the mice's incubation and survival time [221]. The first human study was conducted in Italy treating 21 patients with probable CJD with 100 mg per day of Doxycycline from the diagnosis until their death [222]. A very similar trial was performed in Germany and in both cases the scientists noticed an increase in the survival time of the treated compared to the untreated (placebo treated) patients [223]. These positive results led to another trial conducted between Italy and France. But in this case, even if the type of treatment was the same, the results were not confirmed, because there were no significative differences between the treated and control groups [224]. A new trial started in these last years in Italy by Forloni et al. They are performing a preventive study with Doxycycline in patients with the genetic risk of developing FFI syndrome [225]. The study should end in 2023 [197].

Drug	Country	Patient recruitment	Number	Primary endpoint
Flupirtine	Germany	sCJD and genetic TSEs	28	ADAS-cog
PPS	UK	vCJD, iCJD and genetic TSEs	7	Survival
PPS	Japan	sCJD and iCJD	11	Survival
Quinacrine	France	sCJD and genetic TSEs	32	Survival
Quinacrine	UK	sCJD and genetic TSEs	107	Survival and rating scales
Quinacrine	USA	sCJD	51	Survival
Doxycycline	France/Italy	sCJD and genetic TSEs	121	Survival
Doxycycline	Germany	sCJD	100	Survival

Tabelle 5. Detailed information of some clinical trials. ADAS-cog, cognitive component of the AD assessment scale [199].

As it is possible to understand reading above, even if there have been steps forward in the drug development and the treatment of prion diseases, so far there is still no therapy able to modify the course of these disorders.

1.5.2 Approaches to therapy in TSEs

As it is mentioned above, the drug discovery and in general the devising therapeutic approaches is a very challenging area in prion diseases. Nowadays, there are many different types of strategies.

1.6.2.1 Repurposing approach

In the previous chapter, it is shown that all the human trials were performed using molecules that were already employed for other disorders (i.e. acyclovir as antiviral). The use of existing drug to cure and treat new diseases is called "repurposing". Recently, this approach has been commonly used to find therapies for orphan diseases, such TSEs. An orphan disease is a disorder that has not been adopted by the pharmaceutical industry because it is a rare disease or a common disease, and it is far more prevalent in developing countries than in the developed world. The identification of possible drug repurposing can happen by serendipity, target searching and observation of side effects. The advantages to use this approach are many: the critical information, such as drug-likeness, pharmacokinetic features, dosing, safety and tolerability, are already available; the time saved, because in this way it is possible to avoid several years of the drug development; the lack of human risk in terms of side effects [226, 227].

The most common strategy used to do drug repositioning is the *in silico* screening of compound libraries for new targets. *In-silico* term refers to a mathematical equation able to explain a biological phenomenon. It is quite common in the drug repositioning for prion diseases to use a quantitative structure-activity relationship (QSAR) model to screen a huge library of compounds in order to select only the molecules that have a good predicted biological activity and then confirm the result with *in vitro* studies [228].

All the compounds used in clinical trials for prion diseases represent a good example of drug repurposing [195].

1.5.2.2 The use of small molecules to block the prion replication

Another possible approach is to use compounds that can block the prion replication. From the knowledge of prion cell biology, this blocking could happen in a direct mechanism by which the compound induces the stabilization of PrP^{C} and/or the destabilization of PrP^{Sc}; or by an indirect mechanism, by which the molecule interacts with other components of the prion replication. It is not so easy to identify compounds with these abilities, but even if they are obtained, they still face high hurdles to qualify as drug candidates. Because they also need to

reach the appropriate cellular compartment, have an acceptable ratio of toxic to therapeutic dose and the capacity to cross the BBB effectively [195]. Designing molecules with a deliberate activity, is a task for the computational chemists. Once the molecules are designed and computationally screened, they are tested in cell lines chronically infected with prions (next chapter) and *in vitro* experiments to confirm their activity and mechanism of action. If the ability of the compound to clear the level of PrP^{Sc} is really good and it is not toxic, the compound could be tested in an animal model, usually mice or hamsters.

Starting from the fact that the structure of PrP^{Sc} is poorly defined, they can have different strains [229], the chaperones and other proteins involved in the prion replication are not so well known, the most sensate approach is to target PrP^{C} [230]. On the cellular prion protein, there are some binding sites, where a molecule can stick and block the contact with PrP^{Sc}, thus avoiding the prion conversation and propagation. Below there is a list of chemical scaffolds reported to have an anti-prion activity binding PrP^{C} (Figure 7):

- Acridine and phenothiazine were chosen by Korth in 2001 as possible anti-prion candidates for their ability to cross the BBB. In prion infected neuroblastoma mice cell line (ScN2a), the two molecules that exhibited a strong activity were Quinacrine (EC_{50}=0.3 μM) and Chlorpromazine (EC_{50}=3 μM) [209, 231]. Unfortunately, neither one of these two have the same activity in an animal model (or a human). For the Quinacrine, it is due to the fact that this molecule reaches the brain in a low concentration [214]. NMR and SPR studies demonstrated the ability of Quinacrine to bind the globular domain of human recombinant PrP (residues 121-230) [232]. Recent articles showed that Chlorpromazine does not have a strong binding with PrP^{C} (K_D > 400 μM) and that the anti-prion activity is mainly due to its capability to promote a relocalization of the PrP^{C} from the cell membrane [233, 234].
- In the beginning of 2000s, Caughey and its collaborators screened cyclic tetrapyrroles. They consist of a planar aromatic ring scaffold, able to coordinate metal ions. One of them, the cationic tetrapyrrole Fe(III)-TMPyP was shown to have an EC_{50}=1.6 μM in RML-PK1 cells and to bind the globular domain of PrP^{C} with a K_D=4.52 μM [235, 236]. But Fe(III)-TMPyP is not prone to cross the BBB, so it was not tested in an animal model [237].
- GN8 is a derivate of the Diphenylmethane. This molecule was identified through an *in-silico* screening design to select compounds able to bind the PrP^{C}. *In vitro* experiments determined the binding of GN8 to the residues 159 and 196 of PrP^{C} C-terminal domain and EC_{50}=1.35 μM in cells [125]. It has been shown that GN8 and

some of its derivatives have the ability to prolong the survival time in prion-infected mice [238]. The results obtained in both *in vitro* and *in vivo* experiments failed to confirm its anti-prion activity and ability to bind PrP^{C} [230].

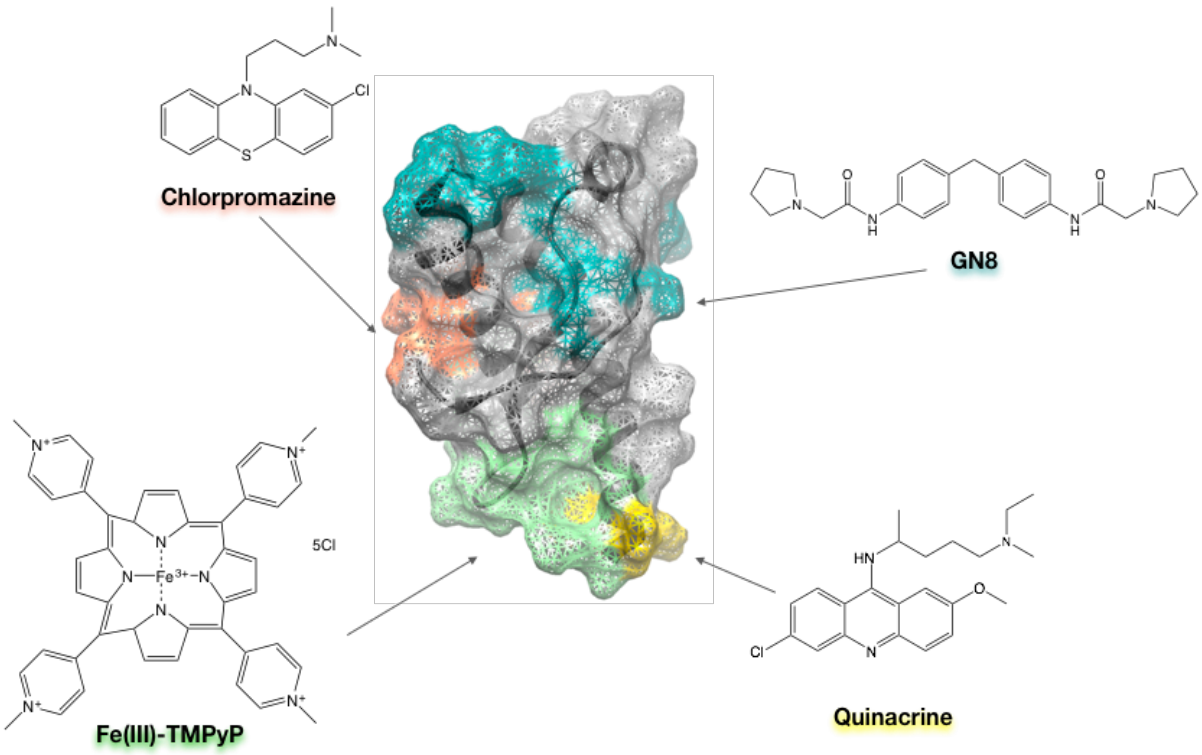

Figure 7. Proposed binding regions on PrP^{C} of the different compounds. (Modified from [230])

1.5.2.3 Immunotherapy

Both active and passive immunization approaches in AD have been shown to clear the Aβ misfolded protein. These results suggested to apply the immunization strategy in prion diseases. The challenge in this field is the self-tolerance for the PrP^{Sc}, because it is just a modified form of PrP^{C}.

The active immunization led to a prevention of prion diseases in a mouse model, using an oral administration with PrP^{C} expressed in an attenuated Salmonella vector. Sadly, it has been shown that the use of this strategy could result in adverse effects, such as autoimmune meningoencephalitis and degeneration in hippocampal and cerebellar neurons. While the passive approach seems to prolong the survival time just when it is administered before or immediately after the exposure to PrP^{Sc} [239, 240].

1.5.2.4 PrP^C silencing and activation of Unfolded Protein Response pathway

Assuming that *Prnp* knockout mice are resistant to prion infection, another proposed approach, in literature, is the PrP^C silencing. In 2008, Mallucci's group used lentivirally mediated RNAi for treatment of prion infected mice. Even if localized to the hippocampus, a single administration of these viruses increases the lifespan of the mice, protects neurons from degeneration, reduces prion accumulation and prevents the onset of behavioral dysfunction [241].

The same group focused the attention also to the unfolded protein response (UPR) pathway, that is a cell protective mechanism which acts to restore the level of the proteins in the face of a misfolding load, reducing the protein synthesis through the activation of PERK enzyme. In 2013, they treated prion infected mice with GSK2606414, a PERK inhibitor. This treatment prevents UPR-mediated repression and promoting the neuroprotection, it abolishes the development of clinical prion diseases in infected mice [242].

1.6 Experimental models

For the discovery of new anti-prion drugs, cell cultures are considered as the most relevant first screening step. Over the last twenty years, many groups of scientists have attempted to find cellular cultures supporting prion diseases agent replication. In addition to the advantages of screening drugs with potential therapeutic values, cell cultures can analyze the biological properties of PrP^C and PrP^{Sc}, have the possibility to determine the nature of the infectious agent, the factors governing its propagation and the biological markers of the infection.

The direct approach to propagate prions *ex vivo* consists of putting the infectious agents in contact with the cell and checking whether replication occurs. The simplest way to obtain the infectious agents is to extract them from infected brain homogenates. The infectious fraction is pretreated for 30 min at 80°C and sonicated to reduce the risk of transmitting conventional viral and bacterial agents. After exposure to the culture, cells are washed and split several times. To check whether replication is occurring, it is necessary to test for the generation of new molecules of PrP^{Sc}. Several techniques are used to detect the presence of PrP^{Sc}. The most common one is the SDS-PAGE analysis of cell lysates treated with protease K, followed by Western blot analysis using anti-PrP antibodies.

There are different strains of prion protein depending on the species of origin, which can reduce the effectiveness of prion propagation. To avoid this species-barrier phenomenon, the

PrP^{Sc} present in the inoculum has the same species origin as the one expressed by cultured cells. In 1970 the group of Clarke [243] was the first to infect TSE culture cells successfully, followed by the groups of Chesebro [244] and Prusiner mainly using mouse neuroblastoma N2a cell lines [245]. Still today N2a is the most common cell line used. Another widely used one is the hypothalamic cell line called GT1. These cells are well differentiated, originate from the central nervous system and are established from gonadotropin-releasing hormone neurons immortalized by genetically targeted tumorigenesis in transgenic mice. Many other cells are prion-susceptible, as shown in Table 8. From different published works, it is possible to conclude that: only some strains can replicate in one particular cell line, only some cells from culture become infected and sub-cloning could improve the susceptibility to prions, the PrP expression level is an important factor for the detection of a successful infection, the propagation of prions induces only subtle changes in the phenotype of cultures.

As mentioned above, the cell culture model is largely used to carry out a prescreening test of potential anti-prion drugs. The advantage of cell culture screening is crucial, since it is not possible to begin the screening *in vivo* using a huge library of compounds. Therefore, cell screening assay makes it possible to identify a reasonable number of *in vitro* active molecules to use for *in vivo* experiments [246].

1.7 Aims of the research

The absence of a therapy to cure prion diseases is an active field of research. Not only for these disorders but especially because TSEs are now considered as the prototype of neurodegenerative diseases. This challenge is due to many factors, such as the difficulty to diagnose the disease in a pre-symptomatic stadium, to develop a molecule able to cross the BBB and still be efficient and to detect the most appropriate targets. As mentioned above, the two main targets used to block the prion conversion are the stabilization of the PrP^{C} and the destabilization of the PrP^{Sc}. *In-silico* approach is one of the most common strategies for drug discovery of prion diseases, used before the *in vitro* studies to detect compounds that can satisfy specific requirements, such as a possible binding of molecule to the target or the need to have a precise biological activity.

In the present thesis, a specific strategy to identify a compound as a possible anti-prion agent has been investigated. In particular the objects of this thesis are:

- *In vitro* identification of a hit compound, starting from a library (Figure 8) of ten molecules. The library was selected using a Quantitative-Structure Activity-Relationship (QSAR) model, built by Dr. Rossetti and Dr. Carloni, able to measure the predicted IC_{50} of the compounds. The *in vitro* screening started with the evaluation of the cell viability of each compound and then with the analysis of anti-prion activity of the compounds measured by the inhibition of PrP^{Sc} level in cell lines chronically infected with prions.

- Understanding the possible mechanism of action of the hit compound. From the literature, it is known that the many compounds with a strong anti-prion activity *in vitro* are the ones able to bind the cellular prion protein. The reason is not known, but a possibility is that these compounds bind the PrP^{C} in the same binding site of the PrP^{Sc}, thus decreasing the prion conversion rate. Also, targeting another component of the prion conversion is a very good strategy, even if the other proteins involved in the conformational change are still not completely known.

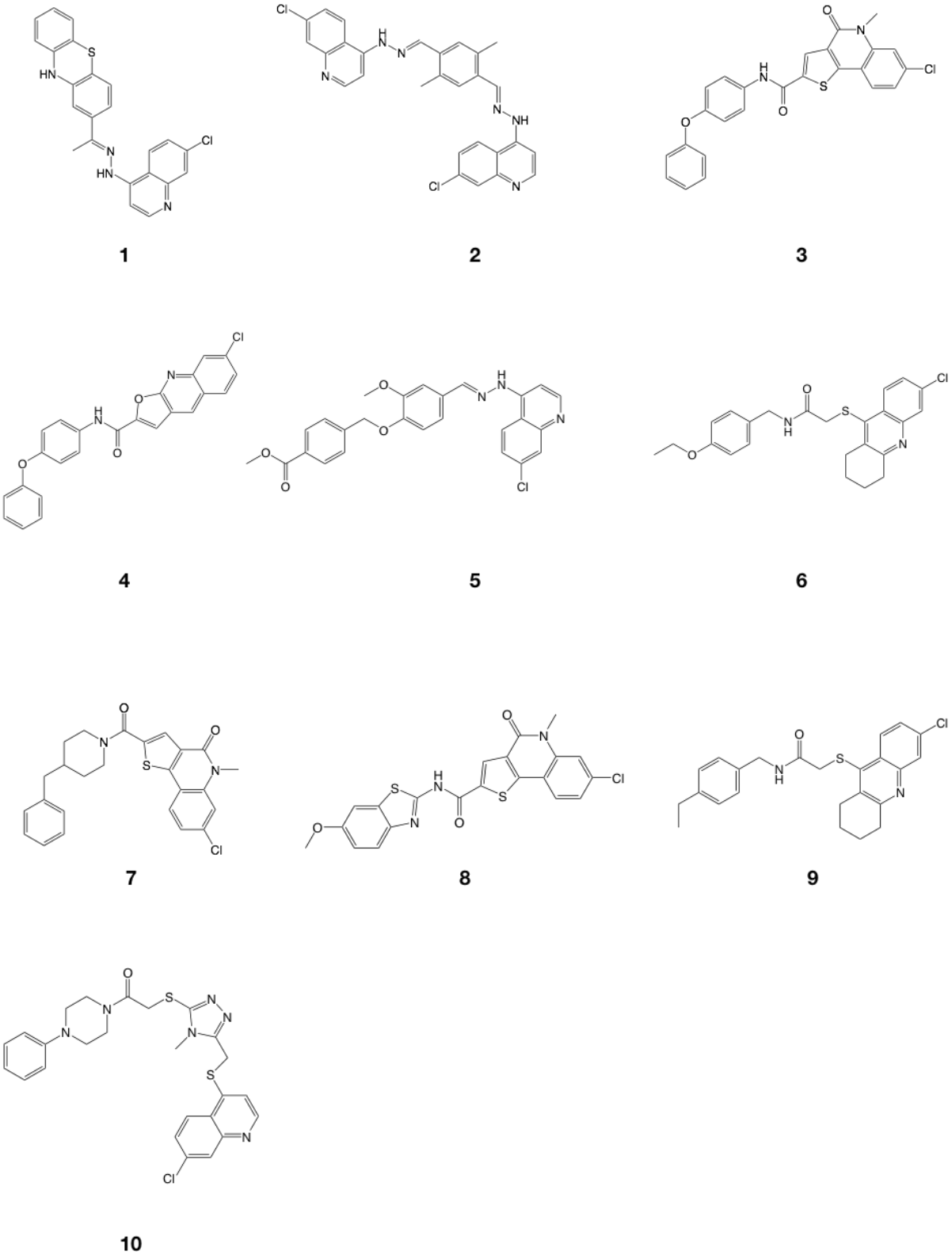

Figure 8. Library of the selected compounds tested *in vitro*.

CHAPTER II

MATERIAL AND METHODS

2.1 Computational details

Note: Computational analysis were performed at the Jülich Research Centre (Stetternich Forest, Kreis Düren, Germany) by Dr. Giulia Rossetti and Dr. Paolo Carloni. For this reason, the related Materials and Methods have been moved to the Appendix II.

2.2 Compound synthesis

Note: Selected compounds were provided by Mcule.com, that is an online drug discovery platform.

2.3 Biological evaluation

In vitro assessment of *in silico* selected compounds.

2.3.1 Cell culture

Mouse neuroblastoma cell line, either the non-infected (N2a) and the chronically infected with Rocky Mountain Laboratory (RML) or with 22L prion strain (ScN2a), were grown in Minimal Essential Medium (MEM)-1% L-glutamax complemented with 10% fetal bovine serum (FBS), 1% non-essential amino acids (NEAA), and 1% penicillin-streptomycin.

Immortalized mouse hypothalamic neurons (GT1) and chronically infected ScGt1 cells, with both RML and 22L prion strains, were grown in Dulbecco's modified Eagle's medium (DMEM)-1% glutammax supplemented with 10% FBS and 1% penicillin-streptomycin.

All cell lines were cultivated in 25 cm^2 flasks at 37 °C under 5% CO_2 or in 10 cm^2 Petri dishes.

2.3.2 Compounds

All the compounds were dissolved in 100% dimethyl sulfoxide (DMSO), to a 10 mM stock solution. From these stock solutions, intermediate dilutions were prepared as needed. For cell treatment, stock solutions were further diluted in 100% Ethanol (EtOH) to a final concentration of 1 mM. Each compound was then diluted in cell culture medium. In the cell medium, the final concentration of DMSO was never above 0.1%. Detailed treatment conditions are provided in following methods. Mock controls were treated with vehicle only under the same conditions.

2.3.3 Assessment of cell viability

N2a, N2a chronically infected with RML or 22L prion strain (ScN2a), GT1 and GT1 chronically infected with RML or 22L prion (ScGT1) cells, were maintained in culture and grown to 80% confluence. The medium was changed and the cells were detached.

The cell density was determined by cell counting using ScepterTM 2.0 Cell Counter (Millipore). The cell density was adjusted to 2.5×10^4 cell/mL with MEM (N2a, ScN2a) or 3×10^4 with DMEM (GT1, ScGT1).

The cell suspension was added to each well of a 96-well, tissue culture-treated, clear bottom, plate (Costar) and the cells were allowed to settle for 1 day at 37 °C under 5% CO_2 prior to the addition of the compounds.

Each compound (dissolved in EtOH) was diluted in the cell medium to a final concentration of 0.1, 1 and 10 μM. After 24 h, cell culture medium was removed and replaced by compound-containing medium.

The plate was incubated at 37 °C under 5% CO_2 for 5 days.

2.3.3.1 MTT assay

The 3-(4,5-dimethylthiazol-2-yl)-2,5-diphenyltetrazolium bromide (MTT, SIGMA) was diluted in phosphate buffer solution (PBS) to a working dilution of 5 mg/mL.

The medium was then removed, and the cells were incubated with the MTT solution for 3 h at 37 °C under 5% CO_2.

After incubation, a solution of DMSO/2-Propanol (1:1) was added to each well and the plate was kept at room temperature (RT) for 30 min before reading. The emission intensity was quantified using a Spectramax Gemini EM (SoftMax Pro).

2.3.3.2 Cell counting KIT-8

Ten µM of CCK-8 solution (ST-8 [2-(2-methoxy-4-nitrophenyl)-3-(4-nitrophenyl)-5-(2,4-disulfophenyl)-*2H*-tetrazolium, monosodium salt) (Dojindo Labroatories) were added to each well of the plate.

The plate was then incubated for 4 hours in the humidified incubator (e.g., at 37°C, 5% CO_2). After that, the absorbance was measured at 450 nm using the microplate reader (Spectramax Gemini EM SoftMax Pro).

2.3.4 PrP^{Sc} and PrP^{C} detection in cell lysates by western blotting

After the treatment with compounds, the amount of PK-resistant PrP^{Sc} was measured in ScN2a and ScGT1 treated with 1 µM of concentration of each compound, then with a titration for compound **1**. After 4 days of treatment, the accumulation of PrP protein was detected by immunoblotting of lysed cells before and after PK digestion.

2.3.4.1 Cell lysates

After removing the medium and washing the cells with PBS, 350 µL of lysis buffer (10 mM Tris-HCl pH 8.0, 150 mM NaCl, 0.5% nonidet P-40, 0.5% deoxycholic acid sodium salt) were added to the flasks/dishes, then the cells were detached using a cell scraper (Falcon) and the lysates were collected and pelleted by centrifugation at 2000 rpm for 10 min at 4 °C in a bench microfuge (Eppendorf).

2.3.4.2 Protein quantification

The total protein amount of the samples was measured by bicinchoninic acid assay (BCA) (Pierce).

First, it was necessary to prepare the Albumin Standards that were used at 1000, 1500 and 2000 µg/mL concentrations, and the Working Reagent (WR). The total volume made depended

on the number of samples and standards to be quantified. The volume was calculated with the following formula:
(# standards + # unknowns) × (# replicates) × (volume of WR per sample) = total volume WR

i.e. (3 standards + 8 unknowns) x (3 replicates) x (100 µL) = 3300 µL of WR

Generally, there were three replicates.

The WR volume was prepared mixing 50 parts of BCA reagent A with 1 part of reagent B (50:1). A 96-well plate was loaded with 5 µL of Blank (distilled water), Albumine Standards and samples (cell lysates) with 100 µL of the Working Reagent mix.

The plate was incubated for 20 minutes at 37°C and then the absorbance was read with SpectraMax reader and the proteins were quantified.

2.3.4.3 PK digestion

Two hundred and fifty µg or 500 µg of protein were digested with 10 µg of PK (Roche) for 1 h at 37 °C.

The reaction was arrested with 2 mM of phenylmethylsulphonyl fluoride (PMSF, SIGMA) and the PK-digested cell lysates were centrifuged at 55000 rpm for 75 min at 6°C in an ultracentrifuge (Beckman Coulter).

After the centrifugation, the supernatants were discarded, and the pellets were re-suspended in 2X or 5X sample loading buffer (125 mM Tris HCl, pH 6.8, 10% 2-mercapethanol, 4% SDS, 0.2% bromophenol blue, 20% glycerol and 200mM DTT) and boiled for 10 min at 100 °C. An amount equal to 30 µg of total proteins was used for the non-PK-digested samples, boiled for 10 min.

2.3.4.4 SDS-page assay and immunoblotting

Samples were loaded onto a 12% Tris-Glycine SDS-PAGE gel for protein separation, then they were transferred to a nitrocellulose membrane (GE Healthcare).

The membrane was blocked with 5% non-fat milk in TBST (Tris 200 mM, NaCl 1.5 mM, 1% Tween-20) for 1 hour at RT and incubated with 1 µg/mL anti-PrP Fab W226, diluted in blocking solution, overnight at 4 °C. After three washes with TBST, the membrane was incubated for 1 h a RT with secondary antibody (goat anti-mouse IgG F(Ab)2 conjugated with horseradish per- oxidase (HRP), DAKO) diluted 1:1000 in blocking solution. After several washes, the signal was detected using enhanced chemiluminescent system (ECL, Amersham Biosciences) and Uvitec Alliance (Cambridge).

Densitometric analysis was performed using Uviband Analysis Software.

Data are expressed as mean ± SD, and the values of the controls are adjusted to 100%.

Each experiment was performed in triplicate.

2.3.4.5 PrP^C detection in cell lysates by western blotting

The same treatment conditions reported above were used for non-infected N2a and GT1 cells. After 5 days of drug treatment, the amount of PrP^C was measured by immunoblotting of lysed cells. Thirty μg of total proteins were used for the analysis. Same protocol as above was used, without PK digestion step. Each experiment was performed in triplicate.

2.3.4.6 PrP^{Sc} quantification by ELISA assay

PK digestion of cell lysates was performed as described above. After ultracentrifugation, pellets were dissolved and denatured in 50 μL of 8 M guanidine hydrochloride (GdnHCl) in coating buffer (0.1 M sodium bicarbonate, pH 8.2) for 1 h and diluted into 500 μL of coating buffer.

Twenty μL of the suspension were transferred to 96-well MaxiSorp ELISA plates (Nunc), with each well containing 180 μL of coating buffer and the plates were sealed and incubated overnight at 4 °C. To increase the immuno-reactivity of PrP^{Sc}, coated proteins were denatured *in situ*. Fifty μL of 8 M GdnHCl were added to each well and incubated for 10 min at room temperature. The ELISA plates were washed three times with TBST and blocked with 200 μL of 3% BSA in TBS (20 mM Tris-HCl, 137 mM NaCl, pH 7.5) for 1 h at 37 °C. After three washes with TBST, the plates were incubated with 100 μL of anti-PrP antibody W226 (1.5 μg/mL) in 1% BSA/TBS, at 37 °C for 2 h. After seven washes with TBST, 100 μL of goat anti-mouse IgG Fab conjugated to HRP diluted 1:1000 in 1% BSA/TBS were added to the plates and incubated at 37 °C for 1 h. Again, plates were washed seven times with TBST, and then developed with 100 μL of 1-step TMB (3,3′,5,5′- tetramethylbenzidine) Turbo ELISA HRP substrate (Pierce).

The reaction was stopped by the addition of 100 μL of 2 M sulfuric acid to the plates. Absorbance at 450 nm was measured using a microplate reader (VersaMax, Molecular Devices). Dose-response curves and IC_{50} values were computed using IGOR (Demo Version 6.32).

2.3.5 PNGase F treatment

PNGase F treatment were performed on N2a cell lysates.

Thirty µg of protein were incubated with 1 µL of Glycoprotein Denaturating Buffer (10X) and water to reach a total reaction volume of 10 µL. Then, the mix is heated at 100 °C for 10 minutes to denature the protein.

The denatured protein was then chilled on ice and centrifuged for 10 seconds. The solution was filled with 2 µl of GlycoBuffer 2 (10X), 2 µl of 10% NP-40 and 6 µl of H_2O. One µl of PNGase F was added and the mix was mixed very gently. The solution was incubated with shaking (350 rmp) at 37°C for 6 hours.

The result was, then, observed by SDS-page.

All the reagents for the protocol were assessed by New England BioLabs.

2.3.6 Ammonium chloride treatment

N2a RML infected cells were treated in absence or in presence of 4 µM of compound **1** with 20 mM of NH_4Cl. The ammonium chloride at this concentration is known to block the lysosomal activity. The results of the treatment were then observed by SDS-page.

2.3.7 Recombinant full-length mouse PrP production and purification

The mouse construct was expressed in competent BL21 Rosetta2 (DE3) cells Escherichia coli (Stratagene).

Freshly transformed overnight culture was inoculated into Luria Bertani (LB) medium and 100 µg/mL ampicillin and 30 µg/mL chloramphenicol. At 0.8 OD_{600} expression was induced with isopropyl b-D galactopyranoside (IPTG) to a final concentration of 1 mM. Cells were grown in a BioStat-B plus fermentor (Sartorius). The cells were lysed by a homogenizer (PandaPLUS 2000) and the inclusion bodies were suspended in buffer containing 25 mM Tris-HCl, 5 mM EDTA, 0.8% TritonX100, pH 8, and then in bi-distilled water several times.

Inclusion bodies containing MoPrP (23-231) were dissolved in 5 volumes of 8 M guanidine hydrochloride (GdnHCl), loaded onto pre-equilibrated HiLoad 26/60 Superdex 200-pg column, and eluted in 25 mM Tris–HCl (pH 8.0), 5 mM ethylenediaminetetraacetic acid, and 5 M

GdnHCl at a flow/rate of 1.5 mL/min. Protein refolding was performed by dialysis against refolding buffer [20 mM sodium acetate and 0.005% NaN_3 (pH 5.5)] using a Spectrapor membrane (molecular weight, 10000). Purified protein was analyzed by SDS-polyacrylamide gel electrophoresis under reducing conditions and Western blot.

2.3.8 Competition assay

A mix of recombinant mouse full length PrP (23-231) and compound **1** was incubated at 37 °C in 350 rpm of shaking for 30 minutes.

The mixes were different:

- PrP : compound **1** = 1:1 = 1μM : 1μM
- PrP : compound **1** = 2:1 = 2μM : 1μM
- PrP : compound **1** = 1:2 = 0.5 μM : 1μM
- PrP : compound **1** = 1:5 = 0.2 μM : 1μM

After 1 hour, the mix and the other treatments (compound **1** alone) were centrifuged many times at 2000 rpm in Nanosep centrifugal device (Merk) with Omega membrane 3 kDa to pass the whole solution through. These tubes are permeable to compound **1** (416.93 Da) but not to the PrP (25 kDa) and to the PrP-compound **1** complex.

The mix and the other treatments were added to the cells as a normal treatment for 4 days. Then the cells were lysed, and the result is observed by SDS-page.

2.3.9 RT-QuIC procedure

After purification, aliquots of the recombinant PrP (23-231) were stored at −80 °C in 10 mM phosphate buffer (pH 5.8). Before each test, the protein solution was allowed to thaw at room temperature and filtered using Millex-GV filter 0.22 μm (Millipore).

The final reaction volume was 100 μL loaded into the plate (ViewPlate-96 F TC/50x1B, Perkin Elmer) and the reagents (Sigma) were concentrated as follow: 150 mM NaCl, 0.002% SDS, 1X PBS, 1 mM EDTA, 10 μM ThT and 0.2 mg PrP ml−1.

The seed consists of sonicated RML-N2a cells. Before the sonication the cells were collected in 100 μl of PBS 1X, after the sonication the sample was quantified using the BCA assay, in order to use it as a seed (1 μg of the protein).

After the addition of 10 µL of seed, the plate was sealed with a sealing film (Perkin Elmer) and inserted into a FLUOstar OPTIMA microplate reader (BMG Labtech). The plate was shaken for 1 minute at 600 rpm (double orbital) and incubated for 1 minute at 45 °C.

Fluorescence readings (480 nm) were taken every 30 minutes (30 ashes per well at 450 nm). Given the rapid response, a specific threshold was set to decrease the likelihood of false positives. A sample was considered positive if the mean of the highest two fluorescence values (AU) of the replicates was higher than 10.000 AU and at least two out of three replicates crossed the threshold that was set at 30 hours. This reaction cutoff was established because in all the experiments there were wells only with PrP (23-231) and in these cases no positive RT-QuIC reactions were observed until after 30 hours.

2.3.10 Immunofluorescence of fixed cells, the surface staining

N2a cells were seeded to semi-confluence in each well of a 24-well plate containing a poly-lysine coated coverslip and an appropriate culture medium coverslip for 24 hours.

After one day of incubation the cells were put on ice for 15 minutes.

Then the cells were stained with the primary antibody (W226 1:200) in culture medium for 20 minutes, always in ice. After this time, the medium was removed, and the cells were washed 2 times with PBS.

The cells were then removed from the ice and were fixed using 4 % of para-formaldehyde (PFA) for 20 minutes. The PFA was discharged and the cells were washed 3 times for 5 minutes with PBS.

Blocking buffer, consisting of 7% Normal Goat Serum (NGS) in PBS, was added to the cells for 1 hour at room temperature. After the blocking, the cells were incubated with a secondary antibody (Goat anti-mouse [GαMo]-AlexaFluor488, Life Technologies) diluted 1:1000 in the incubation buffer (1% NGS, 0.02% triton-100 in PBS) for 1 hour at room temperature in the dark.

After 2 washes of 5 minutes in PBS, the cells were incubated with 0.1-1 µg/ml of DAPI (Life Technologies) in PBS-T for 5 minutes.

The cells were washed 3 times in PBS for 5 minutes and then the coverslips were mounted with a drop (around 4 µL) of Fluoromount-G (Invitrogen). The coverslips were sealed with nail polish to prevent drying and movement under the microscope.

Images were acquired with C1 confocal microscope (Nikon). FITC filter was used for detection of PrP specific staining, while Dapi specific staining was acquired with 500 nm filter.

CHAPTER III

RESULTS

3.1 *In silico* screening

The *in silico* screening was performed using a QSAR model to select a small library of molecules with precise features, such as specific biological activity. The model generation, validation and the virtual screening were done in the Jülich Institute (shown in the related Results chapter Appendix I, Section II).

The *in silico* screening led to a library of 10 molecules (Figure 8), the majority of which are acridine and phenothiazine derivatives. The selection of the compounds was made by calculating the predicted IC_{50} (pIC_{50}) with the QSAR model. The pIC_{50} of each compound is in the nanomolar range (Table 6).

Compound	pIC_{50} (nM)
1	54.9
2	63.9
3	80.1
4	128.8
5	130.2
6	168.0
7	170.7
8	177.9
9	184.2
10	184.6

Table 6. The predicted IC_{50} of compounds selected with the virtual screening.

3.2 Anti-prion effect of the library on N2a-RML cell line

The *in vitro* screening was mainly performed using the neuroblastoma mice cell line chronically infected with RML prion strain.

The screening was performed to assess the ability of the compounds to have an anti-prion activity. The ability of all compounds to reduce PrP^{Sc} level was determined by Western blot densitometry of the PK resistant PrP^{Sc}. After a PK digestion, it is possible to observe only the presence of resistant PrP^{Sc} bands (PrP27–30), while without PK treatment both PrP^{Sc} and PrP^{C} bands are present (Figure 3). The first assessment of the compounds' anti-prion activity was performed at just one concentration, 1 μM.

3.2.1 Cell viability on N2a-RML cell line

In the beginning, we determined the effects of the library compounds on cell viability using two different assays: MTT assay and the CCK-8 kit. They are both sensitive colorimetric assays able to assess the cell metabolic activity, however, they use two different tetrazolium dyes. In the MTT assay, the 3-(4,5-dimethylthiazol-2-yl)-2,5-diphenyltetrazolium bromide is reduced by NAD(P)H-dependent cellular oxidoreductase enzymes to its insoluble formazan, that gives a purple color. While the CCK-8 kit uses the WST-8 [2-(2-methoxy-4-nitrophenyl)-3-(4-nitrophenyl)-5-(2,4-disulfophenyl)-2H-tetrazolium, monosodium salt], which is reduced in a formazan dye upon the reduction with a dehydrogenase, giving an orange color [247].

The treatment concentration was evaluated at 1μM. In Table 7 results for each compound are reported. Compound toxicity is expressed as an average percentage of viable cells treated with the compound, versus control cells without the compound or just with the vehicle. No toxicity was observed in the selected library, using both techniques. The toxicity threshold at this concentration was set below 80%, as it has already been shown in the literature [248].

3.2.2 Inhibition of PrP^{Sc} replication at a concentration of 1 μM

None of the compounds showed cytotoxic effects, so all of them were tested in N2a-RML cells to quantify the presence of PrP^{Sc} protein after the treatment. The ability of compounds to reduce the level of the resistant PrP^{Sc} in prion-infected cells was determined by Western blot

densitometric analysis. Relative amount of PK-resistant PrP^{Sc} was measured in N2a-RML cell lysates.

Although the measured pIC_{50} of each of the compounds was in the nanomolar range, almost none of them showed a strong anti-prion activity at the concentration of 1 μM.

All the treated samples were normalized to the untreated control (Ctrl). The cells treated with the maximum concentration of the solution in which the compounds were dissolved (Mock) were not subjected to a change in the PrP^{Sc} level. Compounds **3**, **4**, **5**, **7**, **8** and **10** in all four independent experiments did not promote a decrease in the level of PrP^{Sc} protein. Compounds **2** and **9** turned out to have mild anti-prion activity, while treating N2a-RML cells with compound **1** resulted with a strong clearance of PrP^{Sc}. Indeed, the level of the PK-resistant prion protein in this case was around 35%, with respect to the control. (Figure 9 and table 8).

Compound	MTT assay	CCK-8 Kit
Ctrl	100	100
Mock	102.3 ± 4.7	98.3 ± 5.3
1	90.0 ± 3.2	87.4 ± 3.4
2	91.1 ± 7.6	89.1 ± 5.6
3	102.9 ± 1.9	100.3 ± 4.8
4	82.6 ± 8.1	82.4 ± 1.2
5	85.8 ± 5.3	93.1 ± 4.6
6	80.1 ± 2.7	83.2 ± 6.2
7	94.2 ± 0.4	87.5 ± 3.9
8	94.9 ± 1.3	91.2 ± 4.0
9	83.5 ± 1.7	80.3 ± 1.6
10	80.6 ± 3.4	82.3 ± 4.5

Table 7. Cell viability values at 1μM treatment. Values are the mean of three experiments, standard deviations are given.

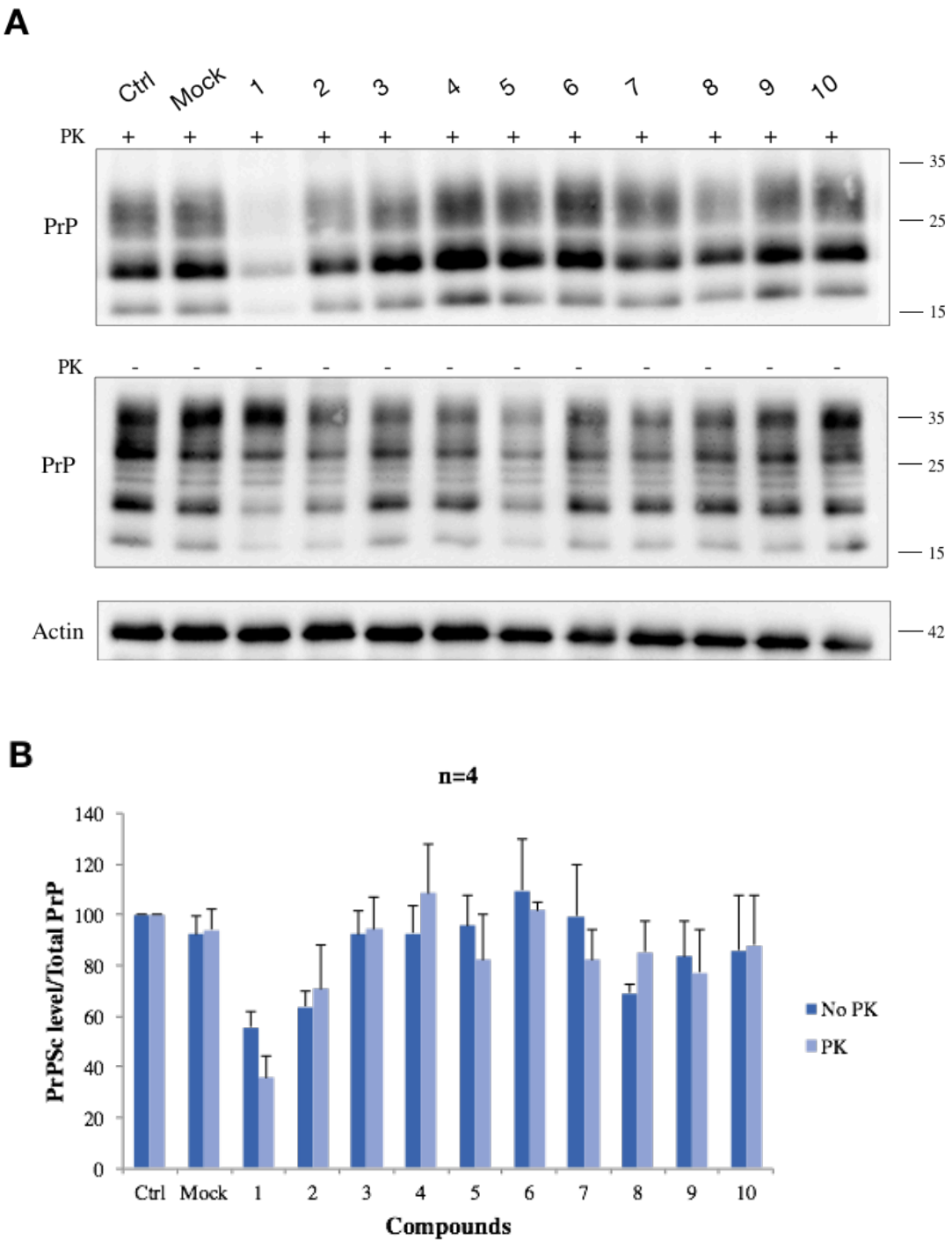

Figure 9. Anti-prion effect evaluation of all compounds at 1 µM of concentration. (**A**) Western blot of N2a-RML cell lysates depicting the presence or absence of prions following the treatment with the compounds before (down) or after (up) PK digestion. The proteinase-K digested cell lysates were detected with W226 anti-PrP monoclonal antibody. Bands represent di-, mono-, and un-glycosylated isoforms at approximately 32, 23 and 18 kDa, respectively. (**B**) Bar graph representations of the percentage of PrP^{Sc} infectivity compared to non-treated control. Error bar is ± standard deviation of four independent experiments.

Compound	−PK	+PK
Ctrl	100	100
Mock	92.4 ± 7.2	94.0 ± 8.1
1	55.7 ± 6.3	35.6 ± 8.8
2	63.8 ± 6.0	70.9 ± 17.3
3	92.5 ± 8.9	94.4 ± 12.8
4	92.6 ± 11.1	108.6 ± 19.3
5	95.6 ± 12.1	82.3 ± 18.0
6	109.5 ± 20.4	101.7 ± 3.1
7	99.6 ± 20.7	82.4 ± 11.8
8	69.1 ± 3.5	85.4 ± 12.1
9	83.5 ± 14.0	77.1 ± 17.3
10	85.8 ± 11.6	88.0 ± 19.9

Table 8. Effect of test compounds on PrP^{Sc} level in N2a-RML cells. N2a-RML cells were incubated with each compound for 5 days. The values under –PK and +PK represent the percentage of the level of total amount of PrP (–PK) and of PrP^{Sc} (+PK) normalized to the control (100%). The values after ± are the standard deviations (SD) calculated from the four independent experiments performed.

3.3 Anti-prion activity of Compound 1 on N2a-RML cells

The results obtained from the anti-prion activity of the whole library on N2a-RML cell revealed a strong effect of compound **1** at 1 μM of concentration. Observing the structure of this molecule, it is immediately evident that compound **1** is a phenothiazine derivative. In 2001 Korth and his collaborators tested this moiety on the same cells [209]. They found that this kind of tricyclic compounds, as acridines, have a good anti-prion activity. It was believed that the effect was due to the their binding to the C-terminal domain of PrP^{C} [233]. However, a recent study [234] demonstrated the ability of some phenothiazines, as Chlopromazine, to promote the relocalization of the cellular PrP from the cell surface to the intracellular compartments.

We decided anyway to proceed with compound **1** and calculate its IC_{50} (the half minimal inhibitory concentration) on N2a-RML cells. Before that, we measured the cell viability of compound **1** at many different concentrations and its non-toxic profile was confirmed with the cell viability assays (Figure 9).

Concentration (µM)	MTT assay	CCK-8 Kit
0	100	100
0.1	100.4 ± 2.7	101.5 ±1.4
0.2	102.0 ± 5.0	98.4 ± 2.5
0.4	98.1 ± 4.9	99.6 ± 3.8
0.6	92.4 ± 1.5	97.5 ±5.4
0.8	89.4 ± 3.1	92.2 ± 7.5
1	90.0 ± 3.2	87.4 ± 3.4
2	87.9 ± 7.9	95.6 ± 3.2
4	98.7 ± 9.6	87.4 ± 9.1
10	89.1 ± 0.7	89.4 ± 7.1

Table 9. Effect of compound **1** on cell viability of N2a-RML at different concentrations. The values represent the % of the viable cells.

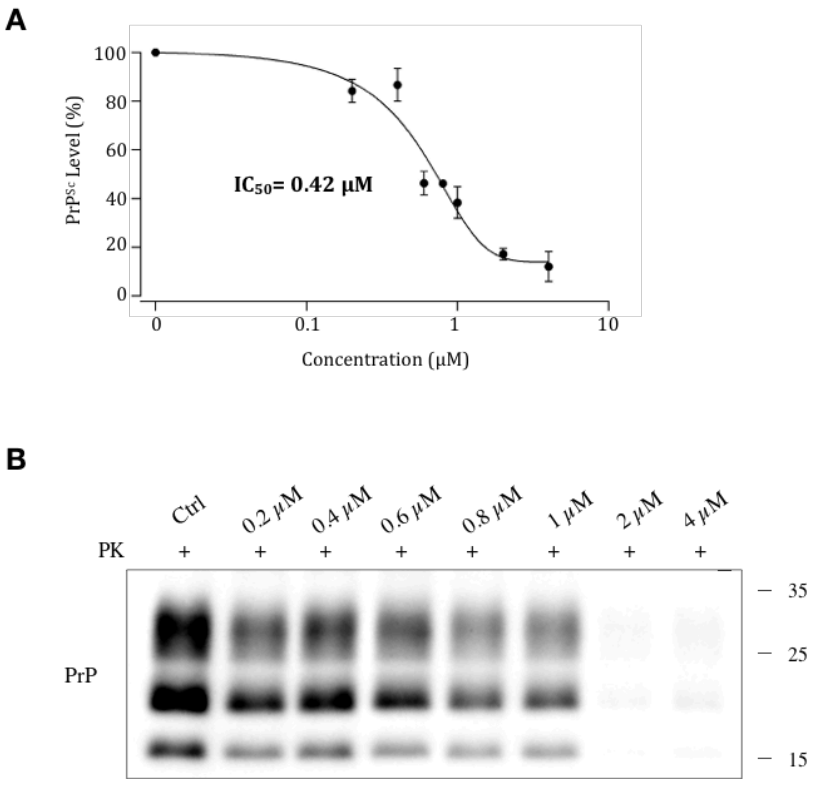

Figure 10. IC_{50} evaluation of compound 1 on N2a-RML. (**A**) Dose-response curve form ELISA assay of 8 different concentration of compound **1**. (B) Western blot of N2a-RML cell lysates treated with compound **1** at the same concentrations used in (A), after digestion with proteinase K.

The IC_{50} was calculated with the ELISA assay, using PK digested samples from N2a-RML cells treated with eight different concentrations of compound **1** (0, 0.2, 0.4, 0.6, 0.8, 1, 2, 4 μM). The results obtained were then confirmed by western blot analysis, using the same PK-digested samples. Each of the two experiments were repeated three times. This experiment established the anti-prion activity of compound **1**, the IC_{50} (calculated with IGOR software) 0.42 ± 0.1 μM (Figure 10).

3.3.1. Anti-prion activity of compound 1 on different cell lines and prion strains

It is known from the literature that several small molecules are active only on precise cell lines and on some prion strains and not on others, these phenomena are called cell and strain specificity [249-251]. Given the fact that the exact mechanisms of action for any anti-prion compound are unknown, it is not easy to explain the reason, in terms of molecular basis, to explain these two aspects. The strain specificity happens probably with compounds that exert their interaction by directly binding to PrP^{Sc}, since the strain specificity seems to derive from differences in PrP^{Sc}.[252].

Starting from the fact that the mechanism of compound **1** as an anti-prion agent is unknown, we decided to test whether at least at high concentrations the interested molecule has the same ability to clear the scrapie prion protein on three other cell lines: N2a chronically infected with 22L mouse prion strain (N2a-22L), hypothalamic mouse cell line (GT1) infected with two prion strains, GT1-RML and GT1-22L.

In Figure 11 (A), the western blots of cell lysates of the previously mentioned cell lines infected with two different prion strains treated or untreated with compound **1** are represented. As it was already shown in the IC_{50} experiments, 4 μM of compound **1** in N2a-RML can bring the level of PrP^{Sc} to around 9.4%, meaning that it promotes a strong clearance of PrP^{Sc}. This activity is maintained in the other cell lines, the treatment on N2a-22L reduces the level of PrP^{Sc} around 5% compared to the untreated sample and around 10% in the GT1-RML and GT1 22L cells (Figure 11 B). Even if it seems to be a bit lower, the total amount of PrP (samples nontreated with proteinase K) also seems to be reduced in all the cell lines. This reduction is probably due to the clearance of PrP^{Sc} visible in the PK-treated samples.

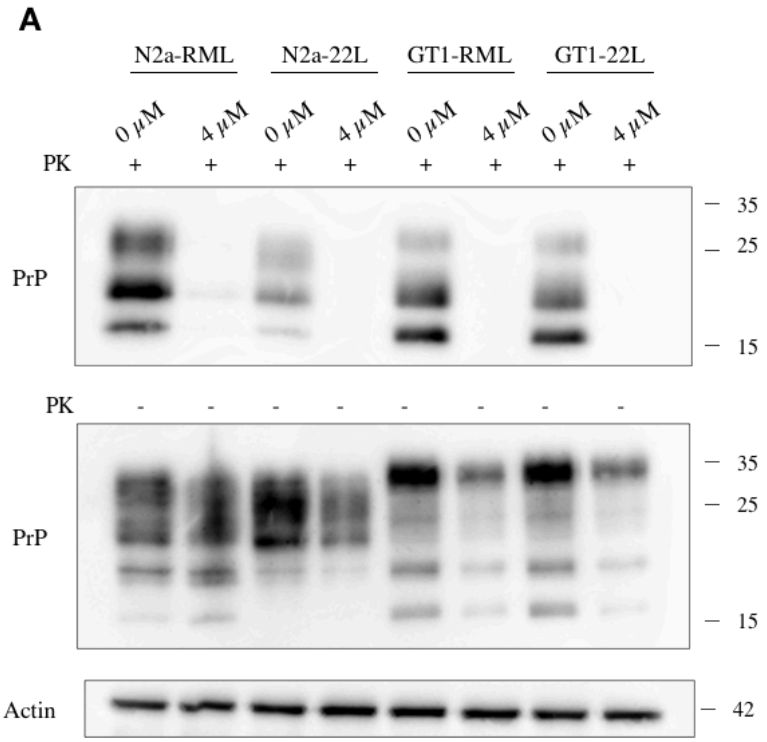

B

Cell line	Concentration (μM)	−PK	+PK
N2a-RML	0	100.0	100.00
	4	62.1 ± 3.4	9.4 ± 2.8
N2a-22L	0	100.0	100.0
	4	48.7 ± 12.4	5.1 ± 4.5
GT1-RML	0	100.0	100.0
	4	42.0 ± 3.8	12.3 ± 5.3
GT1-22L	0	100.0	100.0
	4	39.2 ± 9.6	11.0 ± 8.0

Figure 11. Activity of compound 1 on the total PrP or rPrP^{Sc} on N2a-22L, GT1-RML, GT1-22L. (**A**) One of the three WBs carried out using the cell lysates of treated and untreated cells with compound **1**, before or after PK digestion (**B**) Quantification of the three independent experiments performed. The values under –PK and +PK point the percentage of the level of the total amount of PrP (–PK) and of PrP^{Sc} (+PK) normalized to the control (100 %). The values after ± are the standard deviations (SD) calculated from the four independent experiments performed.

In order to perform this experiment, before the treatment cells were counted and seeded in the same number to administer the compound **1** to the same number of cells in different cell lines. In this way, the results obtained were not due to the number of treated cell, but simply because of the efficacy of compound **1**. Consequently, the different cell lines were collected at a different time, N2a 5 days post seeding, while GT1 8 days post seeding, since it is known that the doubling time in N2a is faster than in GT1 cells.

Even if all the controls are normalized to 100%, it is normal that in the untreated PK-digested samples (upper square in Figure 11 A) the amount of PrP^{Sc} is not the same, this reflects the difference in PrP^{Sc} protein level in different cell lines.

The cell viability of compound **1** was assessed also on N2a-22L, GT1-RML and GT1-22L cells. The compound resulted not to be toxic at 4 μM also on these cells (data not shown).

3.4 Understanding the mechanism of action of compound 1

As already mentioned in the introduction, there are several possible mechanisms of action for a compound with anti-prion activity. Small molecules can block the prion replication using two different strategies: in the direct one, the compound induces the stabilization of the PrP^{C} or the destabilization of the PrP^{Sc}, blocking the prion replication; in the indirect one, the molecule can act on some other protein involved in the prion replication or in the increase of PrP^{Sc} degradation.

In the next experiment we tried to understand which mechanism is used by compound **1** to promote the strong reduction of prions in the cells.

3.4.1 Treatment with ammonium chloride demonstrates the non-involvement of lysosome degradation pathway in the mechanism of action of compound 1

Ammonium chloride (NH_4Cl) is a salt highly soluble in water. In literature, there are several publications that assess the ability of NH_4Cl to inhibit the lysosomal degradation and the phagosomes-lysosomes fusion [253, 254].

The reduction of the level of PrP^{Sc} observed in the WBs of cell lysates, after the treatment with compound **1** (see for example in Figure 10 B), could be due to an increase of the physiological degradation activity of lysosomes promoted by compound **1**. To figure out if the mechanism of

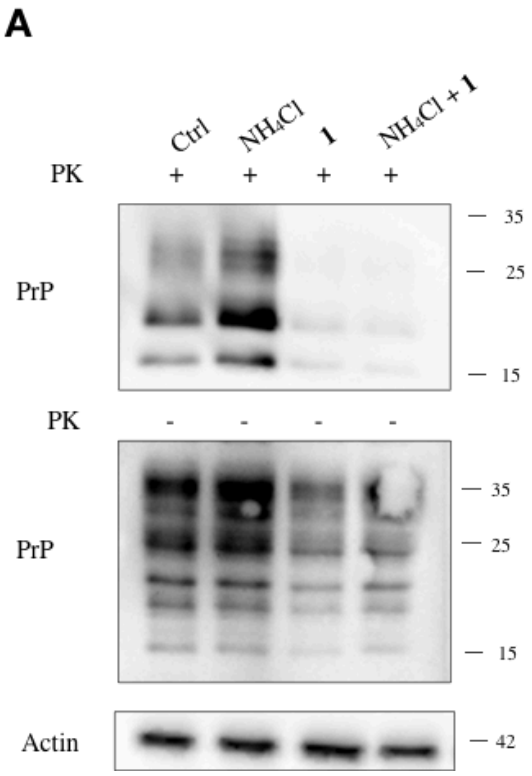

B

Condition	−PK	+PK
Ctrl	100	100
NH_4Cl	126.9 ± 4.1	131.5 ± 9.9
1	47.1 ± 8.3	11.2 ± 5.1
NH_4Cl + **1**	39.8 ± 4.6	9.4 ± 6.4

Figure 12. The mechanism of action of compound 1 does not affect the lysosome degradation. (**A**) WBs of N2a-RML cell lysates in control condition, treatment with either 20 mM of NH_4Cl or 4 μM of compound **1**, and with both 20 mM of NH_4Cl and 4 μM of compound **1**. In the upper square the PrP signal after PK digestion is represented, in the middle the samples without the PK digestion (total PrP) and in the bottom the house-keeping protein, actin. (**B**) Quantification of the three independent experiments. The values under –PK and +PK point the percentage of the level of the total amount of PrP (–PK) and of PrP^{Sc} (+PK) normalized on the control (100%). The values after ± are the standard deviations (SD)

action of compound **1** involves the degradation of the PrP^{Sc}, N2a-RML cells were treated with 20 mM of NH_4Cl in combination with compound **1**. Untreated cells (neither with compound **1** nor NH_4Cl) were used as control, then cells treated just with compound **1** (4 μM) or NH_4Cl (20 mM) and cells treated with both compound **1** and NH_4Cl.

In Figure 12, results of these treatments on the cells are shown. In the samples treated just with 20 mM of NH_4Cl, the level of PrP^{Sc} is 30% higher than in the untreated control. This result is probably due to the inhibition of the lysosome degradation by NH_4Cl, that induces a slowdown of cell clearance pathways and so an increase of misfolded proteins, that cannot be cleared as usual. We expected that in the cells treated with both compound **1** and NH_4Cl the level of PrP^{Sc} would be higher than in the samples treated just with compound **1**, if the compound activity promoted an increase in the lysosome degradation. However, we observed that in the cells treated just with compound **1** and with both compound **1** and NH_4Cl, the level of PrP^{Sc} was almost the same: 11.4% and 9.4%, respectively. A similar pattern observed in PK treated samples was present in the samples untreated with PK, even if less prominent.

After these experiments, we concluded that the lysosomal degradation pathway is not involved in the compound **1** mechanism of action in the decrease of PrP^{Sc}. The next hypothesis was that compound **1** could affect the prion replication stabilizing PrP^{C} or destabilizing the PrP^{Sc}.

3.4.2 Effect of compound 1 on cellular prion protein in uninfected cells

As previously mentioned in the introduction, according to the protein-only hypothesis, the prion replication is the molecular event that allows the self-propagation of prions through the conversion of the PrP^{C} to PrP^{Sc}.

The NH_4Cl treatment revealed that the mechanism of action of compound **1** does not involve the lysosomal degradation pathways. If it is not the degradation, we speculated that another possibility could be blocking the prion replication. To inhibit the prion conversion, compound **1** should bind the cellular prion protein or the scrapie PrP. In order to check if compound **1** binds PrP^{C} and affects its protein level, we decided to treat uninfected N2a and GT1cells for 4 days at 0.1, 1 and 10 μM of concentration, that were already tested for the cell viability on the same cells, using the MTT assay (Table 10). The mock control was used to control a possible influence of the vehicle solution (DMSO-EtOH) on the treatment.

Concentration (µM)	N2a	GT1
Ctrl	100	100
Mock	95.3 ± 2.1	103.2 ± .4.8
0.1	93.6 ± 1.5	96.9 ± 2.9
1.	97.3 ± 4.9	91.4 ± 6.3
10	90.5 ± 8.5	97.4 ±9.2

Table 11. Cell viability of compound 1 on N2a and GT1 by MTT assay. Here, the results of MTT assay of three independent experiments on Na and GT1 are represented. The values under N2a or GT1 are the percentage (%) of the viable cells in the control condition (untreated sample) and after the treatment with vehicle (Mock), 0.1, 1 and 10 µM of compound **1**.

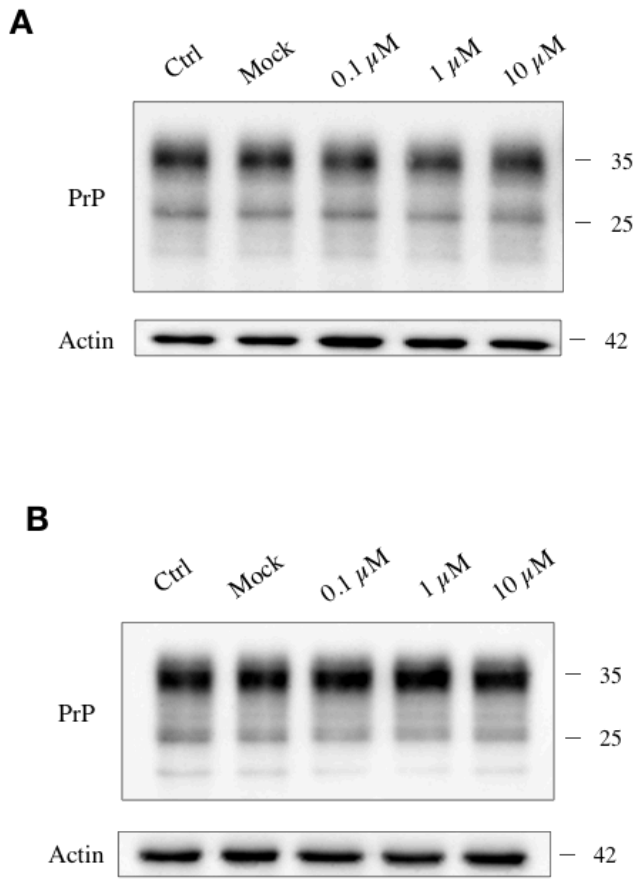

Figure 13. Western blot of compound 1 treatment on N2a (A) and GT1 (B) cell lines. Two representative WBs of the N2a (A) and GT1 (B) cell lysates after treatment with compound **1** at 0.1, 1 and 10 µM of concentration. The Ctrl corresponds to cells without any kind of treatment, while the Mock is the sample treated with the vehicle solution, a mix of DMSO and EtOH in a ratio 1:10.

Once it was shown that the compound **1** was not toxic for the uninfected N2a and GT1, we performed a WB to check if the level of the cellular prion protein in cell lysates of treated samples is affected. In Figure 13 the WBs of the treatment on N2a (A) and GT1 (B) are represented. Neither in N2a nor in GT1 the three concentrations of compound **1** change or affect the PrP^C level.

After these experiments, we concluded that compound **1** is not able to influence the level of PrP^C, however, its ability to bind the cellular prion protein should not be excluded.

3.4.3 Compound 1 does not affect the PrP^C localization from the cell membrane

The treatment of N2a and GT1 with compound **1** for 4 days revealed that it is not able to affect the level of the cellular prion protein. It is still necessary to understand whether the compound **1** binds PrP^C.

In 2017, as already mentioned in the introduction, Stincardini et al. demonstrated that the anti-prion activity of an antipsychotic, Chlorpromazine (CPZ), is not due to its binding to the PrP^C. Indeed, through surface plasmon resonance (SPR) and dynamic mass redistribution (DMR), they estimated that the affinity of CPZ to PrP^C is in a high micromolar range (K_D=421 μM), while the active concentration on infected cells is 100 times lower. This would mean that it is not possible that the mechanism of action of CPZ involves its binding to PrP^C. Knowing that the antipsychotic effect of CPZ involves the clathrin-mediated endocytosis (CME) and that CME allows the recycling of PrP^C from the plasma membrane, they assessed if the CPZ promotes a relocalization of the PrP^C from the cell surface to the intracellular compartments[234].

CPZ and compound **1** are both phenothiazine molecules because they possess the phenothiazine moiety. For this reason, the following experiments were conducted to test if the mechanism of action of compound **1** involves a redistribution of PrP^C.

An immunofluorescence surface staining, without the cell permeabilization, was performed using N2a cells, treated with compound **1** at two different concentrations: 0.4 and 4 μM. PrP^C is marked in green, while the DAPI dye in blue is used to visualize the nucleus. This staining was used to see if the level of the cellular PrP present on the cell surface is affected by treatment with compound **1**. We expected that if compound **1** can promote a relocalization of PrP^C as CPZ, the samples treated with the molecule at 0.4 μM, but especially at 4 μM, would exhibit a

decrease in the level of PrP^C stained in respect to the untreated and the mock controls. On the contrary, we noticed that treated samples had the same pattern staining of the controls.

This experiment allowed us to conclude that anti-prion activity of compound **1** does not implicate a PrP^C redistribution from the cell surface to the intracellular compartments, as is the case for CPZ and other phenothiazine compounds.

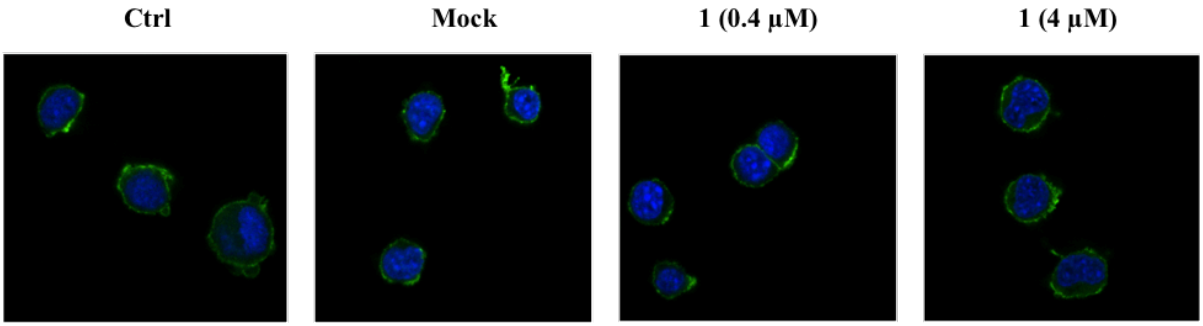

Figure 14. Surface immunofluorescent staining on N2a cells treated with compound 1. As for the other experiments, N2a cells were treated with compound **1** for 4 days. Before the staining the cells were incubated one day in a 24-well plate on the coverslip. Two different concentration of compound **1** were used: 0.4 µM and 4 µM. PrP^C present on the surface is labeled in green, and in blue the nucleus.

3.4.4 Activity of Compound 1 in the prion *in vitro* conversion

After the last-mentioned experiments, we concluded that the mechanism of action of compound **1** does not involve the clearance of PrP^{Sc} by the activation or increase of lysosomal degradation activity. Compound **1** does not change the level of the cellular PrP and the treatment with it on uninfected N2a cells does not affect the redistribution of the PrP^C from the plasma membrane to intracellular compartments. The experiments conducted so far were not able to answer the question if anti-prion activity of the molecule is due to its binding to the cellular PrP, or if this binding is decreasing the PrP^C available for the PrP^{Sc} conversion leading to a reduction in the PK-resistant PrP^{Sc}, visible in the western blots.

In order to have a better comprehension of the mechanism of action of compound **1**, we checked if it is actually able to bind the cellular prion protein. In literature, several techniques are shown to be able to assess molecule-protein interactions, such as the isothermal titration calorimetry (ITC) [255], that can determine the thermodynamic parameters of interactions of small molecules to larger macromolecules in solution; the surface plasmon resonance (SPR) [256], an optical technique able to measure changes in the refractive index caused by

interactions between a mobile molecule and a molecule immobilized on a thin metal film; the bio-layer interferometry (BLI) [257], another optical technique that uses a biological layer, instead of a metal film to immobilize the molecule.

We tried to use the SPR to check a hypothetical binding between compound **1** and the PrP^C and eventually calculate the dissociation constant (K_D) to assess if the anti-prion activity of compound **1** is caused by its binding with the PrP^C. Unfortunately, we had many problems with the solution in which the compound was dissolved, consisting of EtOH and DMSO. For this reason, we tried to avoid the use of SPR and we designed a new protocol to evaluate the possible binding between compound **1** and PrP^C, that we named "competition assay".

In this assay, PrP (23-231) and compound **1** were mixed in different ratios and incubated at 37 °C with constant shaking at 350 rpm for 30 minutes.

The ratios used are shown below:

- PrP : compound **1** = 1:1 = 1μM : 1μM
- PrP : compound **1** = 2:1 = 2μM : 1μM
- PrP : compound **1** = 1:2 = 0.5 μM : 1μM
- PrP : compound **1** = 1:5 = 0.2 μM : 1μM

After 30 minutes of shaking, the mix and compound **1** alone (at the same concentration of 1 μM) were centrifuged several times at 2000 rpm in Nanosep centrifugal device (Merk) with Omega membrane 3 kDa to pass the whole solution through. The centrifugations should not be higher than 1000 rpm to avoid the membrane breakdown. These tubes are permeable for compound **1** (416.93 Da) but not for the PrP (25 kDa) and the hypothetical PrP-compound **1** complex (Figure 15). Regarding the concentration, we have chosen 1 μM instead of 4 μM, so that the concentration of PrP would not be too high.

After several centrifugations, the solution above the membrane contains the molecule with a molecular weight higher than 3 kDa, so it should either be consisted of PrP alone or the PrP-compound **1** complex if the binding has occurred. Meaning that the solution present in the tube's bottom should contain molecules with a molecular weight lower than 3 kDa, such as the compound **1**.

All the solutions were then analyzed using two different approaches: with WB where they were added to the N2a-RML cells and in the RTQuIC where they were loaded into a 96-well plate. If the binding between PrP and compound **1** would occur, a decrease of PK-resistant PrP^{Sc} in the WB and inhibition of the prion aggregation in RTQuIC are expected.

3.4.4.1 Competition assay on N2a-RML cells

Then, the solution from the bottom of the tube after the centrifugation, which should contain just the compound 1, was added to the N2a-RML cells as a normal treatment for 4 days.

As a negative control, we used cells treated just with the vehicle. The cells incubated with 1 µM of compound **1** without the centrifugation in the Nanosep centrifugal device and the N2a-RML treated with 1 µM of compound **1** after the use of Nanosep tubes were utilized as positive controls.

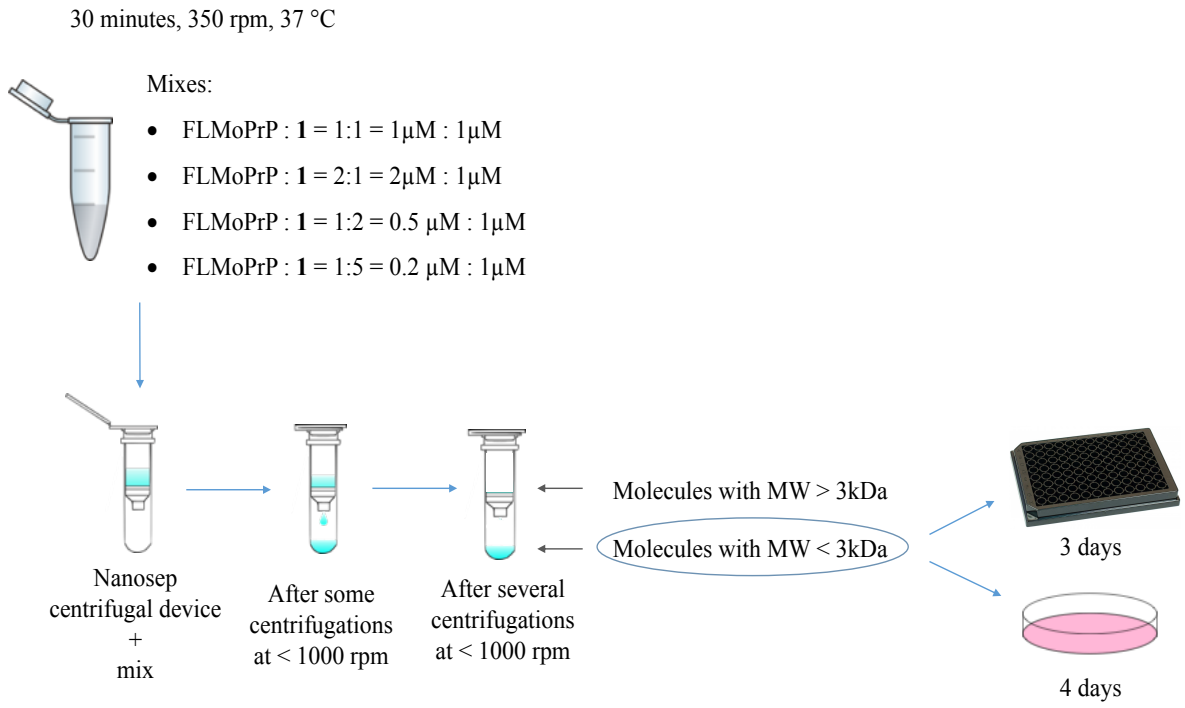

Figure 15. A representation of the competition assay. Different combinations of PrP and compound **1** were incubated for 30 minutes at 350 rpm at 37 °C. After this incubation, the mixes were moved from a normal Eppendorf tube into a Nanosep centrifugal device, which contains a membrane permeable to the molecules with a molecular weight lower than 3 kDa. Several centrifugations at ~1000 rpm allowed the molecules with MW < 3 kDa to cross the membrane and reach the tube's bottom. This solution was used as a treatment and incubated with the N2a-RML cells for 4 days or loaded to a 96-well plate to perform a RTQuIC for 3 days.

After 4 days of treatment, the cells were detached from the Petri's dish and centrifuged. The supernatant was thrown away and the pellet was lysed. WB analysis was used to detect the level of PK-resistant PrP^{Sc} after the treatment. The experiments were repeated three times, so we collected independently three times the cell lysates after the treatment with the solution obtained after the use of the Nanosep device and for each collection we performed a WB. In figure 16 A, it is possible to observe one representative WB obtained. We noticed immediately

that the treatment with compound **1** without the use of Nanosep tube and the treatment with the solution obtained after putting compound **1** alone in the tube caused the same effect on the N2a-RML. In both cases, it is possible to see a strong and a very similar reduction of the PrP^{Sc}. This result confirmed the functionality of the Nanosep device, because it means that compound **1** alone is able to cross the membrane, indeed 3kDa > 416.93Da (**1** MW). Once we concluded this, we checked what happened when the PrP and compound **1** are put in the Nanosep tubes after a pre-incubation at 37 °C with shaking. As it is possible to see in figure 16 A, when the ratio is 2 moles of PrP and 1 mole of compound **1** or 1 mole of PrP and 1 of **1**, the level of PK-resistant PrP^{Sc} is not affected by a strong reduction as it happened after the addition of compound **1** alone.

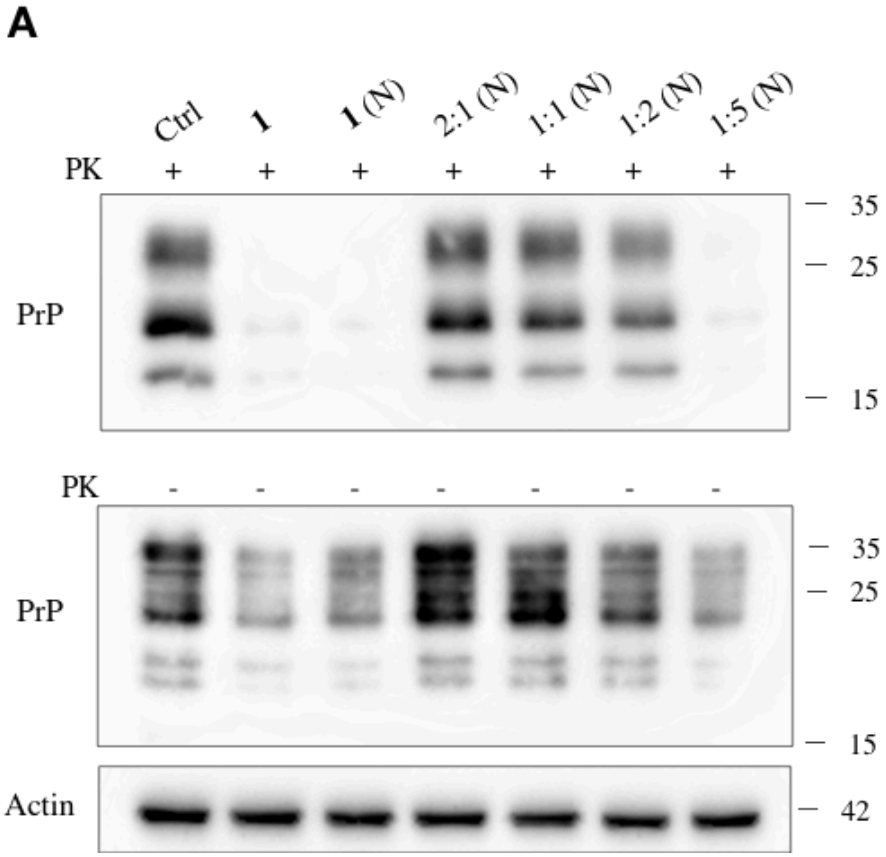

B

Condition	−PK	+PK
Ctrl	100	100
1	48.8 ± 4.5	25.2 ± 7.8
1 (N)	51.7 ± 6.7	22.6 ± 9.5
2:1 (N)	114.4 ± 7.1	108.2 ± 3.8
1:1 (N)	117.6 ± 7.3	90.1 ± 2.9
1:2 (N)	98.4 ± 5.2	65.7 ± 5.7
5:1 (N)	41.0 ± 4.8	13.6 ± 9.0

C

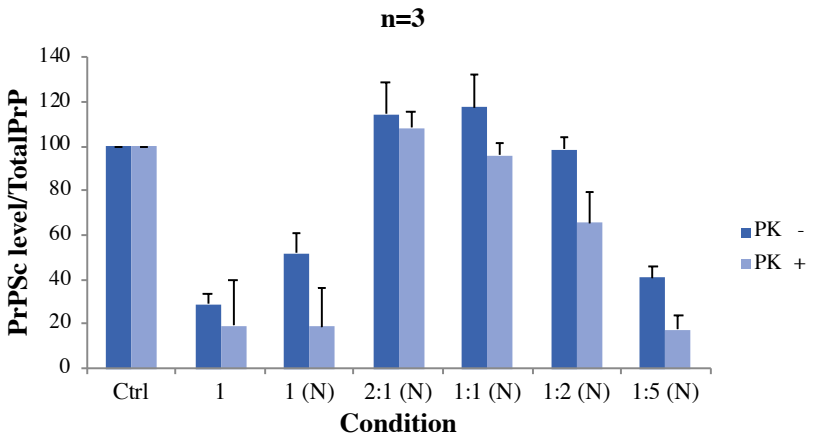

Figure 16. Competition assay in N2a-RML cell line. (**A**) Representative WB of the cell lysates of N2a-RML treated in different conditions. The first line corresponds to the untreated sample, then in order: sample incubated with 1 μM of compound **1**, samples treated with the solution obtained from the bottom part of Nanosep device after several centrifugations of compound **1** alone, cells incubated with the solution obtained from the bottom part of Nanosep device after several centrifugations of a pre-incubated PrP and compound **1** in ratios 2:1, 1:1, 1:2 and 1:5. In the upper part the cell lysates are represented after the PK-digestion (PrP^{Sc}), in the bottom the samples without the PK treatment. (**B**) The table that shows the quantification of the three-independent experiment performed. The values under −PK represent the normalization of the total PrP on the actin, the values under +PK represent the PrP^{Sc} on the total PrP. The values after ± are the standard deviations (SD). (**C**) Histogram of the

values present in the figure 16 B. The total PrP (−PK) is in dark blue, the PrP^{Sc} is in light blue (+PK). The values are normalized to 100%.

This mean that when the two molecules are incubated in the ratios 2:1 and 1:1, there is a binding that does not allow the compound **1** to cross the membrane and it remains attached to the protein, otherwise the results would have the same of those in line **1** and **1 (N)**, since the compound **1** crosses the 3kDa membrane of the Nanosep tubes. After the quantification, this result is even more evident. Treatment directly with compound **1** or after the use of Nanosep device produced a PrP^{Sc} inhibition around 30%, while in the 2:1(N) and 1:1(N) did not cause any or a strong inhibition, the values are around 100% and 90% (figure 16 B and C). When the mixes were prepared in a ratio 1:2, 1 mole of PrP and 2 moles of compound **1**, the level of resistant-PK PrP^{Sc} decrease to 65%, demonstrating that a part of compound **1** was linked to the PrP and the other crossed the Nanosep membrane and affected the level of PrP^{Sc}. We also used a ratio in which the concentration of compound **1** is 5 times higher than the PrP (1:5). The strong inhibition of PrP^{Sc} from 100% to 23.6%, using the ratio 1:5, could be explained again through the binding between PrP and compound **1**. In this case the level of PrP^{Sc} is the same as in the samples treated just with compound **1**, probably because compound **1** is in a large excess causing the majority of it to cross the 3 kDa membrane.

All the results obtained using the different ratios and treating the cells with the solution present in the Nanosep device's bottom, led us to believe that the compound **1** is actually able to bind the PrP.

The level of total PrP followed the same trend of PrP^{Sc}, even if the decrease is less evident. This demonstrates that compound **1** is able to affect just the PrP^{Sc} level, although it binds the PrP^{C}.

3.4.4.2 Competition assay using RTQuIC

RTQuIC analysis was performed using the same solutions obtained after the competition assay, such as in WBs. We decided to check if there were differences in the results using these two different approaches. Both of them have advantages and disadvantages, in the WBs it is possible to see the effect of the treatment on living cells, but it is possible to detect only the presence of PK-resistant PrP^{Sc} and not in low quantity; while in the RTQuIC it is not possible to consider all the other potential factors that are present in cells and that can trigger the spreading of PrP^{Sc}, however, it is able to detect very low amounts of prions.

In the RTQuIC assay, the PrP (23-231) alone was used as a negative control, because it is known that this protein is not able to aggregate in the absence of a seed [258]. Instead, the positive control consists of PrP with a PrP^{Sc} seed. For this purpose, a confluent 10 cm^2 plate of

N2a-RML cells was collected in 50 µl of PBS and then sonicated. The sonicated proteins, present in the sample, were quantified. We tested two different amounts, 1 µg and 10 µg, and tested which one gave the best result in terms of seeding activity and reproducibility. Figure 17 shows the curves using the two different seeds.

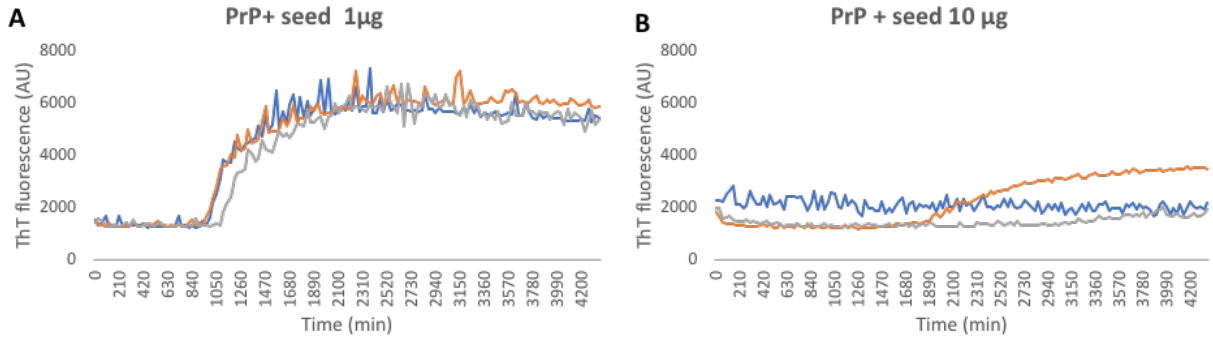

Figure 17. Aggregation curves of PrP (23-231) using 1 µg or 10 µg of the seed. Three independent RTQuIC experiments, each one represented by a specific color. (**A**) The aggregation is promoted by 1 µg of the seed. (**B**) The aggregation of PrP is allowed by 10 µg of the seed.

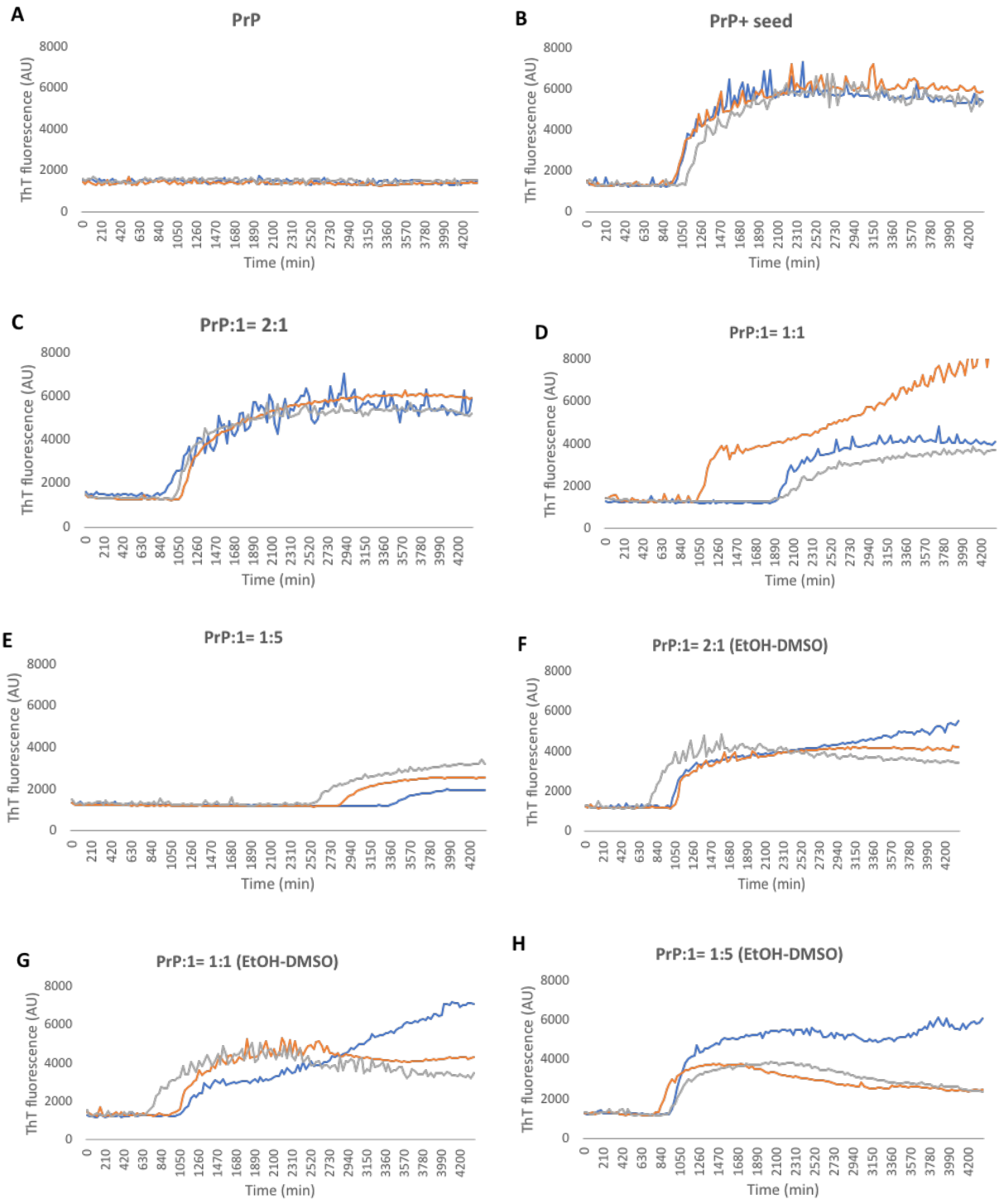

Figure 18. Aggregation curves of PrP after the treatments with the solution obtained with the competition assay. In each plot, the three independent experiments are represented with orange, gray and blue lines. RtQuIC of (**A**) only PrP (23-231), (**B**) PrP with 1 µg of the seed, (**C**) the solution obtained after the pre-incubation and centrifugation in the Nanosep device of the mix consisting PrP and compound **1** in a ratio 2:1, (**D**) 1:1 and (**E**) 1:5. The mock control of the condition (**C**), (**D**) and (**E**) are represented in the (**F**), (**G**) and (**H**).

Using only the seed at 1 μg, we obtained an aggregation curve, for this reason we decided to use 1 μg of seed for the later experiments.

We have set up an RTQuIC protocol, by which the negative control consists of only PrP, that did not show a curve aggregation (Figure 18 A) and the positive control that has a reproducible curve aggregation after about 1050 min (17,5 hours) (Figure 18 B). This protocol was used to check whether the RTQuIC assay could confirm the results obtained in WB analysis.

As before, the same competition assay procedure was performed, but instead of cell treatment, the solutions were added to the 96 well plate.

The experiments confirmed what we saw in the WBs, the solution obtained from the pre-incubation of PrP:compound **1**=2:1 after several centrifugations using the Nanosep device contains prions. Indeed, in figure 18 C it is possible to observe that the aggregation curves have the same ThT fluorescence, around 6000 AU, and the lag phase (1050 min) as the positive control. Also, in the WBs analysis, the level of PrP^{Sc} in this condition was the same of the untreated control. So, these two different assays support our hypothesis that compound **1** binds PrP and so it is not able to cross the 3kDa membrane present on the Nanosep device and to inhibit PrP^{Sc} and its aggregation. When the ratio used is PrP:compound **1**=1:1, the aggregation curves of the three independent experiments are not comparable (figure 18 D). In two experiments (blue and gray lines), the prion aggregation started later than in the positive control, around 1890 (31,5 hours) and the ThT fluorescence is less intense (4500 AU). In the other experiment (orange line) the aggregation started normally, but the fluorescence had an uncommon increase after 2100 min (30 hours), so we decided to not consider it for further analysis. Also, in this case the RTQuIC assay confirmed the WBs results. The increase of the lag phase and the decrease of ThT fluorescence can mean a lower presence of prions and this could correspond to the results of the WB, where after the treatment with the solution obtained from PrP:compound **1**=1:1 mix, the level of PrP^{Sc} started to decrease (figure 16 B and C). These results mean that at the ratio 1:1, almost all molecules of compound **1** bind the PrP, causing just a little inhibition of prions aggregation. In figure 18 E, results from the RTQuIC of PrP treated with the solution obtained after the pre-incubation and centrifugation in the Nanosep tubes of the mix PrP:compound **1** = 1:5 is represented. The delayed aggregation curves (starting around 50 hours) and the low ThT fluorescence (4000 AU) could be due to a low presence of prions, that corresponds exactly to the strong inhibition of the PK-resistant PrP^{Sc} seen in WB. This again could mean that even if compound **1** binds PrP it is in a large excess and can cross the 3kDa membrane. So, when the solution in the bottom of the Nanosep

tube is added to the 96-well plate, there is enough of compound **1** which is able to bind the PrP^C and partially inhibit the aggregation.

We also checked if the EtOH-DMSO reagents, in which the compound **1** is dissolved, affect the reaction. In figure 18 F, G and H the aggregation curves of MoPrP treated with the same amount of EtOH-DMSO present in the corresponding treatments with compound **1** are represented. It is possible to notice that the lag phase and the ThT fluorescence are the same of the positive control (PrP+seed), confirming that the vehicle does not influence the result.

Taking together the WBs and RTQuIC experiments, we conclude that the compound **1** is able to bind the PrP (23-231) and so the cellular prion protein.

3.5 Effect of chronic treatment with compound 1 on N2a-RML cell line

In literature, there are many papers that show the ability of different small molecules to decrease the level of mouse PrP^{Sc} and/or inhibit the prion aggregation [228, 259-262]. Unfortounately, there is still no cure for TSEs. The cause of failure in finding a therapy can be various, such as the inability to cross the BBB, inefficacy in complex model and other many factors that are so far unknown. Another possible cause of the common failure of anti-prion compounds is the drug-prion resistance that can be developed after a continuous chronic treatment and results in a prion strain selection, such as it happened for the Quinacrine treatment in prion-inoculated $MDR^{0/0}$ mice [214].

In order to assess if N2a-RML cells treated with compound **1** can be walking into a strain resistant and to check if it is able to cure the N2a-RML cells, a chronic treatment was performed. We treated N2a-RML cells with 4 μM of compound **1** for 5 passages, that correspond to 20 days of treatment. After this period, the incubation with compound **1** was stopped and the cells were maintained in culture without any treatment for other 5 passages to check if this kind of treatment with compound **1** for 20 days is able to clear completely cells from prions (figure 19).

After 40 days, 10 passages of N2a-RML cells were obtained. For each passage and each experiment, we had 2 Petri dishes, one to continue the experiment, one to collect the cells at each specific step. The cells were detached from the 10 cm^2 Petri dishes, centrifuged for 5 minutes at 1200 rpm and the pellet was collected at -80 °C. This experiment was performed 3

times and each time in double, because we assessed the activity of compound **1** in chronic treatment using both WB analysis and RTQuIC assay.

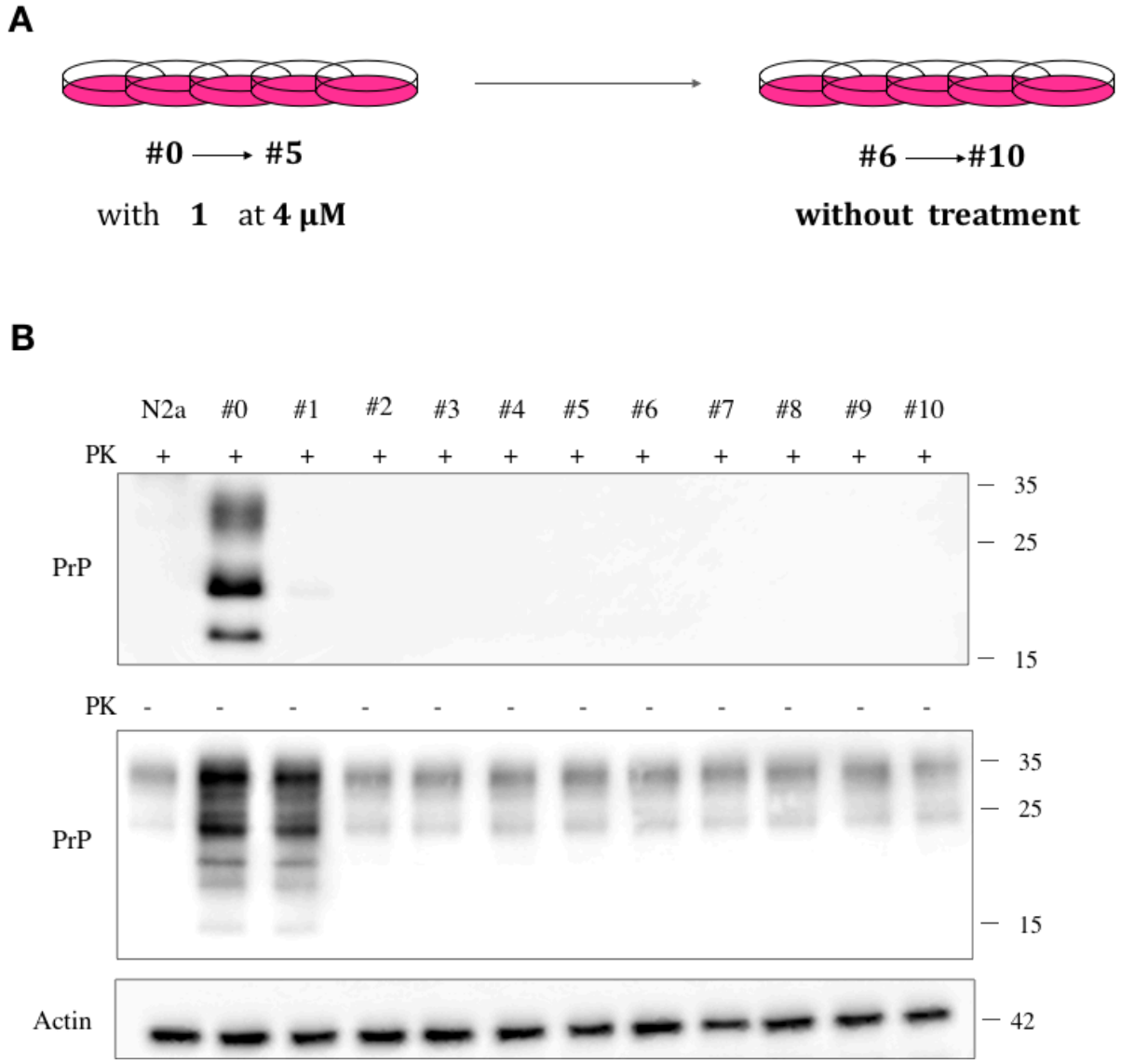

Figure 19. Chronic treatment with compound 1 on N2a-RML cells. (**A**) Schematic representation of the chronic treatment with compound **1**. N2a-RML cells were incubated with 4 µM of compound **1** for 5 passages, after this period the treatment was stopped, and the cells were passaged for others 5 times. (**B**) Representative WB of N2a-RML cell lysates. The upper part corresponds to the PK-resistant PrP^{Sc} detected using the W226 primary antibody. The same was used in the cell lysates not subjected to PK-digestion. In the bottom part the actin is represented, detected using the anti β-actin antibody.

For the WBs, the samples were prepared, as mentioned above, by lysing the pellets in the proper buffer and then boiling in loading buffer. We used the lysates of uninfected N2a cells and the N2a-RML before the treatment (#0) as controls. So, looking at the WB, it is

immediately possible to notice that the PrP^{Sc} in N2a cells is absent, as we expected. Indeed, after PK-digestion no signal was detected. At #0, N2a-RML cells showed the typical pattern of the RML prion strains: the three bands with the mono-glycosylated one more evident. But immediately after the first passage of the 4 μM treatment with compound **1**, PK-resistant PrP^{Sc} is almost absent. In the following passages (from #2 to #10) the PrP^{Sc} is not even detectable. It is very important to focus the attention on the fact that from the #6 to #10 the treatment with 4 μM of compound **1** is stopped. So, the absence of PrP^{Sc} signal in these passages demonstrates that the compound **1** is able to "cure" the N2a-RML cells from prions and that it does not undergo a drug-prion resistance. The level of total PrP was evaluated, observing the samples not treated with PK-digestion. Also, here the uninfected N2a lysate was used as a control. The total PrP does not reflect the results obtained for the PrP^{Sc}, because in this case the #0 and #1 have the exactly same pattern, while in the PK-treated samples the level of PrP was strongly reduced already in the #1. Conversely, the total PrP signal from #2 until #10 is unchanged, but is exactly the same of the PrP^{C} signal from the uninfected N2a cells (line 1). Thus, from the WB it seems that in the samples of N2a-RML with or without the treatment with compound **1** since the #2 the only prion protein present is the cellular prion protein.

The same samples were checked also in the RTQuIC assay. After cell collection, the pellet was dissolved in 50 μl of PBS and then sonicated. The sonicated proteins were quantified, as already mentioned in the previous chapter, and 1 μg of them was used as seed. In figure 20, it is possible to observe the RTQuIC experiments that we performed with the same type of samples used for WBs, to compare the two different approaches. In the control (figure 20 A), without treatment with 4 μM of compound **1**, prion aggregation started after 1050 minutes (17,5 hours). The same result was obtained in the #1, where the ThT fluorescence intensity and the lag phase were identical as in #0. At #1 the aggregation curve obtained in RTQuIC (figure 20 B) reflects the WB result without the digestion with the proteinase K (figure 19 B), but not the result of the PK-digested sample.

While in WB, at #2, in both PK and non-PK treated samples, the PrP^{Sc} seemed completely cleared, in RTQuIC experiments, the lag phase was a little elongated (1260 minutes, 21 hours) and the ThT fluorescence was decreased, for some peaks to 7000 AU in #0 and #1 to 5000 AU in #2 (figure 20 C). The same kind of incongruence was noticed in #3, because in the WB

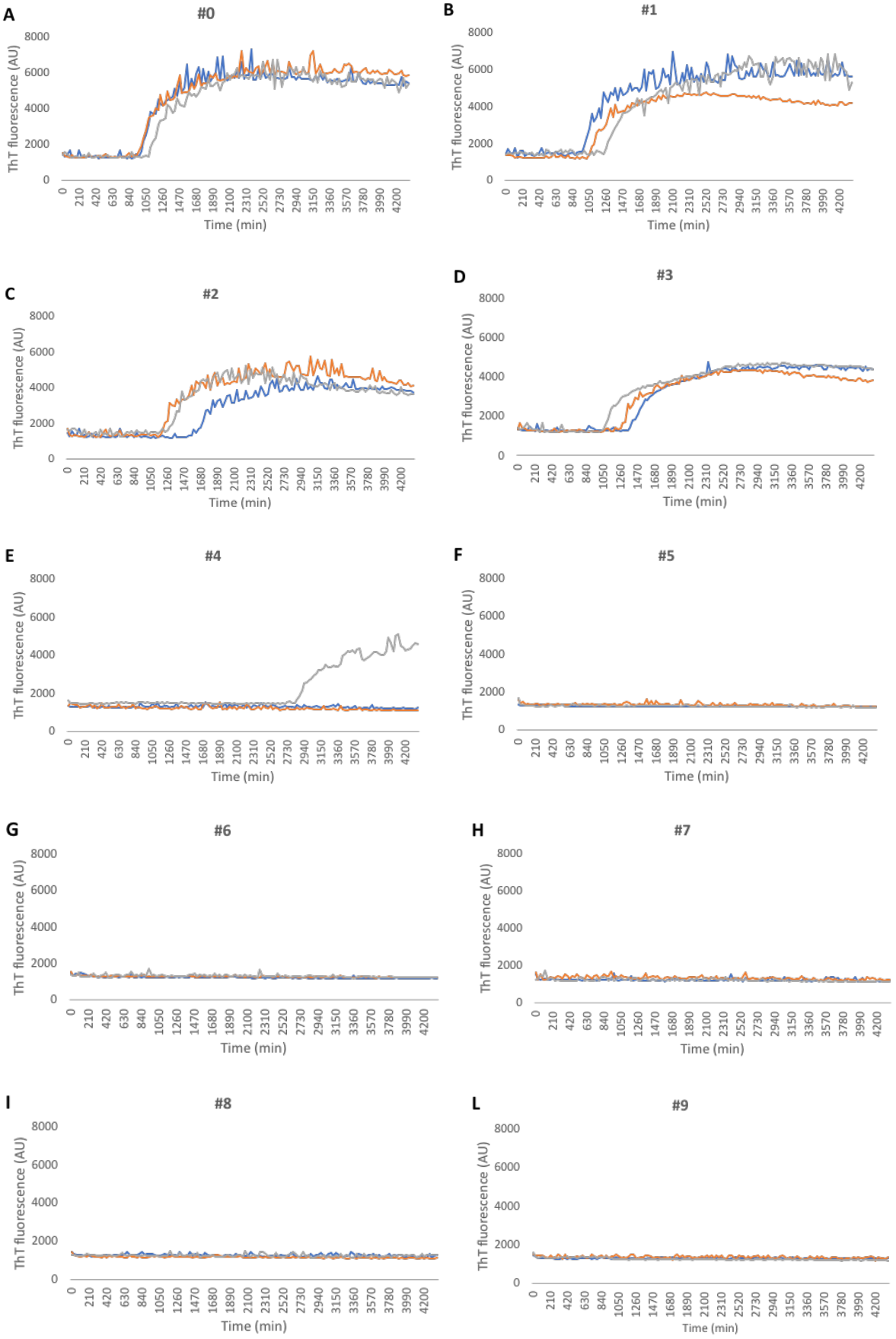
A
#0
B
#1
C
#2
D
#3
E
#4
F
#5
G
#6
H
#7
I
#8
L
#9
ThT fluorescence (AU)
Time (min)
0
2000
4000
6000
8000
0
210
420
630
840
1050
1260
1470
1680
1890
2100
2310
2520
2730
2940
3150
3360
3570
3780
3990
4200

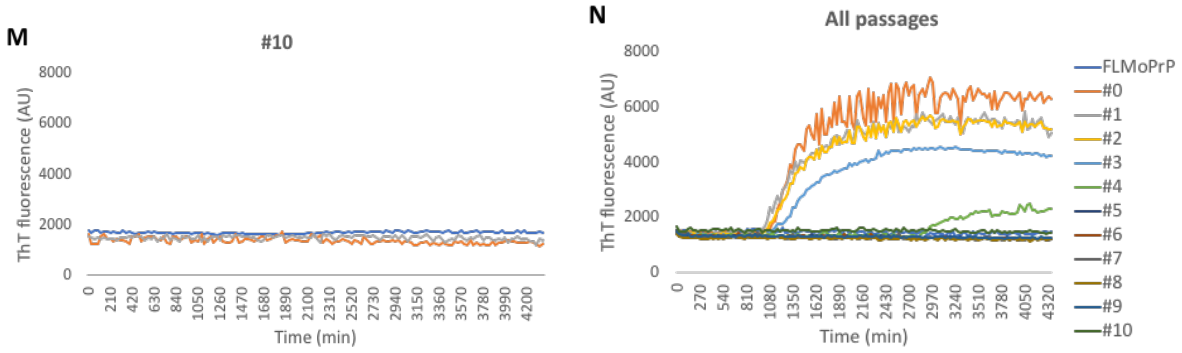

Figure 20. Aggregation curves of PrP after the addition of a seed, obtained from a chronic treatment on N2a-RML cells. In each plot, the three independent experiments are represented with the orange, gray and blue lines. (**A**) RTQuIC performed with 0.2 mg of PrP and using 1 µg of sonicated protein from N2a-RML cells. (**B**) RTQuIC of PrP and using 1 µg of sonicated protein from N2a-RML cells after one treatment with compound **1** at 4µM. In (**C**) the seed derived from a second passage of the treatment with **1**, in (**D**) third passage, in (**E**) fourth, in (**F**) fifth, in (**G**) sixth, in (**H**) seventh, in (**I**) eighth, in (**L**) nineth and in (**M**) the tenth. The average of the three independent experiments of all conditions (**N**).

the PrP^{Sc} signal is completely absent, while in the RTQuIC the presence of prions is evident by the aggregation curve (figure 20 D). At passage #4, in two out of three experiments, the PrP is not able to aggregate, just one sample started the aggregation around 45 hours (2730 minutes) (figure 20 E). We did not consider it as a technical problem, because all the 4 wells of that experiment aggregate at the same time and with the same intensity, rather we believed that after 4 passages of treatment with compound **1**, the prions in almost all the experiment were cleared but it is possible that sometimes they were not completely eliminated. But the fifth treatment with compound **1** is incontrovertibly able to remove all the prions present in the N2a-RML cells and the proof is the absence of an aggregation curve in all the passages after the #5 (figure 20 F-M).

The fact that even after the #5, that corresponds to the treatment interruption, none of the samples demonstrated to have prions using both the RTQuIC assay and WB analysis, confirmed the ability of compound **1** at 4 µM of concentration for 5 times to cure the ScN2a from the RML prion strain.

In figure 20 N, the average of the three independent experiments performed, shows the progressive decrease in prion concentration from #0 to #10. This reduction is mainly characterized with a decrease in the ThT fluorescence, rather than in an increase in the lag phase.

CHAPTER IV

DISCUSSION

Prion diseases or TSEs are triggered by the aberrant misfolding of the cellular prion protein. The conformational change and replication of the PrP^{C} to its pathological isoform (PrP^{Sc}) are followed by aggregation and cell-spreading in the nervous system, that lead to a fatal neurodegeneration. So far, no therapies against TSEs have been identified. Indeed, the scientific community collected just failures and frustration trying to cure or at least modify the course of these disorders. The most common strategy used is the design and screening of small molecules. Many of them were already tested in human clinical trials, but none gave the expected result, probably because the development of anti-prion drugs and the understanding of their mechanism of action are very difficult and challenging tasks.

In collaboration with the Jülich Institute, a quantitative structure-activity relationship model (QSAR) has been developed and by using it a virtual screening of some purchasable compounds has been performed. With the help of the QSAR model, we obtained a library of 10 molecules. The library was then tested *in vitro* study using N2a mouse cell lines chronically infected with prions to assess their anti-prion activity. Compound **1** emerged as the most promising molecule, so we tried to assess its mechanism of action.

In the present section, the results that led to the selection of the compound **1** and to the understanding of its mechanism of action will be discussed.

4.1 Identification of compound 1 as anti-prion agent

The *in silico* screening has been performed through the design of a QSAR model. This model tries to understand the possible relationship that occurs between the activity of a compound and its chemical structure. In order to build a QSAR model, our collaborators used a library of molecules known to have an anti-prion activity on N2a RML cell line [209, 232, 238, 260, 263-269]. The QSAR model is a mathematical equation able to measure the predicted biological

activity of a molecule, in this case the IC_{50} against the PrP^{Sc}. With the aim of identification and selection of new compounds with anti-prion activity, the QSAR model was used to perform a virtual screening of the ZINC database, that contains around 35 million of purchasable, FDA approved molecules. From the compounds obtained with this screening, we selected the ones with a pIC_{50} in the nanomolar range.

The first assessment of the anti-prion activity of the selected library was performed on N2a mouse cells chronically infected with RML prion strain at 1 μM of concentration. In this part of the screening, we tried just to identify the molecules able to reduce the level of PrP^{Sc} that is actually the desired physiological effect, without knowing the mechanism of action. At the beginning, we decided to treat the cells with only one concentration (1μM) of each compound, in order to discard all the molecules that did not reach the intended result. 1 μM was the concentration chosen, because from the QSAR model the molecules were predicted an IC_{50} in the nanomolar range. The cell viability of N2a-RML cells has been tested before to discard any toxic compounds. But none of the compounds showed to have a toxic profile.

The treatments with each compound on N2a-RML cell reveled the strong activity at 1 μM of the compound **1**. Indeed, it is able to induce a reduction of the PK-resistant PrP^{Sc} of more than 65% in N2a-RML cells. Then, we measured, on the same cell line, the IC_{50} of compound **1**, that resulted to be 0.42 μM. Although there is a substantial difference between the pIC_{50} calculated (54.9 nM, table 6) and the IC_{50} calculated on the cells, the strong anti-prion activity of this compound is anyway confirmed. The ability of compound **1** to clear the PrP^{Sc} was confirmed also in other cell lines that we have in our laboratory, the N2a-22L, GT1-RML and GT1-22L. The first part of the *in vitro* screening showed also that compound **1** was the most effective anti-prion agent in the library, as previously evaluated by the QSAR model.

Looking at the structure of this molecule, we noticed that it consists of two main moieties a phenothiazine and a 7-chloro-quinoline fragment, bound by a hydrazine linker (figure 21). We can consider compound **1** as a bivalent ligand with an appropriate linker. The two moieties are very well-known prion recognition motif. In 2001 Korth et al. tested the same phenothiazine moiety and it was already shown to be an anti-prion agent in N2a-RML [209]. They noticed that phenothiazine was not able to inhibit PrP^{Sc} or to strongly decrease its level of PrP^{Sc}, except at 10 μM. So, we concluded that the effect we saw in compound **1** is not only due to the presence of the phenothiazine moiety.

The 7 chloro-quinoline fragment is defined as a prion recognition motif, because several quinoline derivatives were tested as potential anti-prion drugs with excellent results.

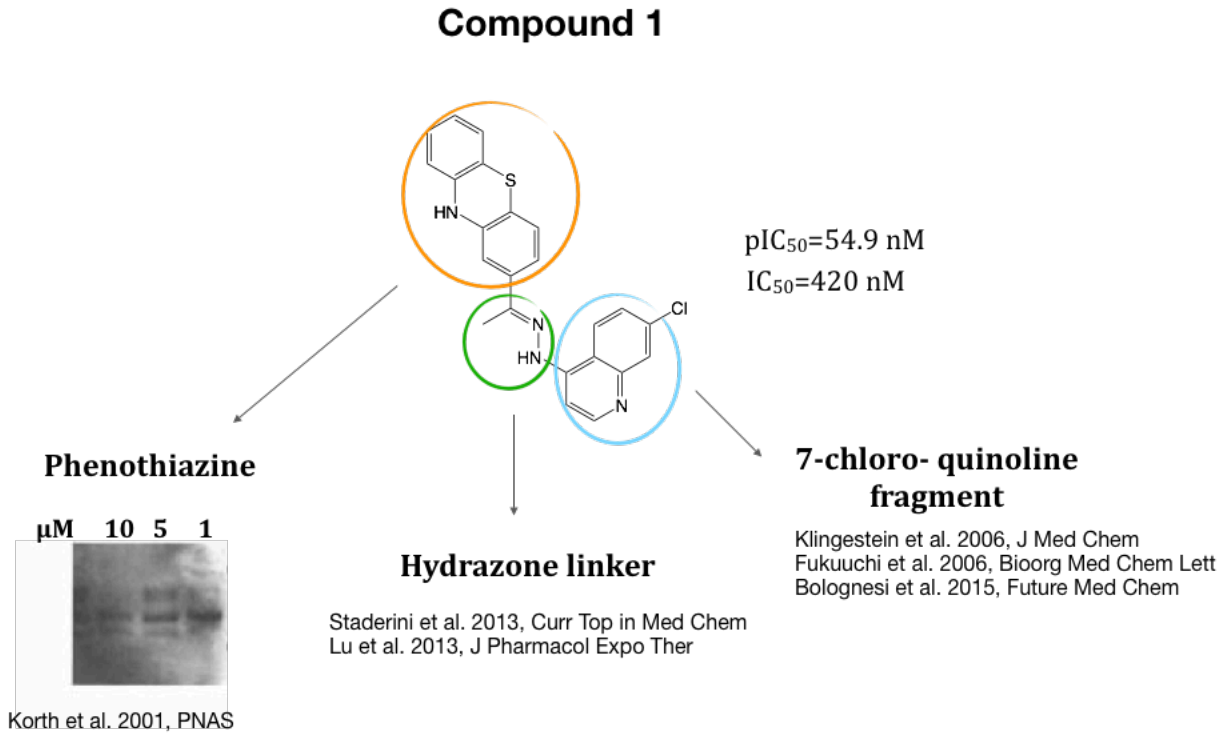

Figure 21. Structure of Compound 1. Compound **1** consists of a phenothiazine, 7-chloro-quinoline fragment and a hydrazone linker. The two moieties are prion recognition structure. Several studies aimed their anti-prion activity. Therefore, the phenothiazine fragment was screened by Korth et al. in 2001.

On the basis of these findings, Korth's group studied the structure-activity relationship of a series of quinoline derivatives as potential antimalarial and anti-prion drugs.

It has been demonstrated that there is a possible overlap between some molecular targets of anti-prion and anti-malarial compounds, because they are able to inhibit at the same nanomolar concentration both scrapie-infected cells and *P. falciparum* growth [264]. As in malarial studies, also bis-quinolines were tested as inhibitors of PrP^{Sc} accumulation in cell cultures. Generally, the bis-quinolines are more effective than normal ones to inhibit the fibril formation *in vitro*, but unfortunately, they show lower efficiency in *in vivo* experiments. Fukuuchi et al. demonstrated that the bis-quinolines tested inhibit PrP biosynthesis and PrP transition to the cell surface and also decrease the amount of substrate available for conversion to PrP^{Sc} [270].

So, we conclude that the strong efficacy of compound **1** to inhibit the prion formation and to decrease the PrP^{Sc} from prion infected cells is due to a synergistic activity of the two moieties and the rigid hydrazone linker between them [271]. Indeed, these three structural elements are very well-known to positively affect the prion inhibition and clearance.

4.2 Understanding the mechanism of action of compound 1

Although, as already mentioned, in literature a variety of small molecules tested *in vitro* screening against prion diseases are present, the majority of them have an unknown mechanism of action. For this reason, when these molecules failed in animal model or human clinical trials, it is very challenging for the scientific community to comprehend the causes of the failure.

The activity of a compound in promoting the clearance of the PrP^{Sc} and inhibit the prion aggregation could be due to several reasons. The two main strategies that an anti-prion agent can adopt in order to obtain the wanted result are:

- The activation of some pathways involved in the prion degradation
- The blocking of the prion conversion

To assess whether the mechanism of action of compound **1** was due to the activation of the lysosome degradation pathway, we treated the N2a-RML cells with 20 mM of NH_4Cl in the presence or absence of 4 μM of compound **1**. Indeed, it is known that the ammonium chloride is able to inhibit the lysosomal degradation and the phagosomes-lysosomes fusion [253, 254]. In the samples treated with just 20 mM of NH_4Cl, the level of PrP^{Sc} was higher than in the untreated control. This result was caused by the inhibition of the lysosomes degradation by NH_4Cl, that induces a slowdown of PrP^{Sc} clearance pathways and so an increase of misfolded proteins, that cannot be cleared as usual. If the compound **1** mechanism of action promotes an increase in the lysosomes degradation, the cells treated with both compound **1** and NH_4Cl should have a higher level of PrP^{Sc} than the samples treated with just compound **1**. But we observed that in the cells treated with just compound **1** and with both compound **1** and NH_4Cl, the level of PrP^{Sc} was almost the same. So, after this experiment we concluded that compound **1** does not affect the lysosome degradation pathways.

Even if in the cells there are other pathways involved in the degradation of misfolded proteins, we decided to assess if the activity of compound **1** causes the blocking of the prion conversion. This blocking could happen in a direct mechanism by which the compound induces the stabilization of PrP^{C} and/or the destabilization of PrP^{Sc} or by an indirect mechanism, by which the molecule interacts with other components of the prion replication.

Starting from the fact that the proteins and the other molecules involved in the mechanism of prion conversion are not so well known, we decided to avoid the screening of the possible protein that can be a target of compound **1** and focus the attention the prion protein.

The structure of PrP^{Sc} is poorly defined [229] and it is very difficult at the same time to imagine a molecule able to bind the PrP^{Sc} and promote its degradation. So, we think that the most sensate approach for an anti-prion agent is to bind PrP^{C} and consequently prevent binding with PrP^{Sc} and in that way, inhibit the prion conversion. On the cellular prion protein, there are some binding sites, where a molecule can stick and block the contact with the PrP^{Sc} avoiding the prion conversation and propagation.

Recently it has been demonstrated that many compounds with a good anti-prion activity, designed to bind the cellular prion protein, exert their function through different mechanisms, rather than just linking to the PrP^{C}. For example, Stincardini et al. in 2017 showed that the antidepressant Chlorpromazine, that was believed to bind the PrP^{C}, actually causes a re-localization of the cellular prion protein from the plasma membrane into intracellular compartments [234]. The chlorpromazine and compound **1** have a similar structure, because they share the phenothiazine moiety (Figure 22). In order to check if this moiety causes the re-localization and to assess if compound **1** has the same behavior, we decided to perform an immunofluorescence assay on uninfected N2a cells labeling the cellular prion protein present on the cell membrane. As it is shown in the results, the treatment with compound **1** does not promote the redistribution of the PrP^{C}. This demonstrates that the phenothiazine moiety is not involved in this mechanism.

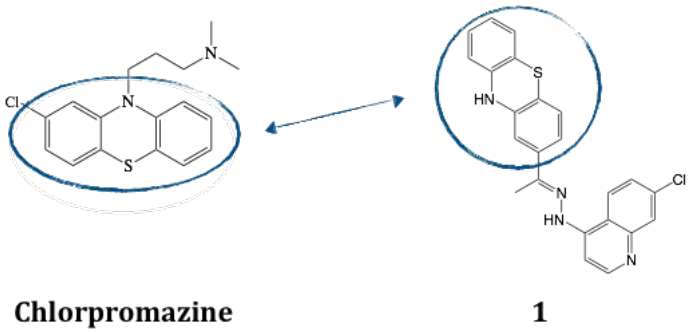

Figure 22. Structures of chlorpromazine and compound 1. These two molecules share the phenothiazine moiety as it is highlighted in the blue circle.

To assess the possibility of a binding between compound **1** and PrP (23-231), we designed a protocol that we named competition assay. In this protocol, we used the PrP (23-231) to mimic the presence of the PrP^{C}. The PrP (23-231) and compound **1** were pre-incubated in tubes in different ratios. The mixes were then centrifuged in the Nanosep device tubes that contain a membrane of 3 kDa. The solution obtained after the centrifugation was used as a treatment in

N2a-RML cells and in RTQuIC experiments. The results obtained using both techniques demonstrate the ability of compound **1** to bind the PrP (23-231).

We also noticed, performing a chronic treatment, that the incubation with compound **1** at 4 μM for 5 passages on N2a-RML cells is able to cure them from prions, because even after additional 5 passages no prions can be detected. This experiment demonstrated at the same time that, as it is already known from the literature, that the RTQuIC assay has a higher sensibility in the detection of prions than WB analysis. In the WBs the PrP^{Sc} was not visible anymore after the second passage, while in the RTQuIC there was a presence of prions until the 4^{th} passage.

In conclusion, in the present thesis we have shown a precise biological protocol for the identification of novel potential therapeutic anti-prion agent. We assessed the ability of the compound **1** to bind the cellular prion protein and so to inhibit the prion conversion.

APPENDIX I

SUPPLEMENTARY RESULTS

PROTEIN EXPRESSION AND PURIFICATION

1. Prion proteins expression in LB medium.

The MoPrP (23-231) was cloned into plasmid pET11a. The recombinant protein was produced in *E. coli* Rosetta2 cells in LB medium.

Large scale protein expression was achieved using a 2 L bioreactor which allows an automated pH, stirrer, temperature and pO2 control. The characteristic fermentation plot of a E. coli BL21(DE3) culture grown in LB medium is presented in Figure 1 B. As we can see from the pO2 curve, bacteria consume oxygen intensively for about 6 hours after induction. The expression in bioreactor allows bacterial yield of 9-10 g/l of paste and a final OD_{600} nm of 7-8. On the basis of expression protocols already established in our laboratory, we confirmed that the PrP expression always results in the formation of insoluble inclusion bodies (Figure 1 C).

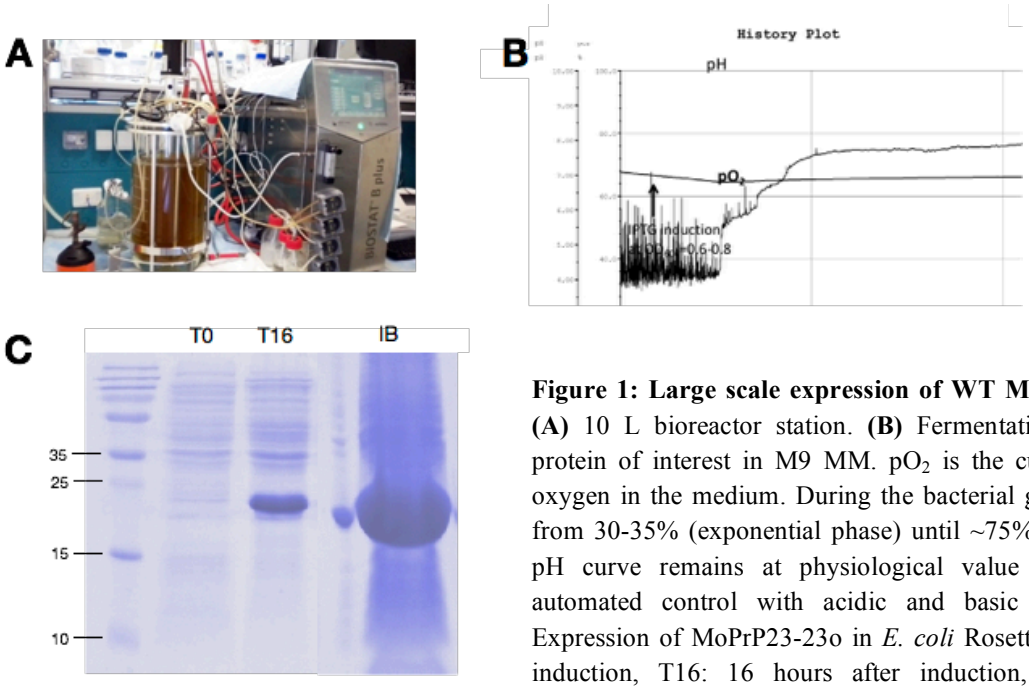

Figure 1: Large scale expression of WT MoPrP (23-231). **(A)** 10 L bioreactor station. **(B)** Fermentation plot of the protein of interest in M9 MM. pO_2 is the curve of soluble oxygen in the medium. During the bacterial growth, it starts from 30-35% (exponential phase) until ~75% (plateau). The pH curve remains at physiological value thanks to the automated control with acidic and basic solutions. **(C)** Expression of MoPrP23-23o in *E. coli* Rosetta 2, T0: before induction, T16: 16 hours after induction, IB: inclusion bodies.

2. Protein purifications and refolding

The main advantages of the expression of prion proteins as insoluble inclusion bodies are the high levels of expression and the possibility to easily purify extremely pure proteins after the first purification step. However, inclusion bodies need to be solubilized in strong denaturant agents (such as GndHCl or urea) before use. Therefore, the purification of the MoPrP(23-231) was achieved in non-native condition due to the presence of 2-6 M GndHCl in the buffers. Another aspect limiting our work with proteins expressed as inclusion bodies is the refolding process. This step always resulted in protein precipitations (approximately 50% of the total amount of refolded protein), which required additional re-solubilization steps with GndHCl of protein precipitates and refolding.

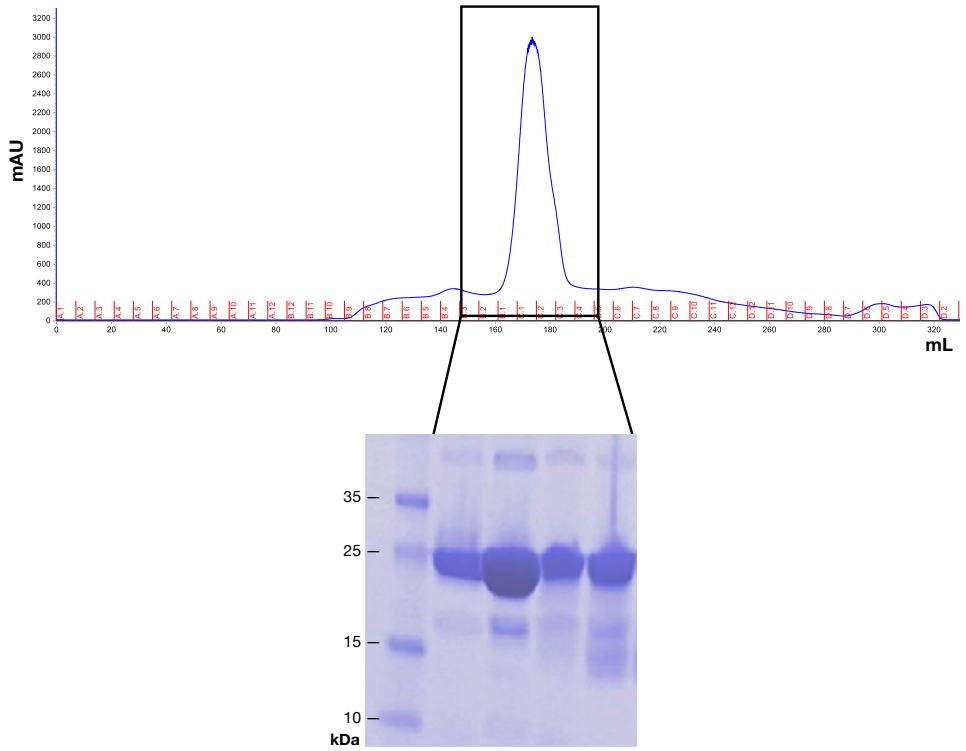

Figure 2. Protein purifications. Size exclusion chromatography profile, and *below* and SDS-PAGE of MoPrP(23-231).

QSAR MODEL

Recent structure deposits (PDB 4MA7, 4MA8) have revealed binding information of tricyclic ligands (Promazine and Chloropromazine) in complex with mouse PrP. Tricyclic derivatives are considered GN8 [125] fused ring derivatives. GN8 is believed to achieve its anti-prion activity by specific binding [125]. The binding site of Promazine derivatives in moPrP is in agreement to docking molecular dynamics NMR studies of GN8. Altogether, it seems that some prion recognition motifs (of GN8 derivatives and 2-3 fused ring analogs) specifically interact with the shallow cavity formed between β1,2 and α2. The particular importance of this region for mediating the PrP^{C}-PrP^{Sc} conversion was later elegantly illustrated by the introduction of a new β0 (residues 118-122) from the HuPrP (23-231)·Nb484 crystal complex (PDB 4KML). Collectively, these studies provide a rationale for investigating the interactions between anti-prion compounds and the shallow cavity in the mechanism of PrP^{C}-PrP^{Sc} conversion. We conducted a brief quantitative structure-activity relationship (QSAR) study to extract binding information from published data using statistical calculations.

Based on the assumption that anti-prion compounds derived from GN8 share similar binding specificity, an anti-prion compound database has been curated from literature for QSAR study. This database contains ca. 200 compounds with known anti-prion activities (IC_{50}) (A total of 14 publications were used, See Table S1). We first subdivided this dataset into 5 datasets by the type of cell line and the incubation time of inhibitors (see Table S2). Next, for each of them we generated a QSAR model. Only the best model, across the five datasets, was considered and therefore presented here. This is the QSAR model based on the ScN2a dataset.

Constitutional, Topological, Geometric, Electrostatic, Hydrophobic and Steric descriptors were generated, plus the drug-likeness (Lipinski's rule of 5 [272]) were calculated by using PaDEL-descriptor [272].

Among those, five selected variables were identified as optimal dimension to develop the final model (see Methods for details). These are LogP, Molecular Weight (MW), No. of Sulfur atoms (Nsulfur), No. Tricyclic scaffold (Ntricyclic) and Molecular size (diameter, D).

The best MLR model obtained with its statistical parameters is shown below:

pIC_{50}= 0.2344(0.066)LogP - 0.0047(0.008)MW + 0.3597(0.1135)NSulfur + 0.6237(0.2450)NTricyclic + 0.2278(0.0242)D + 2.6812

n=38, R^2=0.8028, R^2adj=0.7720, s=0.3440, F=26.0602, Q^2loo=0.7191, Q^2lmo,30%=0.7056, R^2- R^2adj=0.0308

where n is the number of compounds of the training set, R^2 is the coefficient of determination, R^2adj is adjusted R^2 based on the number of independent variables in the model (goodness-of-fit statistic), s is standard error of estimate, F is variance ratio. R^2 (the highest value is in correspondence with the good fitting of the model) should be compared with Q^2_{loo} (Leave One Out - for the highest values and comparable with R^2, the model is robust), $R^2-Q^2_{loo}$ (a lower value is indicative of the model stability), Q^2_{lmo} (leave many out – if comparable with the values of R^2 and Q^2_{LOO} the model is stable).

As shown in the model equation, using only five predictors (molecular descriptors), around 80% of the biological activity of the compounds can be predicted. R^2adj of 0.7720, which is indicative of the convenience to add a new descriptor to the model, is comparable with R^2; Therefore, we can say that no existing overfitting is in the model, as it presents a good fit with minimum number of descriptors.

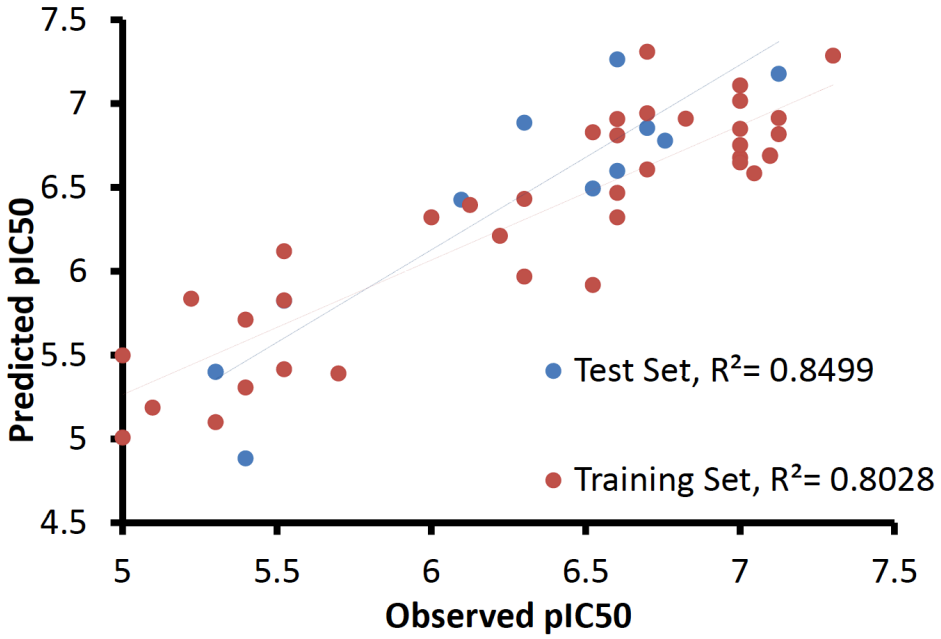

Figure 1. QSAR model obtained by QSARIN software on ScN2a

The fitting and stability of the model were evaluated using internal validation procedures; first, we took into account the parameters of the cross-validation Leave-One-Out (loo). According to the obtained results, it is possible to affirm that the internal predictions are good since the variance explained in the prediction by loo (Q^2loo = 0.7191) has a comparable value with R^2 = 0.8028.

A stronger technique included in the QSARINS is Leaving-Many-Out (lmo), which was developed leaving out the 30% of the dataset to study the behavior of our model. This technique is very useful since in opposite to loo, where for each single disturbance of the data

the influence on the predictions might be weak; in lmo technique, each perturbation of data is significant. The model is considered stable because the R^2 = 0.8028 and Q^2lmo=0.7191 values are comparable.

Virtual Screening

With the aim of performing identification/selection of new compounds with anti-prion activity, the obtained model was used for the virtual screening of the ZINC database (35 million purchasable, http://zinc.docking.org FDA approved molecules). We first filtered the database only considering the ones similar to the chloroquine moiety. Around 5000 compounds were retrieved. Among those, only 2039 compounds respect the Lipinsky rule of 5 and 2029 of these were within the Applicability Domain of our proposed model. The predicted pIC_{50} is shown in Figure 2. The compounds with highest predicted pIC_{50} were tested in the experiments.

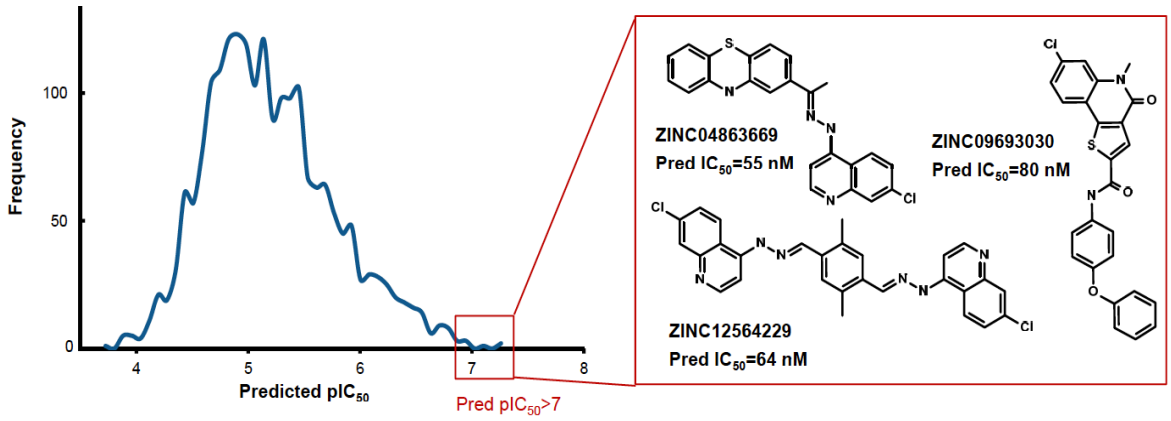

Figure 2. Distribution of the predicted pIC_{50} among the 2029 compounds extracted from the ZINC database. Example of compounds with highest predicted pIC_{50} are highlighted in the red box.

APPENDIX II

SUPPLEMENTARY MATERIALS AND METHODS

Model generation. For the calculation of molecular descriptors, PaDEL-descriptor [Yap CW 2011 J Comput Chem 32 1466 1474] Molinspiration [www.molinspiration.com] were used.
Given the great number of variables calculated, the data were subjected to a filtration process using the QSARINS software [237] and the descriptors that possessed more than 95% of constant values and had more than 90% correlation were eliminated. After that, only 33 descriptors were considered in the selection process to develop the model.
It would be ideal to use all combinations of available descriptors for the calculation of the models; however, the number of combinations is usually so great that it is impossible to calculate all models. Therefore, to reduce the model computation time, all combinations were preliminarily used with only a small number of descriptors per model, in order to explore all combinations of low dimension, using the *all subset* technique, and, later, a *genetic algorithm* (GA) method was applied to develop models based on a larger number of descriptors.
The Multiple Linear Regression (MLR) is the process that we used to obtain a linear relationship between the pIC_{50} values against mPrP and the molecular descriptors, using ordinary least squares (OLS) algorithm in the QSARINS (QSAR-Insubria) software .
For selecting the best model, the equations were ordered by QSARINS, showing the optimum models according to R^2 (the highest value is in correspondence with the good fitting of the model), Q^2_{LOO} (Leave One Out - for the highest values and comparable with R^2, the model is robust), $R^2-Q^2_{LOO}$ (a lower value is indicative of the model stability) and RMSE (should be small and as close as possible between calculation of training, training prediction by LOO and external prediction series XGX).
Assessment of lowest number of variables. We developed several MLR models with low multicollinearity between descriptors and good correlation with the modeled response. The generated population of models were plotted as mean values of R^2 and Q^2_{loo} (with their standard deviations) versus the number of variables of the model, in order to evaluate the

performance of the models against their size and to avoid overfitted models. The values of R^2 and Q^2_{loo} rose as new descriptors and were added to the model. The highest values were achieved by the models of seven variables; however, the models with five variables showed very similar values with three less predictive variables (data not shown) XGX. We therefore selected five variables as optimal dimension to develop the final model. These are LogP, Molecular Weight (MW), No. of Sulfur atoms (Nsulfur), No. Tricyclic scaffold (Ntricyclic) and Molecular size (diameter, D).

Internal validation strategies. In order to control the robustness of the model, we carried out internal validation strategies. First, we used the Q^2_{loo} criterion applying the technique of cross-validation (CV), i.e., iteratively excluding a compound from the dataset (*Leaving One Out*, loo), and then calculating a model with the remaining compounds and making the prediction for the excluded molecule. If the internal predictions were good, the value of Q^2_{loo} was high and comparable with R^2, so the model was considered internally stable and robust. However, a disturbance of a single compound might be too weak to show the real model robustness. QSARINS further includes a stronger technique: *Leaving Many Out* (lmo), which allowed studying the behavior of the model when a larger number of compounds (in this case 30% of the compounds) were excluded. The model was considered stable if the values of R^2 and Q^2 calculated for each iteration of the lmo experiment and their averages (R^2_{lmo} and Q^2_{lmo}) were comparable with the values of R^2 and Q^2_{LOO} of the model.

Validation of the model accordingly to the OECD principles (XGX to be decided XGX). Algorithm QSARINS is a friendly software that can validate the obtained model using OECD principles, in order to increase the confidence of the predictions. According to these principles, the model should have the following: (1) a defined endpoint; (2) an unambiguous algorithm; (3) a defined domain of applicability; (4) appropriate measures of goodness-of-fit, robustness and predictability; and (5) a mechanistic interpretation, if possible [274].

Principle 1 is associated with the endpoint definition where it refers to a physicochemical, biological or pharmacological property that can be measured and, therefore, modeled. The aim of this principle is to ensure transparency in the measurement point predicted by a given model. The endpoint in this work was pIC50 of the compounds against moPrP.

According to *Principle 2*, QSAR models can be expressed in the form of unambiguous algorithms, considering that the algorithm model is the way of relating the descriptors of the chemical structure and activity (endpoint of the model) through mathematical models or rules based on the knowledge developed by one or more experts. The used algorithm was a mathematical model of Multiple Linear Regression detailed in the previous section.

Insubria graph was used for DA (*Principle 3*). This was very useful to assess the reliability of the predictions of experimental compounds, lacking response, and to compare with the predictions of the database XGX.

Following the *Principle 4*, the goodness of the fit was evaluated using the coefficient of determination R^2 and a modified form R^2_{adj} that also evaluated the effectiveness by adding a new descriptor to the model. While the robustness was evaluated with internal validation strategies (see above).

The mechanistic interpretation of the model (*Principle 5*), although it is not mandatory, it is very desirable. In our work, we developed a general interpretation of the model based on docking calculation XGX.

-In order to demonstrate that the model was not the result of a chance correlation, we applied the *Y-scrambling* procedure. In this procedure, responses are placed randomly, so there was no correlation with the descriptors and, as a result, the performance of the models should decay drastically. In this case, if the model in the validation process was good, the values of R^2 and Q^2 of each iteration, and their averages (R^2_{YS} and Q^2_{YS}) must be lesser and lesser with respect to the values of the model.

-In order to assess the model's ability to predict new compounds, an external validation was carried out. The procedure was performed by applying the model equation obtained with the training set, a predictive dataset, i.e., excluding compounds that have never been used for the calculation model. Model performance was evaluated by different criteria such as $RMSE_{ext}$, Q^2-F1, Q^2-F2, Q^2-F3, r^2M, Δr^2_m, CCC, and Golbraikh and Tropsha methods.

Supporting Information

Table S1. Published papers relative to the database's molecules

Cell line	References
GT-FK	• Kimura, T. et al. (2011) Synthesis of GN8 derivatives and evaluation of their antiprion activity in TSE- infected cells. Bioorg. Med. Chem. LeJ. 21, 1502–7 • Kimura, T. et al. (2011) Synthesis of 9-substituted 2,3,4,9-tetrahydro-1H-carbazole derivatives and evaluation of their anti-prion activity in TSE-infected cells. Eur. J. Med. Chem. 46, 5675–5679
ScGT1	• Thuy, N.T.H. (2010), Investigation on anti-prion, neuroprotective and anti-cholinesterase activities of acridine derivatives, National University of Singapore • Korth, C. et al. (2001) ticridine and phenothiazine derivatives as pharmacotherapeutics for prion disease. Proc. Natl. ticad. Sci. U. S. ti. 98, 9836–9841 • Vogtherr, M. et al. (2003) tintimalarial drug quinacrine binds to C-terminal helix of cellular prion protein. J. Med. Chem. 46, 3563–4 • lingenstein, R. et al. (2006) Similar structure-activity relationships of quinoline derivatives for antiprion and antimalarial effects. J. Med. Chem. 49, 5300–5308 • Nguyen Thi, H.T. et al. (2008) tintiprion activity of functionalized 9-aminoacridines related to quinacrine. Bioorganic Med. Chem. 16, 6737–6746
ScN2a	• Gallardo-Godoy, A. et al. (2011) 2-timinothiazoles tis Therapeutic Leads for Prion Diseases. J. Med. Chem. 54, 1010–1021 • Li, Z. et al. (2013) 2-timinothiazoles with Improved Pharmacotherapeutic Properties for Treatment of Prion Disease. ChemMedChem 8, 847–857
ScN2a	• Staderini, M. et al. (2013) A fluorescent styrylquinoline with combined therapeutic and diagnostic activities against Alzheimer's and Prion diseases. ACS Med. ... 4, 225–9
cl3	• Staderini, M. et al. (2013) A fluorescent styrylquinoline with combined therapeutic and diagnostic activities against Alzheimer's and Prion diseases. ACS Med. ... 4, 225–9 • Bongarzone, S. et al. (2010) Parallel Synthesis, Evaluation, and Preliminary Structure−AcTvity RelaAonship of 2,5-Diamino-1,4-benzoquinones as a Novel Class of Bivalent Anti-Prion Compound. J. Med. Chem. 53, 8197–8201 • Bolognesi, M.L. et al. (2010) Discovery of a class of diketopiperazines as antiprion compounds. ChemMedChem 5, 1324–34 • Bongarzone, S. et al. (2011) Hybrid lipoic acid derivatives to attack prion disease on multiple fronts. ChemMedChem 6, 601–5 • Tran, H.N.A. et al. (2010) Synthesis and evaluation of a library of 2,5-bisdiamino-benzoquinone derivaAves as probes to modulate protein–protein interactions in prions. Bioorg. Med. Chem. LeJ. 20, 1866–1868

Table S2. Database subgroups.

	Cell line	Drug treatment	No. of compounds	EC_{50} range (μM)	SE*
GTFK	GT-FK	3 days	11	0.51-8.54	0.01-0.36
GT1	ScGT1	5 days	23	0.15-15.8	0.01-0.9
N2aa	ScN2a	3 days	59	0.05-10	n/a
N2ab	ScN2a	6 days	41	0.021-4.24	n/a
cl3	ScN2a-cl3	5 days	85	0.051-15.644	0.007-0.42

Standard error of mean, SE

References:

1. Soto, C., *Prion hypothesis: the end of the controversy?* Trends Biochem Sci, 2011. **36**(3): p. 151-8.
2. Levenson, R.W., V.E. Sturm, and C.M. Haase, *Emotional and behavioral symptoms in neurodegenerative disease: a model for studying the neural bases of psychopathology.* Annu Rev Clin Psychol, 2014. **10**: p. 581-606.
3. Hardy, J.A. and G.A. Higgins, *Alzheimer's disease: the amyloid cascade hypothesis.* Science, 1992. **256**(5054): p. 184-5.
4. Goedert, M., M.G. Spillantini, and R.A. Crowther, *Tau proteins and neurofibrillary degeneration.* Brain Pathol, 1991. **1**(4): p. 279-86.
5. Spillantini, M.G., et al., *Alpha-synuclein in Lewy bodies.* Nature, 1997. **388**(6645): p. 839-40.
6. Rosen, D.R., *Mutations in Cu/Zn superoxide dismutase gene are associated with familial amyotrophic lateral sclerosis.* Nature, 1993. **364**(6435): p. 362.
7. Neumann, M., et al., *Ubiquitinated TDP-43 in frontotemporal lobar degeneration and amyotrophic lateral sclerosis.* Science, 2006. **314**(5796): p. 130-3.
8. Prusiner, S.B., et al., *Prion protein biology.* Cell, 1998. **93**(3): p. 337-48.
9. Martin, J. and F.U. Hartl, *Molecular chaperones in cellular protein folding.* Bioessays, 1994. **16**(9): p. 689-92.
10. Stefani, M., *Protein misfolding and aggregation: new examples in medicine and biology of the dark side of the protein world.* Biochim Biophys Acta, 2004. **1739**(1): p. 5-25.
11. Sunde, M. and C. Blake, *The structure of amyloid fibrils by electron microscopy and X-ray diffraction.* Adv Protein Chem, 1997. **50**: p. 123-59.
12. Brown, P., *Reflections on a half-century in the field of transmissible spongiform encephalopathy.* Folia Neuropathol, 2009. **47**(2): p. 95-103.
13. Griffith, J.S., *Self-replication and scrapie.* Nature, 1967. **215**(5105): p. 1043-4.
14. Prusiner, S.B., *Novel proteinaceous infectious particles cause scrapie.* Science, 1982. **216**(4542): p. 136-44.
15. Wells, G.A., et al., *A novel progressive spongiform encephalopathy in cattle.* Vet Rec, 1987. **121**(18): p. 419-20.
16. Detwiler, L.A., *Scrapie.* Rev Sci Tech, 1992. **11**(2): p. 491-537.
17. Williams, E.S. and S. Young, *Spongiform encephalopathy of Rocky Mountain elk.* J Wildl Dis, 1982. **18**(4): p. 465-71.
18. Hartsough, G.R. and D. Burger, *Encephalopathy of mink. I. Epizootiologic and clinical observations.* J Infect Dis, 1965. **115**(4): p. 387-92.
19. Medori, R., et al., *Fatal familial insomnia, a prion disease with a mutation at codon 178 of the prion protein gene.* N Engl J Med, 1992. **326**(7): p. 444-9.
20. Masters, C.L., D.C. Gajdusek, and C.J. Gibbs, Jr., *Creutzfeldt-Jakob disease virus isolations from the Gerstmann-Straussler syndrome with an analysis of the various forms of amyloid plaque deposition in the virus-induced spongiform encephalopathies.* Brain, 1981. **104**(3): p. 559-88.
21. Gajdusek, D.C., C.J. Gibbs, and M. Alpers, *Experimental transmission of a Kuru-like syndrome to chimpanzees.* Nature, 1966. **209**(5025): p. 794-6.
22. Ladogana, A., et al., *Mortality from Creutzfeldt-Jakob disease and related disorders in Europe, Australia, and Canada.* Neurology, 2005. **64**(9): p. 1586-91.
23. Aguzzi, A., *Prion diseases of humans and farm animals: epidemiology, genetics, and pathogenesis.* J Neurochem, 2006. **97**(6): p. 1726-39.
24. Prusiner, S.B. and S.J. DeArmond, *Prion diseases and neurodegeneration.* Annu Rev Neurosci, 1994. **17**: p. 311-39.

25. Aguzzi, A. and M. Polymenidou, *Mammalian prion biology: one century of evolving concepts.* Cell, 2004. **116**(2): p. 313-27.
26. Basler, K., et al., *Scrapie and cellular PrP isoforms are encoded by the same chromosomal gene.* Cell, 1986. **46**(3): p. 417-28.
27. Lee, I.Y., et al., *Complete genomic sequence and analysis of the prion protein gene region from three mammalian species.* Genome Res, 1998. **8**(10): p. 1022-37.
28. Premzl, M., et al., *The prion protein gene: identifying regulatory signals using marsupial sequence.* Gene, 2005. **349**: p. 121-34.
29. McKinley, M.P., et al., *Developmental expression of prion protein gene in brain.* Dev Biol, 1987. **121**(1): p. 105-10.
30. Lieberburg, I., *Developmental expression and regional distribution of the scrapie-associated protein mRNA in the rat central nervous system.* Brain Res, 1987. **417**(2): p. 363-6.
31. Rapoport, T.A., *Protein translocation across the eukaryotic endoplasmic reticulum and bacterial plasma membranes.* Nature, 2007. **450**(7170): p. 663-9.
32. Hebert, D.N. and M. Molinari, *In and out of the ER: protein folding, quality control, degradation, and related human diseases.* Physiol Rev, 2007. **87**(4): p. 1377-408.
33. Hegde, R.S., et al., *A transmembrane form of the prion protein in neurodegenerative disease.* Science, 1998. **279**(5352): p. 827-34.
34. Stewart, R.S., B. Drisaldi, and D.A. Harris, *A transmembrane form of the prion protein contains an uncleaved signal peptide and is retained in the endoplasmic Reticulum.* Mol Biol Cell, 2001. **12**(4): p. 881-9.
35. Stahl, N., et al., *Glycosylinositol phospholipid anchors of the scrapie and cellular prion proteins contain sialic acid.* Biochemistry, 1992. **31**(21): p. 5043-53.
36. Abid, K., R. Morales, and C. Soto, *Cellular factors implicated in prion replication.* FEBS Lett, 2010. **584**(11): p. 2409-14.
37. Sarnataro, D., et al., *PrP(C) association with lipid rafts in the early secretory pathway stabilizes its cellular conformation.* Mol Biol Cell, 2004. **15**(9): p. 4031-42.
38. Taylor, D.R., et al., *Assigning functions to distinct regions of the N-terminus of the prion protein that are involved in its copper-stimulated, clathrin-dependent endocytosis.* J Cell Sci, 2005. **118**(Pt 21): p. 5141-53.
39. Taylor, D.R. and N.M. Hooper, *The prion protein and lipid rafts.* Mol Membr Biol, 2006. **23**(1): p. 89-99.
40. Sunyach, C., et al., *The mechanism of internalization of glycosylphosphatidylinositol-anchored prion protein.* Embo j, 2003. **22**(14): p. 3591-601.
41. Aguzzi, A. and A.M. Calella, *Prions: protein aggregation and infectious diseases.* Physiol Rev, 2009. **89**(4): p. 1105-52.
42. Lawson, V.A., et al., *Prion protein glycosylation.* J Neurochem, 2005. **93**(4): p. 793-801.
43. Hornemann, S., C. Schorn, and K. Wuthrich, *NMR structure of the bovine prion protein isolated from healthy calf brains.* EMBO Rep, 2004. **5**(12): p. 1159-64.
44. Christen, B., et al., *NMR structure of the bank vole prion protein at 20 degrees C contains a structured loop of residues 165-171.* J Mol Biol, 2008. **383**(2): p. 306-12.
45. Zahn, R., et al., *NMR solution structure of the human prion protein.* Proc Natl Acad Sci U S A, 2000. **97**(1): p. 145-50.
46. Lopez Garcia, F., et al., *NMR structure of the bovine prion protein.* Proc Natl Acad Sci U S A, 2000. **97**(15): p. 8334-9.
47. Antonyuk, S.V., et al., *Crystal structure of human prion protein bound to a therapeutic antibody.* Proc Natl Acad Sci U S A, 2009. **106**(8): p. 2554-8.

48. Eghiaian, F., et al., *Insight into the PrPC-->PrPSc conversion from the structures of antibody-bound ovine prion scrapie-susceptibility variants.* Proc Natl Acad Sci U S A, 2004. **101**(28): p. 10254-9.
49. Abskharon, R.N., et al., *Probing the N-terminal beta-sheet conversion in the crystal structure of the human prion protein bound to a nanobody.* J Am Chem Soc, 2014. **136**(3): p. 937-44.
50. Legname, G., *Elucidating the function of the prion protein.* PLoS Pathog, 2017. **13**(8): p. e1006458.
51. Caughey, B.W., et al., *Secondary structure analysis of the scrapie-associated protein PrP 27-30 in water by infrared spectroscopy.* Biochemistry, 1991. **30**(31): p. 7672-80.
52. Gasset, M., et al., *Perturbation of the secondary structure of the scrapie prion protein under conditions that alter infectivity.* Proc Natl Acad Sci U S A, 1993. **90**(1): p. 1-5.
53. Viles, J.H., M. Klewpatinond, and R.C. Nadal, *Copper and the structural biology of the prion protein.* Biochem Soc Trans, 2008. **36**(Pt 6): p. 1288-92.
54. Pan, T., et al., *Cell-surface prion protein interacts with glycosaminoglycans.* Biochem J, 2002. **368**(Pt 1): p. 81-90.
55. Yin, S., et al., *Human prion proteins with pathogenic mutations share common conformational changes resulting in enhanced binding to glycosaminoglycans.* Proc Natl Acad Sci U S A, 2007. **104**(18): p. 7546-51.
56. Mashima, T., et al., *Unique quadruplex structure and interaction of an RNA aptamer against bovine prion protein.* Nucleic Acids Res, 2009. **37**(18): p. 6249-58.
57. Taylor, D.R. and N.M. Hooper, *The low-density lipoprotein receptor-related protein 1 (LRP1) mediates the endocytosis of the cellular prion protein.* Biochem J, 2007. **402**(1): p. 17-23.
58. Muramoto, T., et al., *Recombinant scrapie-like prion protein of 106 amino acids is soluble.* Proc Natl Acad Sci U S A, 1996. **93**(26): p. 15457-62.
59. Aguzzi, A., F. Baumann, and J. Bremer, *The prion's elusive reason for being.* Annu Rev Neurosci, 2008. **31**: p. 439-77.
60. Brown, D.R., J. Herms, and H.A. Kretzschmar, *Mouse cortical cells lacking cellular PrP survive in culture with a neurotoxic PrP fragment.* Neuroreport, 1994. **5**(16): p. 2057-60.
61. Forloni, G., et al., *Neurotoxicity of a prion protein fragment.* Nature, 1993. **362**(6420): p. 543-6.
62. Barmada, S., et al., *GFP-tagged prion protein is correctly localized and functionally active in the brains of transgenic mice.* Neurobiol Dis, 2004. **16**(3): p. 527-37.
63. Moya, K.L., et al., *Immunolocalization of the cellular prion protein in normal brain.* Microsc Res Tech, 2000. **50**(1): p. 58-65.
64. Kanaani, J., et al., *Recombinant prion protein induces rapid polarization and development of synapses in embryonic rat hippocampal neurons in vitro.* J Neurochem, 2005. **95**(5): p. 1373-86.
65. Linden, R., et al., *Physiology of the prion protein.* Physiol Rev, 2008. **88**(2): p. 673-728.
66. Manson, J., et al., *The prion protein gene: a role in mouse embryogenesis?* Development, 1992. **115**(1): p. 117-22.
67. Hidaka, K., et al., *The cellular prion protein identifies bipotential cardiomyogenic progenitors.* Circ Res, 2010. **106**(1): p. 111-9.
68. Tremblay, P., et al., *Developmental expression of PrP in the post-implantation embryo.* Brain Res, 2007. **1139**: p. 60-7.
69. Hirsch, T.Z., S. Martin-Lanneree, and S. Mouillet-Richard, *Functions of the Prion Protein.* Prog Mol Biol Transl Sci, 2017. **150**: p. 1-34.

70. Benvegnu, S., I. Poggiolini, and G. Legname, *Neurodevelopmental expression and localization of the cellular prion protein in the central nervous system of the mouse.* J Comp Neurol, 2010. **518**(11): p. 1879-91.
71. Viegas, P., et al., *Junctional expression of the prion protein PrPC by brain endothelial cells: a role in trans-endothelial migration of human monocytes.* J Cell Sci, 2006. **119**(Pt 22): p. 4634-43.
72. Bueler, H., et al., *Normal development and behaviour of mice lacking the neuronal cell-surface PrP protein.* Nature, 1992. **356**(6370): p. 577-82.
73. Manson, J.C., et al., *129/Ola mice carrying a null mutation in PrP that abolishes mRNA production are developmentally normal.* Mol Neurobiol, 1994. **8**(2-3): p. 121-7.
74. Nishida, N., et al., *A mouse prion protein transgene rescues mice deficient for the prion protein gene from purkinje cell degeneration and demyelination.* Lab Invest, 1999. **79**(6): p. 689-97.
75. Sakaguchi, S., et al., *Loss of cerebellar Purkinje cells in aged mice homozygous for a disrupted PrP gene.* Nature, 1996. **380**(6574): p. 528-31.
76. Moore, R.C., et al., *Ataxia in prion protein (PrP)-deficient mice is associated with upregulation of the novel PrP-like protein doppel.* J Mol Biol, 1999. **292**(4): p. 797-817.
77. Rossi, D., et al., *Onset of ataxia and Purkinje cell loss in PrP null mice inversely correlated with Dpl level in brain.* Embo j, 2001. **20**(4): p. 694-702.
78. Li, A., et al., *Identification of a novel gene encoding a PrP-like protein expressed as chimeric transcripts fused to PrP exon 1/2 in ataxic mouse line with a disrupted PrP gene.* Cell Mol Neurobiol, 2000. **20**(5): p. 553-67.
79. Herms, J., et al., *Evidence of presynaptic location and function of the prion protein.* J Neurosci, 1999. **19**(20): p. 8866-75.
80. Siskova, Z., et al., *Brain region specific pre-synaptic and post-synaptic degeneration are early components of neuropathology in prion disease.* PLoS One, 2013. **8**(1): p. e55004.
81. Wulf, M.A., A. Senatore, and A. Aguzzi, *The biological function of the cellular prion protein: an update.* BMC Biol, 2017. **15**(1): p. 34.
82. Tobler, I., et al., *Altered circadian activity rhythms and sleep in mice devoid of prion protein.* Nature, 1996. **380**(6575): p. 639-42.
83. Mastrianni, J.A., et al., *Prion protein conformation in a patient with sporadic fatal insomnia.* N Engl J Med, 1999. **340**(21): p. 1630-8.
84. Lugaresi, E., et al., *Fatal familial insomnia and dysautonomia with selective degeneration of thalamic nuclei.* N Engl J Med, 1986. **315**(16): p. 997-1003.
85. Huber, R., T. Deboer, and I. Tobler, *Prion protein: a role in sleep regulation?* J Sleep Res, 1999. **8 Suppl 1**: p. 30-6.
86. Gasperini, L., et al., *Prion protein and copper cooperatively protect neurons by modulating NMDA receptor through S-nitrosylation.* Antioxid Redox Signal, 2015. **22**(9): p. 772-84.
87. Lassle, M., et al., *Stress-inducible, murine protein mSTI1. Characterization of binding domains for heat shock proteins and in vitro phosphorylation by different kinases.* J Biol Chem, 1997. **272**(3): p. 1876-84.
88. Chiarini, L.B., et al., *Cellular prion protein transduces neuroprotective signals.* Embo j, 2002. **21**(13): p. 3317-26.
89. Gauczynski, S., et al., *The 37-kDa/67-kDa laminin receptor acts as the cell-surface receptor for the cellular prion protein.* Embo j, 2001. **20**(21): p. 5863-75.
90. Chen, S., et al., *Prion protein as trans-interacting partner for neurons is involved in neurite outgrowth and neuronal survival.* Mol Cell Neurosci, 2003. **22**(2): p. 227-33.

91. Santuccione, A., et al., *Prion protein recruits its neuronal receptor NCAM to lipid rafts to activate p59fyn and to enhance neurite outgrowth.* J Cell Biol, 2005. **169**(2): p. 341-54.
92. Vassallo, N. and J. Herms, *Cellular prion protein function in copper homeostasis and redox signalling at the synapse.* J Neurochem, 2003. **86**(3): p. 538-44.
93. Roucou, X. and A.C. LeBlanc, *Cellular prion protein neuroprotective function: implications in prion diseases.* J Mol Med (Berl), 2005. **83**(1): p. 3-11.
94. Guitart, K., et al., *Improvement of neuronal cell survival by astrocyte-derived exosomes under hypoxic and ischemic conditions depends on prion protein.* Glia, 2016. **64**(6): p. 896-910.
95. Meyer-Luehmann, M., et al., *Exogenous induction of cerebral beta-amyloidogenesis is governed by agent and host.* Science, 2006. **313**(5794): p. 1781-4.
96. Clavaguera, F., et al., *Transmission and spreading of tauopathy in transgenic mouse brain.* Nat Cell Biol, 2009. **11**(7): p. 909-13.
97. Prusiner, S.B., *Cell biology. A unifying role for prions in neurodegenerative diseases.* Science, 2012. **336**(6088): p. 1511-3.
98. Aguzzi, A. and T. O'Connor, *Protein aggregation diseases: pathogenicity and therapeutic perspectives.* Nat Rev Drug Discov, 2010. **9**(3): p. 237-48.
99. Colby, D.W. and S.B. Prusiner, *Prions.* Cold Spring Harb Perspect Biol, 2011. **3**(1): p. a006833.
100. Gambetti, P., et al., *A novel human disease with abnormal prion protein sensitive to protease.* Ann Neurol, 2008. **63**(6): p. 697-708.
101. Colby, D.W., et al., *Protease-sensitive synthetic prions.* PLoS Pathog, 2010. **6**(1): p. e1000736.
102. Solassol, J., C. Crozet, and S. Lehmann, *Prion propagation in cultured cells.* Br Med Bull, 2003. **66**: p. 87-97.
103. Peretz, D., et al., *Strain-specified relative conformational stability of the scrapie prion protein.* Protein Sci, 2001. **10**(4): p. 854-63.
104. Morales, R., K. Abid, and C. Soto, *The prion strain phenomenon: molecular basis and unprecedented features.* Biochim Biophys Acta, 2007. **1772**(6): p. 681-91.
105. Bessen, R.A. and R.F. Marsh, *Distinct PrP properties suggest the molecular basis of strain variation in transmissible mink encephalopathy.* J Virol, 1994. **68**(12): p. 7859-68.
106. Collinge, J., et al., *Molecular analysis of prion strain variation and the aetiology of 'new variant' CJD.* Nature, 1996. **383**(6602): p. 685-90.
107. Telling, G.C., et al., *Evidence for the conformation of the pathologic isoform of the prion protein enciphering and propagating prion diversity.* Science, 1996. **274**(5295): p. 2079-82.
108. Parchi, P., et al., *Molecular basis of phenotypic variability in sporadic Creutzfeldt-Jakob disease.* Ann Neurol, 1996. **39**(6): p. 767-78.
109. Safar, J. and S.B. Prusiner, *Molecular studies of prion diseases.* Prog Brain Res, 1998. **117**: p. 421-34.
110. Moda, F., et al., *Synthetic prions with novel strain-specified properties.* PLoS Pathog, 2015. **11**(12): p. e1005354.
111. Pattison, I.H., *The relative susceptibility of sheep, goats and mice to two types of the goat scrapie agent.* Res Vet Sci, 1966. **7**(2): p. 207-12.
112. Race, R., et al., *Subclinical scrapie infection in a resistant species: persistence, replication, and adaptation of infectivity during four passages.* J Infect Dis, 2002. **186 Suppl 2**: p. S166-70.

113. Gibbs, C.J., Jr. and D.C. Gajdusek, *Experimental subacute spongiform virus encephalopathies in primates and other laboratory animals.* Science, 1973. **182**(4107): p. 67-8.
114. Nonno, R., et al., *Efficient transmission and characterization of Creutzfeldt-Jakob disease strains in bank voles.* PLoS Pathog, 2006. **2**(2): p. e12.
115. Carlson, G.A., *Prion Protein and Genetic Susceptibility to Diseases Caused by Its Misfolding.* Prog Mol Biol Transl Sci, 2017. **150**: p. 123-145.
116. Salman, M.D., *Chronic wasting disease in deer and elk: scientific facts and findings.* J Vet Med Sci, 2003. **65**(7): p. 761-8.
117. Williams, E.S. and M.W. Miller, *Chronic wasting disease in deer and elk in North America.* Rev Sci Tech, 2002. **21**(2): p. 305-16.
118. Arnot, C., et al., *Chronic wasting disease (CWD) potential economic impact on cervid farming in Alberta.* J Toxicol Environ Health A, 2009. **72**(17-18): p. 1014-7.
119. Chiu, A., E. Goddard, and B. Parlee, *Caribou consumption in northern Canadian communities.* J Toxicol Environ Health A, 2016. **79**(16-17): p. 762-97.
120. Benestad, S.L., et al., *First case of chronic wasting disease in Europe in a Norwegian free-ranging reindeer.* Vet Res, 2016. **47**(1): p. 88.
121. Kim, T.Y., et al., *Additional cases of Chronic Wasting Disease in imported deer in Korea.* J Vet Med Sci, 2005. **67**(8): p. 753-9.
122. Race, B., et al., *Lack of Transmission of Chronic Wasting Disease to Cynomolgus Macaques.* J Virol, 2018.
123. Prusiner, S.B., et al., *Transgenetic studies implicate interactions between homologous PrP isoforms in scrapie prion replication.* Cell, 1990. **63**(4): p. 673-86.
124. Nicholson, E.M., et al., *Differences between the prion protein and its homolog Doppel: a partially structured state with implications for scrapie formation.* J Mol Biol, 2002. **316**(3): p. 807-15.
125. Kuwata, K., et al., *Hot spots in prion protein for pathogenic conversion.* Proc Natl Acad Sci U S A, 2007. **104**(29): p. 11921-6.
126. Aguzzi, A., et al., *Interventional strategies against prion diseases.* Nat Rev Neurosci, 2001. **2**(10): p. 745-9.
127. Veith, N.M., et al., *Immunolocalisation of PrPSc in scrapie-infected N2a mouse neuroblastoma cells by light and electron microscopy.* Eur J Cell Biol, 2009. **88**(1): p. 45-63.
128. Vey, M., et al., *Subcellular colocalization of the cellular and scrapie prion proteins in caveolae-like membranous domains.* Proc Natl Acad Sci U S A, 1996. **93**(25): p. 14945-9.
129. Taraboulos, A., D. Serban, and S.B. Prusiner, *Scrapie prion proteins accumulate in the cytoplasm of persistently infected cultured cells.* J Cell Biol, 1990. **110**(6): p. 2117-32.
130. Bueler, H., et al., *Mice devoid of PrP are resistant to scrapie.* Cell, 1993. **73**(7): p. 1339-47.
131. Saborio, G.P., B. Permanne, and C. Soto, *Sensitive detection of pathological prion protein by cyclic amplification of protein misfolding.* Nature, 2001. **411**(6839): p. 810-3.
132. Colby, D.W., et al., *Prion detection by an amyloid seeding assay.* Proc Natl Acad Sci U S A, 2007. **104**(52): p. 20914-9.
133. Atarashi, R., et al., *Real-time quaking-induced conversion: a highly sensitive assay for prion detection.* Prion, 2011. **5**(3): p. 150-3.
134. Watts, J.C. and S.B. Prusiner, *Mouse models for studying the formation and propagation of prions.* J Biol Chem, 2014. **289**(29): p. 19841-9.
135. Fraser, H., *Neuronal spread of scrapie agent and targeting of lesions within the retino-tectal pathway.* Nature, 1982. **295**(5845): p. 149-50.

136. Bonda, D.J., et al., *Human prion diseases: surgical lessons learned from iatrogenic prion transmission.* Neurosurg Focus, 2016. **41**(1): p. E10.
137. Kimberlin, R.H. and C.A. Walker, *Pathogenesis of mouse scrapie: effect of route of inoculation on infectivity titres and dose-response curves.* J Comp Pathol, 1978. **88**(1): p. 39-47.
138. Kimberlin, R.H. and C.A. Walker, *Competition between strains of scrapie depends on the blocking agent being infectious.* Intervirology, 1985. **23**(2): p. 74-81.
139. Llewelyn, C.A., et al., *Possible transmission of variant Creutzfeldt-Jakob disease by blood transfusion.* Lancet, 2004. **363**(9407): p. 417-21.
140. Cobb, N.J. and W.K. Surewicz, *Prion diseases and their biochemical mechanisms.* Biochemistry, 2009. **48**(12): p. 2574-85.
141. Cashman, N.R. and B. Caughey, *Prion diseases--close to effective therapy?* Nat Rev Drug Discov, 2004. **3**(10): p. 874-84.
142. Uraki, R., et al., *Blocking of FcR suppresses the intestinal invasion of scrapie agents.* PLoS One, 2011. **6**(3): p. e17928.
143. Mishra, R.S., et al., *Protease-resistant human prion protein and ferritin are cotransported across Caco-2 epithelial cells: implications for species barrier in prion uptake from the intestine.* J Neurosci, 2004. **24**(50): p. 11280-90.
144. Gough, K.C. and B.C. Maddison, *Prion transmission: prion excretion and occurrence in the environment.* Prion, 2010. **4**(4): p. 275-82.
145. Mabbott, N.A. and G.G. MacPherson, *Prions and their lethal journey to the brain.* Nat Rev Microbiol, 2006. **4**(3): p. 201-11.
146. Press, C.M., R. Heggebo, and A. Espenes, *Involvement of gut-associated lymphoid tissue of ruminants in the spread of transmissible spongiform encephalopathies.* Adv Drug Deliv Rev, 2004. **56**(6): p. 885-99.
147. Buschmann, A. and M.H. Groschup, *Highly bovine spongiform encephalopathy-sensitive transgenic mice confirm the essential restriction of infectivity to the nervous system in clinically diseased cattle.* J Infect Dis, 2005. **192**(5): p. 934-42.
148. Espinosa, J.C., et al., *Progression of prion infectivity in asymptomatic cattle after oral bovine spongiform encephalopathy challenge.* J Gen Virol, 2007. **88**(Pt 4): p. 1379-83.
149. Lezmi, S., et al., *PrP(d) accumulation in organs of ARQ/ARQ sheep experimentally infected with BSE by peripheral routes.* Acta Biochim Pol, 2006. **53**(2): p. 399-405.
150. Marin-Moreno, A., et al., *Transmission and Replication of Prions.* Prog Mol Biol Transl Sci, 2017. **150**: p. 181-201.
151. Soto, C., et al., *Pre-symptomatic detection of prions by cyclic amplification of protein misfolding.* FEBS Lett, 2005. **579**(3): p. 638-42.
152. Serrano-Pozo, A., et al., *Neuropathological alterations in Alzheimer disease.* Cold Spring Harb Perspect Med, 2011. **1**(1): p. a006189.
153. Dickson, D.W., *Parkinson's disease and parkinsonism: neuropathology.* Cold Spring Harb Perspect Med, 2012. **2**(8).
154. Budka, H., *Neuropathology of prion diseases.* Br Med Bull, 2003. **66**: p. 121-30.
155. Glatzel, M., et al., *Extraneural pathologic prion protein in sporadic Creutzfeldt-Jakob disease.* N Engl J Med, 2003. **349**(19): p. 1812-20.
156. Hill, A.F., et al., *Investigation of variant Creutzfeldt-Jakob disease and other human prion diseases with tonsil biopsy samples.* Lancet, 1999. **353**(9148): p. 183-9.
157. Hansen, H.C., et al., *Clinical changes and EEG patterns preceding the onset of periodic sharp wave complexes in Creutzfeldt-Jakob disease.* Acta Neurol Scand, 1998. **97**(2): p. 99-106.
158. Steinhoff, B.J., et al., *Accuracy and reliability of periodic sharp wave complexes in Creutzfeldt-Jakob disease.* Arch Neurol, 1996. **53**(2): p. 162-6.

159. Tschampa, H.J., et al., *Patients with Alzheimer's disease and dementia with Lewy bodies mistaken for Creutzfeldt-Jakob disease.* J Neurol Neurosurg Psychiatry, 2001. **71**(1): p. 33-9.
160. Wieser, H.G., K. Schindler, and D. Zumsteg, *EEG in Creutzfeldt-Jakob disease.* Clin Neurophysiol, 2006. **117**(5): p. 935-51.
161. Collins, S., et al., *Recent advances in the pre-mortem diagnosis of Creutzfeldt-Jakob disease.* J Clin Neurosci, 2000. **7**(3): p. 195-202.
162. Zeidler, M., et al., *The pulvinar sign on magnetic resonance imaging in variant Creutzfeldt-Jakob disease.* Lancet, 2000. **355**(9213): p. 1412-8.
163. Coulthard, A., et al., *Quantitative analysis of MRI signal intensity in new variant Creutzfeldt-Jakob disease.* Br J Radiol, 1999. **72**(860): p. 742-8.
164. Will, R.G., et al., *Diagnosis of new variant Creutzfeldt-Jakob disease.* Ann Neurol, 2000. **47**(5): p. 575-82.
165. Zerr, I., et al., *Updated clinical diagnostic criteria for sporadic Creutzfeldt-Jakob disease.* Brain, 2009. **132**(Pt 10): p. 2659-68.
166. Jimi, T., et al., *High levels of nervous system-specific proteins in cerebrospinal fluid in patients with early stage Creutzfeldt-Jakob disease.* Clin Chim Acta, 1992. **211**(1-2): p. 37-46.
167. Chohan, G., et al., *The role of cerebrospinal fluid 14-3-3 and other proteins in the diagnosis of sporadic Creutzfeldt-Jakob disease in the UK: a 10-year review.* J Neurol Neurosurg Psychiatry, 2010. **81**(11): p. 1243-8.
168. Bahl, J.M., et al., *The diagnostic efficiency of biomarkers in sporadic Creutzfeldt-Jakob disease compared to Alzheimer's disease.* Neurobiol Aging, 2009. **30**(11): p. 1834-41.
169. Hsich, G., et al., *The 14-3-3 brain protein in cerebrospinal fluid as a marker for transmissible spongiform encephalopathies.* N Engl J Med, 1996. **335**(13): p. 924-30.
170. Henry, C. and R. Knight, *Clinical features of variant Creutzfeldt-Jakob disease.* Rev Med Virol, 2002. **12**(3): p. 143-50.
171. Boellaard, J.W., P. Brown, and J. Tateishi, *Gerstmann-Straussler-Scheinker disease-the dilemma of molecular and clinical correlations.* Clin Neuropathol, 1999. **18**(6): p. 271-85.
172. Schiermeier, Q., *Testing times for BSE.* Nature, 2001. **409**(6821): p. 658-9.
173. Hamad, A., et al., *Iatrogenic Creutzfeldt-Jakob disease at the millennium.* Neurology, 2001. **56**(7): p. 987.
174. Barria, M.A., D. Gonzalez-Romero, and C. Soto, *Cyclic amplification of prion protein misfolding.* Methods Mol Biol, 2012. **849**: p. 199-212.
175. Tattum, M.H., et al., *Discrimination between prion-infected and normal blood samples by protein misfolding cyclic amplification.* Transfusion, 2010. **50**(5): p. 996-1002.
176. Murayama, Y., et al., *Sulfated dextrans enhance in vitro amplification of bovine spongiform encephalopathy PrP(Sc) and enable ultrasensitive detection of bovine PrP(Sc).* PLoS One, 2010. **5**(10).
177. Haley, N.J., et al., *Detection of CWD prions in urine and saliva of deer by transgenic mouse bioassay.* PLoS One, 2009. **4**(3): p. e4848.
178. Concha-Marambio, L., et al., *Detection of prions in blood from patients with variant Creutzfeldt-Jakob disease.* Sci Transl Med, 2016. **8**(370): p. 370ra183.
179. Redaelli, V., et al., *Detection of prion seeding activity in the olfactory mucosa of patients with Fatal Familial Insomnia.* Sci Rep, 2017. **7**: p. 46269.
180. Moda, F., et al., *Prions in the urine of patients with variant Creutzfeldt-Jakob disease.* N Engl J Med, 2014. **371**(6): p. 530-9.
181. Bougard, D., et al., *Detection of prions in the plasma of presymptomatic and symptomatic patients with variant Creutzfeldt-Jakob disease.* Sci Transl Med, 2016. **8**(370): p. 370ra182.

182. Moda, F., *Protein Misfolding Cyclic Amplification of Infectious Prions.* Prog Mol Biol Transl Sci, 2017. **150**: p. 361-374.
183. Atarashi, R., et al., *Simplified ultrasensitive prion detection by recombinant PrP conversion with shaking.* Nat Methods, 2008. **5**(3): p. 211-2.
184. Atarashi, R., et al., *Ultrasensitive human prion detection in cerebrospinal fluid by real-time quaking-induced conversion.* Nat Med, 2011. **17**(2): p. 175-8.
185. Wilham, J.M., et al., *Rapid end-point quantitation of prion seeding activity with sensitivity comparable to bioassays.* PLoS Pathog, 2010. **6**(12): p. e1001217.
186. Orru, C.D., et al., *Prion disease blood test using immunoprecipitation and improved quaking-induced conversion.* MBio, 2011. **2**(3): p. e00078-11.
187. Foutz, A., et al., *Diagnostic and prognostic value of human prion detection in cerebrospinal fluid.* Ann Neurol, 2017. **81**(1): p. 79-92.
188. Caughey, B., et al., *Amplified Detection of Prions and Other Amyloids by RT-QuIC in Diagnostics and the Evaluation of Therapeutics and Disinfectants.* Prog Mol Biol Transl Sci, 2017. **150**: p. 375-388.
189. Zanusso, G., et al., *Detection of pathologic prion protein in the olfactory epithelium in sporadic Creutzfeldt-Jakob disease.* N Engl J Med, 2003. **348**(8): p. 711-9.
190. Zanusso, G., M. Bongianni, and B. Caughey, *A test for Creutzfeldt-Jakob disease using nasal brushings.* N Engl J Med, 2014. **371**(19): p. 1842-3.
191. Masujin, K., et al., *Detection of Atypical H-Type Bovine Spongiform Encephalopathy and Discrimination of Bovine Prion Strains by Real-Time Quaking-Induced Conversion.* J Clin Microbiol, 2016. **54**(3): p. 676-86.
192. John, T.R., H.M. Schatzl, and S. Gilch, *Early detection of chronic wasting disease prions in urine of pre-symptomatic deer by real-time quaking-induced conversion assay.* Prion, 2013. **7**(3): p. 253-8.
193. Haley, N.J., et al., *Antemortem Detection of Chronic Wasting Disease Prions in Nasal Brush Collections and Rectal Biopsy Specimens from White-Tailed Deer by Real-Time Quaking-Induced Conversion.* J Clin Microbiol, 2016. **54**(4): p. 1108-16.
194. Schmitz, M., et al., *The real-time quaking-induced conversion assay for detection of human prion disease and study of other protein misfolding diseases.* Nat Protoc, 2016. **11**(11): p. 2233-2242.
195. Bolognesi, M.L. and G. Legname, *Approaches for discovering anti-prion compounds: lessons learned and challenges ahead.* Expert Opin Drug Discov, 2015. **10**(4): p. 389-97.
196. Costanzo, M. and C. Zurzolo, *The cell biology of prion-like spread of protein aggregates: mechanisms and implication in neurodegeneration.* Biochem J, 2013. **452**(1): p. 1-17.
197. Gandini, A. and M.L. Bolognesi, *Therapeutic Approaches to Prion Diseases.* Prog Mol Biol Transl Sci, 2017. **150**: p. 433-453.
198. Gravitz, L., *Drugs: a tangled web of targets.* Nature, 2011. **475**(7355): p. S9-11.
199. Mead, S. and F. Tagliavini, *Clinical trials.* Handb Clin Neurol, 2018. **153**: p. 431-444.
200. Terzano, M.G., et al., *The effect of amantadine on arousal and EEG patterns in Creutzfeldt-Jakob disease.* Arch Neurol, 1983. **40**(9): p. 555-9.
201. Neri, G., et al., *[Amantadine in Creutzfeldt-Jakob disease. Review of the literature and case contribution].* Riv Neurobiol, 1984. **30**(1): p. 47-56.
202. David, A.S., R. Grant, and J.P. Ballantyne, *Unsuccessful treatment of Creutzfeldt-Jakob disease with acyclovir.* Lancet, 1984. **1**(8375): p. 512-3.
203. Newman, P.K., *Acyclovir in Creutzfeldt-Jakob disease.* Lancet, 1984. **1**(8380): p. 793.
204. Kovanen, J., M. Haltia, and K. Cantell, *Failure of interferon to modify Creutzfeldt-Jakob disease.* Br Med J, 1980. **280**(6218): p. 902.

205. Furlow, T.W., Jr., R.J. Whitley, and F.J. Wilmes, *Repeated suppression of Creutzfeldt-Jakob disease with vidarabine.* Lancet, 1982. **2**(8297): p. 564-5.
206. Pocchiari, M., S. Schmittinger, and C. Masullo, *Amphotericin B delays the incubation period of scrapie in intracerebrally inoculated hamsters.* J Gen Virol, 1987. **68 (Pt 1)**: p. 219-23.
207. Masullo, C., et al., *Failure to ameliorate Creutzfeldt-Jakob disease with amphotericin B therapy.* J Infect Dis, 1992. **165**(4): p. 784-5.
208. Dervaux, A., et al., *Psychiatric features of vCJD similar in France and UK.* Br J Psychiatry, 2001. **178**: p. 276.
209. Korth, C., et al., *Acridine and phenothiazine derivatives as pharmacotherapeutics for prion disease.* Proc Natl Acad Sci U S A, 2001. **98**(17): p. 9836-41.
210. Barret, A., et al., *Evaluation of quinacrine treatment for prion diseases.* J Virol, 2003. **77**(15): p. 8462-9.
211. Haik, S., et al., *Compassionate use of quinacrine in Creutzfeldt-Jakob disease fails to show significant effects.* Neurology, 2004. **63**(12): p. 2413-5.
212. Collinge, J., et al., *Safety and efficacy of quinacrine in human prion disease (PRION-1 study): a patient-preference trial.* Lancet Neurol, 2009. **8**(4): p. 334-44.
213. Geschwind, M.D., et al., *Quinacrine treatment trial for sporadic Creutzfeldt-Jakob disease.* Neurology, 2013. **81**(23): p. 2015-23.
214. Ghaemmaghami, S., et al., *Continuous quinacrine treatment results in the formation of drug-resistant prions.* PLoS Pathog, 2009. **5**(11): p. e1000673.
215. Martinez-Lage, J.F., et al., *Creutzfeldt-Jakob disease acquired via a dural graft: failure of therapy with quinacrine and chlorpromazine.* Surg Neurol, 2005. **64**(6): p. 542-5, discussion 545.
216. Floel, A., et al., *Anticonvulsants for Creutzfeldt-Jakob disease?* Lancet, 2003. **361**(9353): p. 224.
217. Perovic, S., et al., *Effect of flupirtine on Bcl-2 and glutathione level in neuronal cells treated in vitro with the prion protein fragment (PrP106-126).* Exp Neurol, 1997. **147**(2): p. 518-24.
218. Otto, M., et al., *Efficacy of flupirtine on cognitive function in patients with CJD: A double-blind study.* Neurology, 2004. **62**(5): p. 714-8.
219. Todd, N.V., et al., *Cerebroventricular infusion of pentosan polysulphate in human variant Creutzfeldt-Jakob disease.* J Infect, 2005. **50**(5): p. 394-6.
220. Bone, I., et al., *Intraventricular pentosan polysulphate in human prion diseases: an observational study in the UK.* Eur J Neurol, 2008. **15**(5): p. 458-64.
221. Forloni, G., et al., *Tetracyclines and prion infectivity.* Infect Disord Drug Targets, 2009. **9**(1): p. 23-30.
222. De Luigi, A., et al., *The efficacy of tetracyclines in peripheral and intracerebral prion infection.* PLoS One, 2008. **3**(3): p. e1888.
223. Zerr, I., *Therapeutic trials in human transmissible spongiform encephalo-pathies: recent advances and problems to address.* Infect Disord Drug Targets, 2009. **9**(1): p. 92-9.
224. Haik, S., et al., *Doxycycline in Creutzfeldt-Jakob disease: a phase 2, randomised, double-blind, placebo-controlled trial.* Lancet Neurol, 2014. **13**(2): p. 150-8.
225. Forloni, G., et al., *Preventive study in subjects at risk of fatal familial insomnia: Innovative approach to rare diseases.* Prion, 2015. **9**(2): p. 75-9.
226. Ashburn, T.T. and K.B. Thor, *Drug repositioning: identifying and developing new uses for existing drugs.* Nat Rev Drug Discov, 2004. **3**(8): p. 673-83.
227. Duraes, F., M. Pinto, and E. Sousa, *Old Drugs as New Treatments for Neurodegenerative Diseases.* Pharmaceuticals (Basel), 2018. **11**(2).

228. Zaccagnini, L., et al., *Identification of novel fluorescent probes preventing PrP(Sc) replication in prion diseases.* Eur J Med Chem, 2017. **127**: p. 859-873.
229. Baskakov, I.V., *The many shades of prion strain adaptation.* Prion, 2014. **8**(2).
230. Barreca, M.L., et al., *Pharmacological Agents Targeting the Cellular Prion Protein.* Pathogens, 2018. **7**(1).
231. Ryou, C., et al., *Differential inhibition of prion propagation by enantiomers of quinacrine.* Lab Invest, 2003. **83**(6): p. 837-43.
232. Vogtherr, M., et al., *Antimalarial drug quinacrine binds to C-terminal helix of cellular prion protein.* J Med Chem, 2003. **46**(17): p. 3563-4.
233. Baral, P.K., et al., *Structural basis of prion inhibition by phenothiazine compounds.* Structure, 2014. **22**(2): p. 291-303.
234. Stincardini, C., et al., *An antipsychotic drug exerts anti-prion effects by altering the localization of the cellular prion protein.* PLoS One, 2017. **12**(8): p. e0182589.
235. Caughey, W.S., et al., *Inhibition of protease-resistant prion protein formation by porphyrins and phthalocyanines.* Proc Natl Acad Sci U S A, 1998. **95**(21): p. 12117-22.
236. Priola, S.A., A. Raines, and W.S. Caughey, *Porphyrin and phthalocyanine antiscrapie compounds.* Science, 2000. **287**(5457): p. 1503-6.
237. Rajora, M.A., J.W.H. Lou, and G. Zheng, *Advancing porphyrin's biomedical utility via supramolecular chemistry.* Chem Soc Rev, 2017. **46**(21): p. 6433-6469.
238. Kimura, T., et al., *Synthesis of GN8 derivatives and evaluation of their antiprion activity in TSE-infected cells.* Bioorg Med Chem Lett, 2011. **21**(5): p. 1502-7.
239. Weissmann, C. and A. Aguzzi, *Approaches to therapy of prion diseases.* Annu Rev Med, 2005. **56**: p. 321-44.
240. Roettger, Y., et al., *Immunotherapy in prion disease.* Nat Rev Neurol, 2013. **9**(2): p. 98-105.
241. White, M.D., et al., *Single treatment with RNAi against prion protein rescues early neuronal dysfunction and prolongs survival in mice with prion disease.* Proc Natl Acad Sci U S A, 2008. **105**(29): p. 10238-43.
242. Moreno, J.A., et al., *Oral treatment targeting the unfolded protein response prevents neurodegeneration and clinical disease in prion-infected mice.* Sci Transl Med, 2013. **5**(206): p. 206ra138.
243. Clarke, M.C. and D.A. Haig, *Multiplication of scrapie agent in cell culture.* Res Vet Sci, 1970. **11**(5): p. 500-1.
244. Race, R.E., L.H. Fadness, and B. Chesebro, *Characterization of scrapie infection in mouse neuroblastoma cells.* J Gen Virol, 1987. **68 (Pt 5)**: p. 1391-9.
245. Bosque, P.J. and S.B. Prusiner, *Cultured cell sublines highly susceptible to prion infection.* J Virol, 2000. **74**(9): p. 4377-86.
246. Vilette, D., *Cell models of prion infection.* Vet Res, 2008. **39**(4): p. 10.
247. Berridge, M.V., P.M. Herst, and A.S. Tan, *Tetrazolium dyes as tools in cell biology: new insights into their cellular reduction.* Biotechnol Annu Rev, 2005. **11**: p. 127-52.
248. Poncet-Montange, G., et al., *A survey of antiprion compounds reveals the prevalence of non-PrP molecular targets.* J Biol Chem, 2011. **286**(31): p. 27718-28.
249. Kawasaki, Y., et al., *Orally administered amyloidophilic compound is effective in prolonging the incubation periods of animals cerebrally infected with prion diseases in a prion strain-dependent manner.* J Virol, 2007. **81**(23): p. 12889-98.
250. Adjou, K.T., et al., *Differential effects of a new amphotericin B derivative, MS-8209, on mouse BSE and scrapie: implications for the mechanism of action of polyene antibiotics.* Res Virol, 1996. **147**(4): p. 213-8.
251. Kocisko, D.A., et al., *Comparison of protease-resistant prion protein inhibitors in cell cultures infected with two strains of mouse and sheep scrapie.* Neurosci Lett, 2005. **388**(2): p. 106-11.

252. Miller-Vedam, L. and S. Ghaemmaghami, *Strain specificity and drug resistance in anti-prion therapy.* Curr Top Med Chem, 2013. **13**(19): p. 2397-406.
253. Hart, P.D. and M.R. Young, *Ammonium chloride, an inhibitor of phagosome-lysosome fusion in macrophages, concurrently induces phagosome-endosome fusion, and opens a novel pathway: studies of a pathogenic mycobacterium and a nonpathogenic yeast.* J Exp Med, 1991. **174**(4): p. 881-9.
254. Seguin, S.J., et al., *Inhibition of autophagy, lysosome and VCP function impairs stress granule assembly.* Cell Death Differ, 2014. **21**(12): p. 1838-51.
255. Krell, T., et al., *Characterization of molecular interactions using isothermal titration calorimetry.* Methods Mol Biol, 2014. **1149**: p. 193-203.
256. Patching, S.G., *Surface plasmon resonance spectroscopy for characterisation of membrane protein-ligand interactions and its potential for drug discovery.* Biochim Biophys Acta, 2014. **1838**(1 Pt A): p. 43-55.
257. Shah, N.B. and T.M. Duncan, *Bio-layer interferometry for measuring kinetics of protein-protein interactions and allosteric ligand effects.* J Vis Exp, 2014(84): p. e51383.
258. Kang, H.E., et al., *Prion Diagnosis: Application of Real-Time Quaking-Induced Conversion.* Biomed Res Int, 2017. **2017**: p. 5413936.
259. Ghaemmaghami, S., et al., *Discovery of 2-aminothiazoles as potent antiprion compounds.* J Virol, 2010. **84**(7): p. 3408-12.
260. Bolognesi, M.L., et al., *Discovery of a class of diketopiperazines as antiprion compounds.* ChemMedChem, 2010. **5**(8): p. 1324-34.
261. Herrmann, U.S., et al., *Structure-based drug design identifies polythiophenes as antiprion compounds.* Sci Transl Med, 2015. **7**(299): p. 299ra123.
262. Hyeon, J.W., et al., *Anti-Prion Screening for Acridine, Dextran, and Tannic Acid using Real Time-Quaking Induced Conversion: A Comparison with PrPSc-Infected Cell Screening.* PLoS One, 2017. **12**(1): p. e0170266.
263. Kimura, T., et al., *Synthesis of 9-substituted 2,3,4,9-tetrahydro-1H-carbazole derivatives and evaluation of their anti-prion activity in TSE-infected cells.* Eur J Med Chem, 2011. **46**(11): p. 5675-9.
264. Klingenstein, R., et al., *Similar structure-activity relationships of quinoline derivatives for antiprion and antimalarial effects.* J Med Chem, 2006. **49**(17): p. 5300-8.
265. Gallardo-Godoy, A., et al., *2-Aminothiazoles as therapeutic leads for prion diseases.* J Med Chem, 2011. **54**(4): p. 1010-21.
266. Staderini, M., et al., *A Fluorescent Styrylquinoline with Combined Therapeutic and Diagnostic Activities against Alzheimer's and Prion Diseases.* ACS Med Chem Lett, 2013. **4**(2): p. 225-9.
267. Bongarzone, S., et al., *Parallel synthesis, evaluation, and preliminary structure-activity relationship of 2,5-diamino-1,4-benzoquinones as a novel class of bivalent anti-prion compound.* J Med Chem, 2010. **53**(22): p. 8197-201.
268. Bongarzone, S., et al., *Hybrid lipoic acid derivatives to attack prion disease on multiple fronts.* ChemMedChem, 2011. **6**(4): p. 601-5.
269. Tran, H.N., et al., *Synthesis and evaluation of a library of 2,5-bisdiamino-benzoquinone derivatives as probes to modulate protein-protein interactions in prions.* Bioorg Med Chem Lett, 2010. **20**(6): p. 1866-8.
270. Fukuuchi, T., et al., *Metal complexes with superoxide dismutase-like activity as candidates for anti-prion drug.* Bioorg Med Chem Lett, 2006. **16**(23): p. 5982-7.
271. Staderini, M., *Modulation of prion by small molecules: form monovalent to bivalent and multivalent ligands.* Current Topics in medicinal chemistry, 2013.
272. Yap, C.W., *PaDEL-descriptor: an open source software to calculate molecular descriptors and fingerprints.* J Comput Chem, 2011. **32**(7): p. 1466-74.